IDENTIFICATION OF NOVEL LIGANDS OF WDR47, USING YEAST TWO-HYBRID ANALYSIS

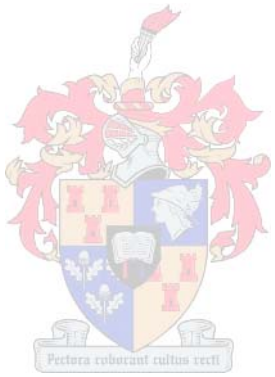

L. McGillewie

Thesis presented in partial fulfilment of the requirements for the degree of Masters of Science in Medical Sciences (Medical Biochemistry) at Stellenbosch University.

Promoter: Dr Craig Kinnear

Co-promoter: Prof Johanna C. Moolman-Smook

December 2009

DECLARATION

By submitting this thesis electronically, I declare that the entirety of the work contained therein is my own, original work, that I am the owner of the copyright thereof (unless to the extent explicitly otherwise stated) and that I have not previously in its entirety or in part submitted it for obtaining any qualification.

Date……14 October 2009…….

ABSTRACT

The mammalian neocortex contributes to the increasing functional complexity of the mammalian brain, partly because of its striking organisation into distinct neuronal layers. The development of the neocortex has been well studied because disrupted neurodevelopment results in several human diseases.

The basic principles of neocortical development have been well established for some time; however the molecular mechanisms have only recently been identified. One major advance in our understanding of these molecular mechanisms was the discovery of Reelin, an extracellular matrix protein that directs the migration of neurons to their final positions in the developing neocortex.

Reelin is a large multi-domain protein that exerts its functions by binding to its ligands on the cell surface and initiating a signal transduction cascade that ultimately results in cytoskeletal rearrangements. Several investigations have been undertaken to elucidate the functions of each of these domains to gain a better understanding reelin's functions.

We have previously identified the WR40 repeat protein 47 (WDR47), a protein of unknown function, as a novel putative ligand for the N-terminal reeler domain of reelin. To gain better understanding into the functional significance of this interaction, the present study sought to identify novel WDR47- interacting proteins. In order to achieve this, a cDNA encoding a polypeptide that contains the two N-terminal domains of WDR47, i.e. the Lis homology and the C-terminal Lis homology domain (CTLH) was used as bait in a Y2H screen of a foetal brain cDNA library. Putative WDR47 ligands were subsequently verified using 3D *in vivo* co-localisation.

Results of these analyses showed that SCG10, a microtubule destabilizing protein belonging to the stathmin family of proteins, interacted with the N-terminal of WDR47. The identification of SCG10 as a novel WDR47 interacting protein not only sheds some light on the role and function of WDR47 but also aids in a better understanding of the reelin pathway and cortical lamination. Moreover, the data presented here, may also provide researchers with new avenues of research into molecular mechanisms involved in neuronal migration disorders.

OPSOMMING

The mammalian neocortex contributes to the increasing functional complexity of the mammalian brain, partly because of its striking organisation into distinct neuronal layers. The development of the neocortex has been well studied because disrupted neurodevelopment results in several human diseases.

The basic principles of neocortical development have been well established for some time; however the molecular mechanisms have only recently been identified. One major advance in our understanding of these molecular mechanisms was the discovery of Reelin, an extracellular matrix protein that directs the migration of neurons to their final positions in the developing neocortx.

Reelin is a large multidomain protein that exerts its functions by binding to its ligands on the cell surface and initiating a signal transduction cascade that ultimately results in cytoskeletal rearrangements. Several investigations have been undertaken to elucidate the functions of each of these domains to gain a better understanding reelin's functions.

We have previously identified the WR40 repeat protein 47 (WDR47), a protein of unknown function, as a novel putative ligand for the N-terminal reeler domain of reelin. To gain better understanding into the functional significance of this interaction, the present study sought to identify novel WDR47- interacting proteins. In order to achieve this, a cDNA encoding a polypeptide that contains the two N-terminal domains of WDR47, ie the Lis homology and the C-terminal Lis homology domain (CTLH) was used as 'bait' in a Y2H screen of a foetal brain cDNA library. Putative WDR47 ligands were subsequently verified using 3D in vivo co-localisation.

Results of these analyses showed that SCG10, a microtubule destabilizing protein belonging to the stathmin family of proteins, interacted with the N-terminal of WDR47. The identification of SCG10 as a novel WDR47 interacting protein not only sheds some light on the role and function of WDR47 but also aids in a better understanding of the reelin pathway and cortical lamination. Moreover, the data presented here, may also provide researchers with new avenues of research into molecular mechanisms involved in neuronal migration disorders.

TABLE OF CONTENTS

ACKNOWLEDGEMENTS

I would like to express my sincere gratitude to the following people who have helped me reach for the stars in the past few years:

My mentor, Dr Craig Kinnear, firstly thank you for your patience. You have always believed in me and stood by me through the good, the bad and the ugly. You have been an inspiration, not only as a brilliant scientist but as a person who I truly admire. In the last few years, you became my family away from home. Thank you for everything, I am honoured to have been your student.

Professor JC Moolman-Smook, for all the guidance both in my scientific career and in my personal growth, and for always encouraging me to strive for nothing but the best.

Mr Ben Loos, Department of Physiology (University of Stellenbosch), for the technical assistance and patience at the fluorescence microscope throughout the co-localisation assays.

To everyone in the MAGIC lab, you have not only been colleagues but many of you have become friends I will cherish forever. Thank you for all the laughs, especially to Chrizette 'Jimmy' Uys. The NRF for giving me the funding and financial support to complete this project.

My amazing family, I could not have wished for more. Dad (David McGillewie) thank you for giving me the opportunity to spread my wings and for always being there and supporting me (in every way), and for always being so understanding you truly are an inspiration... I love you pops. Mom (Helena McGillewie), you are my guardian angel, my pillar of strength, you have always believed in me against all the odds. Thank you for always giving me nothing but the very best, and for always loving me the way only a mother can... I love you. To my brother, Danetjie, you are my best friend, thank you for always being there no matter what, words cannot describe how much I love you. Lastly, ouma Joey, I hope I have made you proud... each day that goes by you are in my thoughts, I miss you so very much!

Jaco Rossouw, you have been by my side every step of the way no matter how difficult things got. Thank you for your endless support and love, you really are my one in a million. Love you always...

Lastly, and most importantly dear God: you have given me everything, the opportunity to become the best I can be, you have given me the most wonderful family... without you, I would not be where I am today. Thank you.

LIST OF ABBREVIATIONS

3D	Three-dimensional
5'-UTR	Five prime untranslated region
aa	Amino acid
AD	Activation domain
ADE2	Phosphoribosylaminoimidazole carboxylase gene
Ade	Adenine
Amp	Ampicillin
ApoER2	Apolipoprotein E receptor 2
APS	Ammonium persulphate
ASD	Autism spectrum disorders
ATP	Adenosine triphosphate
BD	Binding domain
BLAST	Basic local alignment search tool
BLASTN	Basic local alignment search tool (nucleotide)
BLASTP	Basic local alignment search tool (protein)
bp	Base pair
BRET	Bioluminescence resonance energy transfer
cDNA	Complementary DNA
Cdk5	Cyclin dependant kinase 5
Cfu	Colony forming units
CGE	Caudal ganglionic eminence
CIAP	*Calf intestinal alkaline phosphatase*
CNR	Cadherin-related neuronal receptors
CP	Cortical plate
CR	Cajal-Retzius cells
CS	Cockayne syndrome
CTLH	C-terminal to the Lis homology domain
Cul5	Cullin 5
Cul7	Cullin 7
dATP	Deoxy-adenosine triphospate
dCTP	Deoxy-cytidine triphosphate
ddH_2O	Double distilled water
dGTP	Deoxy-guanosine triphosphate
Dab1	Disabled-1
DCX	Doublecortin
DMSO	Dimethyl sulphoxide

DNA	Deoxyribonucleic acid
dNTP	Deoxy-nucleotide triphosphate
DTT	1,4-Dithiothreitol
dTTP	Deoxy-thymidine triphosphate
E.coli	*Escherichia coli*
EDTA	Ethylene-diamine-tetra-acetic acid
EGF	Epidermal growth factor
FCD	Focal cortical dysplasia
GABA	Gamma-aminobutyric acid
GAD67	Glutamate decarboxylase 67
GE	Ganglionic eminence
GFP	Green fluorescent protein
GH	Glycine-histidine
GSK3β	Glycogen synthase kinase 3 beta
Guk1	Guanylate kinase 1
HCl	Hydrochloric acid
HIS3	Imidazoleglycerolphosphate dehydratase gene
His	Histidine
HRM	Heterozygous *reeler* mouse
IZ	Intermediate zone
kb	Kilo bases
kDa	Kilo Dalton
Kan	Kanamycin
KOAc	Potassium acetate
L	Litre
LB	Luria-Bertani broth
Leu	Leucine
LGE	Lateral ganglionic eminence
LiAc	Lithium acetate
LIMK1	LIM kinase 1
LIS	Type 1 lissencephaly
LisH	Lis homology domain
M	Molar
MAP	Microtubule associated proteins
MAP1B	Microtubule associated protein 1 B
MCD	Malformations of cortical development
MCS	Multiple cloning site

MEL1	Alpha-galactosidase gene
MGE	Medial ganglionic eminence
MIT	Microtubules
MITOC	Microtubule organization centre
mTor	Mammalian target of rapamycin
MRC	Medical Research Council
MZ	Marginal zone
mg	Milligram
ml	Millilitre
mM	Millimolar
mRNA	Messenger RNA
NA	Numerical aperture
NaCl	Sodium chloride
NaOH	Sodium hydoroxide
NGF	Neuronal growth factor
NH_4	Ammonium
NMDA	*N*-methyl-*D*-aspartate
^oC	Degrees Celsius
OCD	Obsessive-compulsive disorder
OD	Optical density
ORF	Open reading frame
PAFAH1B1	β subunit of platelet activating factor acetylhydrolase gene
PBS	Phosphate buffered saline
PCI	Phenol/chloroform/isoamyl alcohol
PCR	Polymerase chain reaction
PDE	Phosphodiesterase
PEG	Polyethylene glycol
PEP	Two-phosphoenolpyruvate
Pi	Inorganic phosphate
PI3K	Phosphatidylinositol 3-kinase
PKA	Protein kinase A
PKB	Protein kinase B
PP	Preplate
PTB	Phosphotyrosine binding
QDO	Quadruple dropout
RET	Non-radiative energy transfer
RFP	Red fluorescent protein

RNA	Ribonucleic acid
Rpm	Revolutions per minute
RSA	Republic of South Africa
S. cerevisiae	*Saccharomyces cerevisiae*
SB	Sodium borate
SCG10	Superior cervical ganglion10
SD	Synthetic dropout
SDS	Sodium dodecyl sulphate
SFK	Src family tyrosine kinases
SNAPIN	SNARE associated protein
SNARE	*N*-ethyl maleimide sensitive factor adaptor protein receptor
SP	Subplate
SVZ	Sub-ventricular zone
Ser	Serine
Ta	Annealing temperature
TBST	Tris-buffered saline Tween 20
TDO	Triple dropout
TE	Tris-EDTA
TEMED	N,N,N',N'-Tetramethylethylenediamine
Tm	Melting temperature
Trp	Tryptophan
TUBA1A	Alpha tubulin gene
TxRed	Texas red fluorescent dye
UK	United Kingdom
USA	United States of America
UV	Ultraviolet
VAMP	vesicle-associated protein synaptobrevin
VLDLR	Very low density lipoprotein receptor
VZ	Ventricular zone
WD	Tryptophan-aspartic acid
www	World wide web
X-α-Gal	X-alpha-galactosidase
XLIS	x-linked Lissencephaly
Y2H	Yeast two hybrid
YFP	Yellow fluorescent protein
YPDA	Yeast peptone dextrose adenine
µl	Microlitre

LIST OF FIGURES

migrating cell up along the radial glial fiber until its' correct position within the cortical plate is reached (Taken from Cooper, 2008).

Figure 1.7. Tangential migrating cortical interneurons arising from the medial ganglionic eminence. (a) Cortical interneurons born in the ganglionic emenences migrate tangentially (red arrow) around the cortical notch to the developing cortex. **(b)** Cortical interneurons migrate tangentially within the cortex and subsequently change direction in order to enter the cortical plate. The solid red arrows indicate the path travelled by the cortical interneurons, while the broken red arrow shows that some cortical interneurons have been found to descend radially from the marginal zone into the cortical plate and others continue radially into the deeper cortical layers. Abbreviations: IZ, intermediate zone, LGE, lateral ganglionic eminence, LV, lateral ventricle; MGE, medial ganglionic eminence; MZ, marginal zone; SVZ, subventricular zone, VZ, ventricular zone. (Taken from Kriegstein and Noctor, 2004).

Figure 1.8. Cyto-architectural abnormalities in the *reeler* mouse. In the *reeler* cortex, the preplate forms normally with the exception that the first cohort of early-born migrating neurons are unable to split the preplate due to the absence of reelin; thus the subplate remains adjacent to the marginal zone forming a 'superplate' (SPP, a cell dense area containing the Cajal-Retzius cells, subplate neurons and few cortical plate neurons). The cortical plate then forms underneath the 'superplate', as later generated neurons are not able to migrate past their earlier born predecessors which leads to the formation of a disorganised and inverted (outside-in) cortical plate as neurons are not able to arrange themselves into distinct neuronal layers (Taken from Gupta *et al.,* 2002).

Figure 1.9. Schematic representation of the reelin structure. The open reading frame predicts a secreted extracellular matrix glycoprotein of 3641 amino acids with a relative molecular mass of 388kDa. At the N terminal reelin contains a cleavable signal peptide, followed by a region with 25% identity to that of F-spondin (controls cell migration and neurite outgrowth). This is followed by the characteristic presence of a series of eight internal reelin repeats, each repeat is composed of 350-390 amino acids and is composed of two related subrepeats A and B, which are separated by an EGF-like motif. The epitope for the CR-50 antibody is located upstream of the reelin repeats; oncebound, this antibody blocks the reelin-induced kinase cascade both *in vitro* and *in vivo*. The C-terminal is an area rich in arginine residues, which are required for reelin secretion from the Cajal-Retzius cells during corticogenesis (Taken from Kubo and Nakajima, 2002; Rice and Curran, 2001).

Figure 4.1. **Schematic representation of the microtubule destabilizing protein SCG10.** The N-terminal blue represents the palmitoylation domain responsible for membrane anchoring of SCG10 to growth cone vesicles. The purple represents the regulatory sub-domain of the conserved stathmin-like domain, while the red triangles represent the serine phosphorylation sites. The green represents the interacting sub-domain of the stathmin-like domain, which is responsible for the tubulin interaction and MIT destabilizing activity of SCG10.

Figure 4.2. Shows the dynamic instability of microtubules in light of SCG10. Microtubules are polymer structures composed of α/β heterodimers. GTP-bound tubulin is added to the plus end of growing microtubules. Microtubules are also dynamic polymers which are capable of switching between phases of growth (rescue) and shrinkage (catastrophe). SCG10 increase the dynamic instability of microtubules by promoting catastrophe and by sequestering tubulin, thus dynamic instability is crucial in neurite extension and elongation (Taken from Grenningloh *et al.*,2003).

LIST OF TABLES

CHAPTER ONE: INTRODUCTION

CHAPTER ONE: INTRODUCTION

1.1 NEUROLOGICAL AND NEURODEVELOPMENTAL DISORDERS

Neurological and behavioural disorders are major health problems endemic to all countries around the world, and cause great suffering to affected individuals as well as to their family members. According to the World Bank, neurological and behavioural disorders combined account for approximately 13% of the Global Disease Burden; a burden greater than that of AIDS, tuberculosis and malaria combined (11.4%) (World Bank. Data and Statistics, http://go.worldbank.org). Moreover, these disorders are among the ten leading causes of disability in the United States and other developed countries (World Health Organization, http://www.who.int/mental_health).

Global estimates from the World Health Organisation (WHO) showed that in 2004 approximately 154 million people suffer from depression, 24 million people suffer from Alzheimer's and other dementias, 25 million people suffer from schizophrenia and a staggering one million people die due to suicide each year (World Health Organization, http://www.who.int/healthinfo). It is further estimated that 1 in 4 families have at least one family member suffering from some form of neurological disorder (World Health Organization, http://www.who.int/healthinfo). Despite the increasing number of affected individuals, some low income countries, in which neurological disorders seem to thrive due to adverse circumstances and malnutrition (World Health Organization, http://www.who.int/healthinfo), spend less than 1% of the countries health budget on mental health. These and many more daunting statistics highlight the increasing numbers of affected individuals, and the need for a better understanding of such debilitating disorders in order to develop better diagnostic methods and treatments.

Our laboratory has undertaken a keen interest in neuro-psychiatric disorders, particularly obsessive-compulsive disorder (OCD) and schizophrenia both of which are severely debilitating illnesses. Even though it is well known that both OCD and schizophrenia are multifactorial disorders in which both genetic and environmental factors play essential roles, their precise aetiologies remain relatively unknown. This is partly due to the intricacy of the human central nervous system as well as the complex nature of human behaviour. However, in recent years, several lines of evidence have emerged suggesting these disorders are, in part, caused by defects in neurodevelopment (Hyde *et al.,* 1992; Marenco and Weinberger, 2000; Rosenberg *et al.,* 1997; Weinberger, 1987) (section 1.5). Therefore in order to fully elucidate the intricate pathophysiologies of neurologic disorders such as OCD and schizophrenia, a clearer understanding of the processes involved in neurodevelopment may be helpful.

In an effort to gain a better understanding of the underlying mechanisms governing neurodevelopment, the present study sought to investigate some of the molecular mechanisms involved in this process. More

specifically, the focus of this investigation is the identification of novel molecular components involved in the development of the mammalian neocortex, as this highly evolved brain structure has been implicated in the pathogenesis of OCD, schizophrenia and several other devastating neurological disorders (Fish, 1957; Hyde *et al.,* 1992; Marenco and Weinberger, 2000; Rosenberg *et al.,* 1997; Watt, 1972; Weinberger, 1987). For this reason, the sections that follow will describe both cellular and molecular mechanisms involved in the development of the mammalian neocortex.

1.2 THE MAMMALIAN CEREBRAL CORTEX

The largest region of the mammalian forebrain is composed of cerebral hemispheres which make up the cerebral cortex. This specific region of the brain is highly convoluted to increase the surface area, and is responsible for numerous functions such spatial reasoning, sensory perception, generation of motor commands, and, in humans, for conscious thought, language and higher cognition (Figure 1.1) (Douglas and Martin, 2007; Kaas, 2000; Kaas, 2007). It is believed that the complexity of this brain region gives rise to its superior functions (Douglas and Martin, 2007; Herculano-Houzel *et al.,* 2007; Kaas, 2007). The newest evolved part of the cerebral cortex is a region known as the neocortex, this region is unique to mammals and differs greatly in appearance, size and convolutions between species, and in humans the neocortex occupies 90% of the cerebral cortex housing billions of neurons (Figure 1.1) (Douglas and Martin, 2007; Herculano-Houzel *et al.,* 2007; Kaas, 2007).

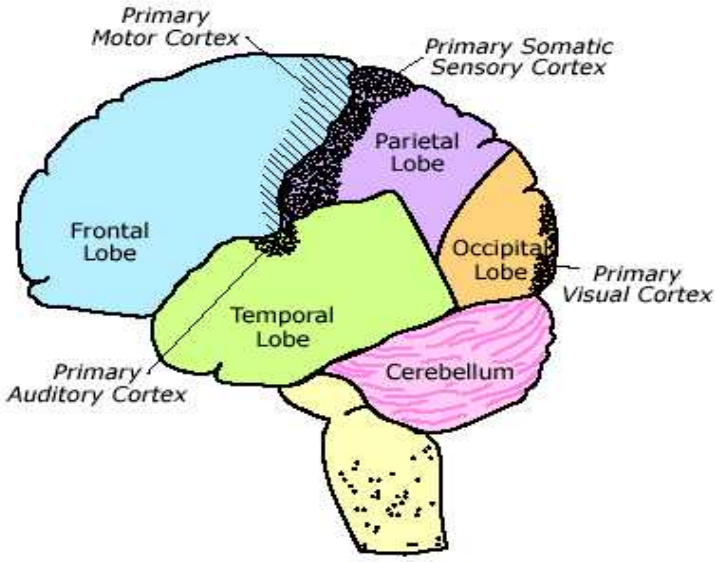

Figure 1.1. Regions within the mammalian brain. The mammalian neocortex in composed of the frontal lobe, the parietal lobe, the occipital lobe and the temporal lobe (Taken from, http://www.aphorgcviimagesbrain).

A striking feature of the mammalian neocortex, which contributes to its functional complexity, is its organization into six distinct neuronal layers (Gupta, 2002; Kriegstein *et al.,* 2006; Rakic, 1995). The development of such an organised and intricate structure is a highly complex process and requires a finely regulated molecular developmental programme (Couillard-Despres *et al.,* 2001). A crucial step in the development and lamination of the neocortex into these layers is the migration of neurons from their place of birth (in the ventricular zone) across an ever changing microenvironment to their final resting places within respective layers (Bielas *et al.,* 2004; Kriegstein *et al.,* 2006; Rakic, 1995). Another notable developmental characteristic of the mammalian neocortex is the inside-out arrangement of these six neuronal layers, in which later born neurons migrate past earlier born neurons (Aboitiz *et al.,* 2001). As the cortex matures and expands, this task becomes ever more challenging as the distances through which neurons must traverse increases. It is crucial that during development and lamination of this remarkably intricate brain structure that each neuron migrates and settles in its proper position. This is ultimately accomplished by cues from the surrounding extracellular matrix and neighbouring cells as well as the cytoskeletal machinery within neurons themselves (Couillard-Despres *et al.,* 2001).

1.3 DEVELOPMENT OF THE CEREBRAL CORTEX

The formation of the neocortex can be divided into three broad crucial steps: neuronal proliferation, neuronal migration, and cortical organization (Barkovich *et al.,* 2005; Geurrini *et al.,* 2008) (Figure 1.2). The sections that follow will briefly elaborate on each of these phases, with special emphasis on neuronal migration as anomalies in the different modes of migration result in several neurological disorders. Some of these disorders are caused by abnormal cortical lamination and irregular neuronal organisation due to anomalies in neuronal migration.

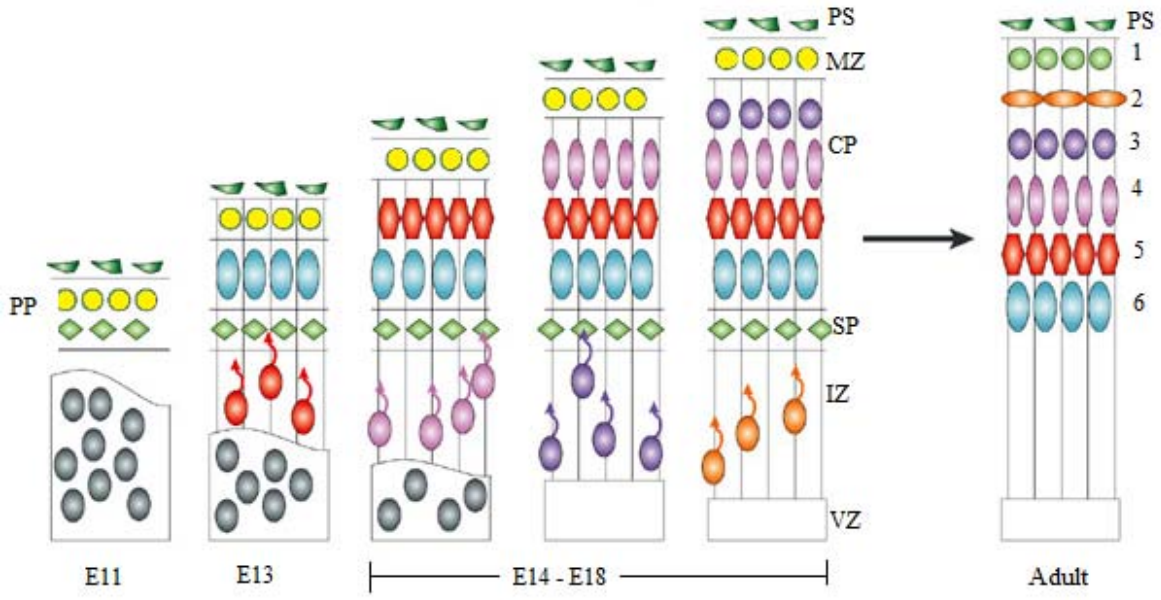

Figure 1.2. Mouse embryonic development of the neocortex. Embryonic cortical development results in the formation of a distinct six layered adult neocortex. First wave of postmitotic neurons migrate out of the ventricular zone (VZ) towards the pial surface (PS) via radial glial cells (vertical bars), this causes the preplate (PP) to be split into the marginal zone (MZ) containing the Cajal-Retzius cells (yellow) and the subplate (SP, green diamonds); creating the cortical plate (CP). Each successive wave of migrating neurons move through the intermediate zone (IZ) and expand the CP in an 'inside-out' fashion, as later born neurons bypass their earlier born predecessors and settle within the more superficial layers near the PS. In adulthood, the SP degenerates forming the characteristic laminar structure of the neocortex (Taken from Gupta *et al.,* 2002).

1.3.1 Cell proliferation

During the proliferation phase, neuronal stem cells proliferate and differentiate into either young neurons or glial cells deep within the ventricular zone (VZ) (Figure 1.2). During this stage a layer known as the preplate (PP) is formed above the proliferative VZ (Bielas *et al.,* 2004; Couillard-Despres *et al.,* 2001; Rickmann and Wolff, 1981) (Figure1.2). The preplate is composed of the first wave of postmitotic neurons to migrate out of the VZ (Bielas *et al.,* 2004), including the subplate neurons as well as the earliest generated Cajal-Retzius (CR) cells which run adjacent to the pial surface (Marin-Padilla, 1998) (Figure1.2).

1.3.2 Neuronal migration

The formation of the six layered neocortex is orchestrated by the extraordinarily ordered migration of postmitotic neurons from the VZ. The first migratory phase involves the movement of postmitotic neurons from the VZ, in an upward direction, towards the brain's pial surface, the surface closest to the membranous layer covering the brain under the skull (Bielas *et al.,* 2004; Kubo and Nakajima 2002). At this stage, a layer known as the preplate (PP) is formed (Bielas *et al.,* 2004; Couillard-Despres *et al.,* 2001; Rickmann and Wolff, 1981) (Figure1.2). Subsequently, a second set of postmitotic neurons migrate from the VZ, which move past their earlier born predecessors and split the preplate into the superficial marginal zone (MZ) and the subplate (Figure 1.2), creating an intermediate layer known as the cortical plate (CP) (Figure 1.2) (Bielas

et al., 2004; Couillard-Despres *et al.,* 2001; Kubo and Nakajima, 2002;). Following the creation of the cortical plate, sets of postmitotic neurons continue to migrate from the VZ, passing through the subplate to form the ordered layers of the cortical plate.

An autoradiographic study that dates the birth of migratory neurons in mice, showed that the layering of cortical plate neurons occur in an inside-out fashion, in which the earlier born neurons constitute the deeper cortical layers, while later born neurons migrate past the aforementioned neurons and form the more superficial cortical layers (Angevine *et al.,* 1961; Gupta *et al.,* 2002; Kubo and Nakajima 2002). Once the cortical plate has been formed, the subplate disintegrates leaving behind the characteristic six-layered neocortex. It is important to note that each wave of postmitotic neurons at some stage come in into contact with the MZ. The relevance of this is not yet properly understood, but it is postulated that an extracellular cue within the MZ containing the Cajal-Retzius cells is responsible for guiding migrating neurons to their correct final orientation within the inside out laminated neocortex (Bielas *et al.,* 2004).

The above mentioned model of neuronal migration is the widely accepted model that was first documented by the Boulder Committee in 1970 (Boulder Committee, 1970). However, several studies of mechanisms involved in neuronal migration has shown that this model is only applicable to pyramidal projection neurons, which are the excitatory glutamatergic neurons in the neocortex (Anderson *et al.,* 2002; Mione *et al.,* 1997; Parnavelas *et al.,* 2000; Tan *et al.,* 1998). In recent years, several investigations have demonstrated that GABA-containing inhibitory cortical interneurons, which are born in the ganglionic eminence (GE), follow a different mode of migration to their excitatory counterparts. Whereas pyramidal projection neurons migrate radially from the VZ towards the pial surface, cortical interneurons migrate from the GE, round the corticostriatal notch and follow tangentially orientated paths to enter the neocortex (Anderson *et al.,* 1997; 2002; Lavdas *et al.,* 1999; Wichterle *et al.,* 2001). Thus, two forms of neuronal migration have been identified to date and have been termed radial and tangential to denote the directions in which each the neurons migrate (Ayala *et al.,* 2007).

1.3.2.1 Radial migration

In a landmark electron microscopic investigation of the foetal monkey neocortex conducted in 1972, Rakic demonstrated that migrating neurons are intimately associated with radial glial fibers, which suggested that these glial fibers could act as scaffolds for neuronal migration (Kanatani *et al.,* 2005; Rakic, 1972). This notion was supported by more recent investigations which showed that radial fibers are present during neocortical development and that their radial processes extended the entire cortical wall (Mission *et al.,* 1991). It should be noted, however, that in a later microscopic investigation of early mouse neocortical slices, Shoumakimas and Hinds did not find a dependable association between glial fibers and migrating neurons, which suggested that during the early stages of neo-corticogenesis, neurons do not require radial glial fibers for migration (Shoumakimas and Hinds, 1978). Taken together, these studies suggested that there

are two modes of radial migration. Later, these were termed glial-guided locomotion and somal or nuclear translocation (Borrel *et al.,* 2006; Nadarajah *et al.,* 2003; Rakic, 2007).

Time lapse studies of mouse embryonic neocortices, conducted by Nadarajah and colleagues confirmed that each of these modes of radial migration occurred at different stages of development. At embryonic day E12-13 in mice, somal translocation was used to split the preplate, while glial-guided locomotion traversed neurons across the cortical plate at embryonic days E15-16 (Nadarajah *et al.,* 2003). Thus, it seems that during the early stages of corticogenesis, while the cortical wall is relatively thin (shorter distance), neurons migrate via somal translocation; whereas later during corticogenesis, as the cortical wall thickens and the distance to the pial surface increases, neurons migrate by glial-guided locomotion (Nadarajah and Parnavelas, 2002).

1.3.2.1.1 Somal translocation during early corticogenesis

During somal translocation, neurons extend a long radially directed leading process (Figure 1.3) with branched ends from the VZ, which terminates at the pial surface. This is followed by a short transient trailing process (Ayala *et al.,* 2007; Cooper, 2008; Gupta *et al.,* 2002; Kubo and Nakajima, 2002) (Figure 1.3). Since this type of migration is independent of the radial glial guides it is unaffected by the signalling cascades and molecular cues that regulate glial guided locomotion (Nadarajah and Parnavelas, 2002). The attachment of the leading process to the pial surface is followed by the ascendant movement of the cell body (including the nuclei), ultimately resulting in the shortening of the leading process overtime (Ayala *et al.,* 2007; Cooper, 2008; Gupta *et al.,* 2002; Kubo and Nakajima, 2002) (Figure 1.3). The driving force for this type of movement is not yet understood, although Miyata and colleagues believe that a spring-like mechanism (due to force generated in the stretching and twisting of the rising leading process) propels these neurons towards the pial surface (Miyata and Ogawa, 2007) (Figure 1.4). This mode of radial migration is smoother, faster and more continuous than glial-guided locomotion, essentially resulting in a faster mode of migration (Cooper, 2008; Nadarajah and Parnavelas, 2002).

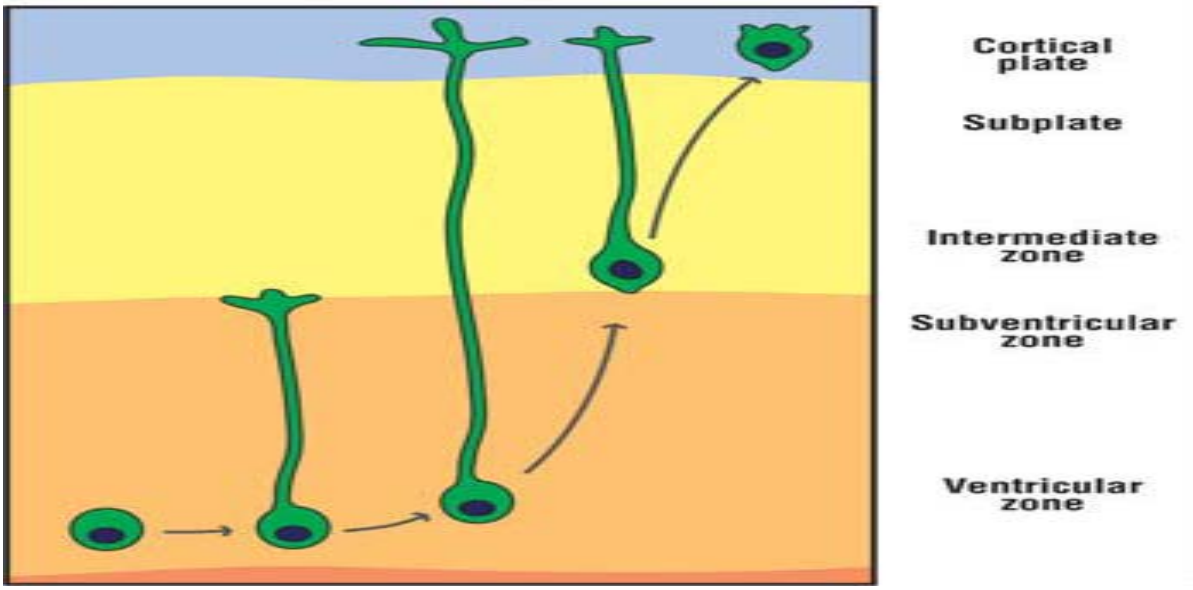

Figure 1.3. Somal translocation during early corticogenesis. Neuronal cells (green) extend a long branched leading process from the ventricular zone towards the pial surface; once implanted within the pial surface, the entire cell and cell body is retracted upwards shortening the leading process. This causes the neuronal cell to be moved or translocated to its' final position within the cortical plate (Taken from Bielas *et al.,* 2004).

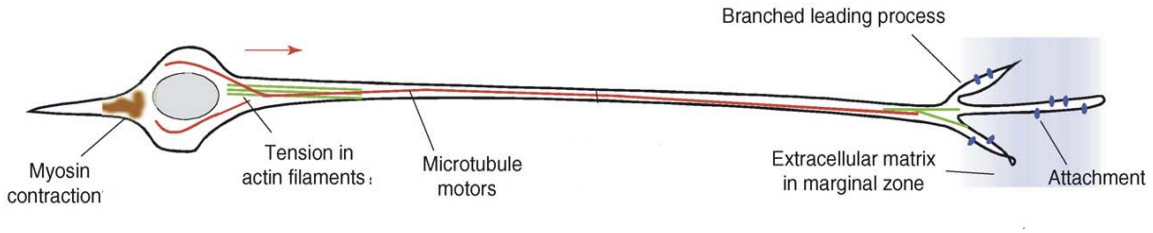

Figure 1.4. The cytoskeletal rearrangements that drive somal translocation. The leading process extends towards the pial surface; once attached to the pial surface cytoskeletal rearrangements are responsible for the retraction of the trailing process and the cell body containing the nucleus (Taken from Cooper, 2008).

1.3.2.1.2 Glial-guided locomotion during the later stages of corticogenesis

As the thickness of the cortical plate increases with each successive wave of migrating neurons, neurons change their mode of migration from somal translocation to glial-guided locomotion, a mode of migration characterized by the use of radial glia as guidance tracks (Couillard-Despres *et al.,* 2001; Kanatani *et al.,* 2005; Nadarajah *et al.,* 2003). During glial-guided migration, locomoting neurons are not attached to the pial surface; instead these neurons migrate up towards the MZ via radial glial guides which are anchored in the MZ. These neurons maintain a shorter, unbranched, freely motile leading process. Both the leading edge and cell soma move together along the radial glial fiber via a repetitive cycle of events (Guota *et al.,* 2002; Nadarajah *et al.,* 2001; Nadarajah *et al.,* 2003). Each cycle involves the extension of the leading edge which results in the nucleus moving forward. The trailing process is then retracted and the cell migrates due to the mechanical strain within the cell and the release of adhesive contacts at the trailing process (Cooper, 2007; Nadarajah *et al.,* 2001). This cycle is then repeated (Cooper, 2007; Nadarajah *et al.,* 2001) (Figure 1.5).

Attachment of migrating neurons to the radial glial involves integrins and gap junctions. These interactions allow the cell body to squeeze and manoeuvre through the cortex as the cellular density increase throughout corticogenesis (Cooper, 2007) (Figure 1.6). This mode of migration is characteristically slow and jerky, with short bursts of forward movement intermingled with stationary/paused phases (Cooper, 2007; Nadarajah and Parnavelas, 2002).

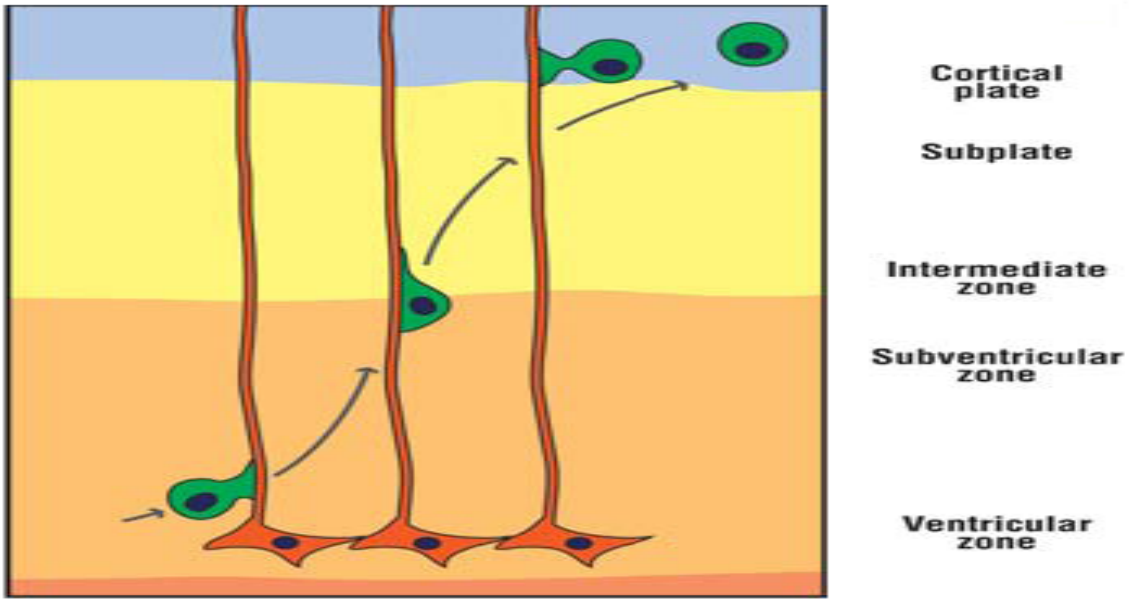

Figure 1.5. Glial guided locomotion during later stages of corticogenesis. Migrating neurons (green) use radial glial fibers (orange) as guidance tracts to reach their final destinations within the cortical plate. These radial glial tracts are anchored in the ventricular zone and extend to the pial surface (Taken from Bielas *et al.,* 2004).

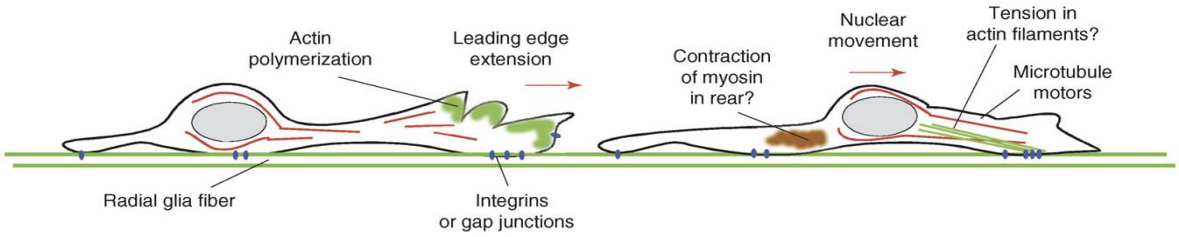

Figure 1.6 The cytoskeletal rearrangements during glial guided locomotion. Migrating neurons attach via integrins and/or gap junctions to the radial glial fibers (green); cytoskeletal rearrangements move the migrating cell up along the radial glial fiber until its' correct position within the cortical plate is reached (Taken from Cooper, 2008).

Importantly neither of the two types of radial migration are cell-type specific (Ayala *et al.,* 2007). As neurons migrate towards the pial surface they dynamically change their morphology and mode of migration (Honda *et al.,* 2003; Kubo and Nakajima, 2002). Nadarajah and colleagues noted that glial guided locomoting cells switch to somal translocation in the final stages of their migration as the leading edge approaches the pial surface (Nadarajah *et al.,* 2001). They showed that at embryonic day 15-16 in mice,

previously generated neurons have already split the PP and the CP is rapidly expanding. During this period glial-guided locomotion is the dominant form of migration, although somal translocation is simultaneously occurring in the upper half of the developing neocortex (Gupta *et al.,* 2002). As development continues, the cortical wall thickens and neurons cannot translocate the full width of the neocortex; thus neurons first migrate via locomotion and then switch to somal translocation once they have moved far enough through the neocortex to attach their leading process to the pial surface (Gupta *et al.,* 2002; Nadarajah *et al.,* 2001). Neuroanatomical studies of the inverted laminar organisation of the mammalian neocortex have shown that the first neurons to arrive in the cortex are phylogenetically the oldest, whereas later born cortical neurons are a more recent evolutionary addition (Marin-Padilla, 1978; Goffinet, 1983). Thus, it was postulated that somal translocation is an earlier evolutionary mode of neuronal migration (used to migrate neurons across shorter cortical distances), whereas glial-guided locomotion evolved to migrate and guide neurons across greater cortical distances (more convoluted, hence more complex cortical organisation) (Rakic, 1972; Nadarajah *et al.,* 2001).

1.3.2.2 Tangential migration

In contrast to earlier investigations that only pointed to radial migration as the mode of migration adopted by cortical neurons, several *in vitro* and *in vivo* studies have provided clear evidence for non-radial migratory routes taken by cortical interneurons (Anderson *et al.,* 1997; Mione *et al.,* 1997; Sussman *et al.,* 1999; Walsh and Cepko, 1993). These neurons were found to migrate tangentially across the plain of the glial fibres. Furthermore, recent investigations have shown that most cortical interneurons originate in the primordia of the basal ganglial- the lateral, medial and caudal ganglionic eminences (LGE, MGE and CGE, respectively) and subsequently migrate to the cortex (de Carlos *et al.,* 1996; Ware *et al.,* 1999). In rodents and in humans, the primary source of interneurons is the MGE (Anderson *et al.,* 2001; Lavidas *et al.,* 1999; Polleux *et al.,* 2002; Wichterle *et al.,* 1999, 2001), however, in humans, a significant amount of cortical interneurons have been shown to originate from progenitors in the cortical sub-ventricular zone (SVZ) (Lectinic *et al.,* 2002; Rakic and Zecevic, 2003).

During cortical development, the first waves of tangentially migrating interneurons are mostly found in the lower intermediate zone (IZ) and SVZ and also in the MZ and subplate (Anderon *et al.,* 2001; Ang *et al.,* 2003; Lavdas *et al.,* 1999; Tanaka *et al.,* 2003; Wichterle *et al.*, 1999). Several investigation have been undertaken to elucidate the migratory paths of these interneurons from the MGE to the cortex. These include studies in which MGE neurons were fluorescently labelled and subsequently cultured *in vitro* (Anderson *et al.,* 2001; de Carlos *et al.,* 1996; Nadarajah *et al.,* 2002; Lavdas *et al.*, 1999; Tamamaki *et al.,* 1997), studies of transgenic animals (Anderson *et al.,* 1997; Casarosa *et al.,* 1999; Sussel *et al.,* 1999) and studies of tagged transplanted tissues (Anderson *et al.,* 2001; Nery *et al.,* 2002; Polleux *et al.,* 2002; Wichterle *et al.,* 2001). However, a recent investigation that made use of real time imaging of green fluorescent protein- labelled glutamate decarboxylase 67 (Gad67-GFP) has provided researchers with a more accurate picture. In their

study, Tanaka and co-workers used Gad67-GFP knock in embryonic mice and showed that the migration of cortical interneurons primarily occur in two streams, in the cortical MZ and in the IV-SVZ (Tanaka *et al.,* 2003). Once interneurons enter the cerebral cortex, they migrate tangentially and then enter the cortical plate by changing their orientation and migrating radially to their final positions (Tanaka *et al.,* 2003) (Figure 1.7). Interneurons migrating tangentially from the IV-SVZ have been shown to turn and migrate radially, or even obliquely, in order to enter the cortical plate from the bottom (Figure 1.7b) (Ang *et al.,* 2003; Nadarajah *et al.,* 2002; Polleux *et al.,* Tanaka *et al.,* 2003), while interneurons migrating tangentially in the MZ have been shown to enter the cortical plate from above (Figure 1.7b) (Ang *et al.*, 2003; Tanaka *et al.*, 2003).

Several lines of evidence have suggested that tangentially migrating interneurons make use of corticofugal fibres as scaffolds for their migration (Anderson *et al.,* 2001; Denaxa *et al.,* 2001; Lavdas *et al.,* 1999), while a functional association between these interneurons and radial glial has also been suggested (Polleux *et al.,* 2002). This possible association between interneurons and radial glial was further investigated in a study by Yokota and co-workers (Yukako *et al.,* 2007). Since previous investigation showed that tangentially migrating interneurons eventually switches to radial migration, these investigators sought to determine what influence, if any, the radial glial grid exerts on the migration of interneurons in the developing cortex. In their investigation, they made use of transgenic mice which were engineered so that only GE-derived neurons were tagged with green fluorescent protein (GFP), while radial glial were tagged with a red fluorescent protein (RFP). They further monitored the interneuronal migration *in utero* in developing embryos using two-photon microscopy. These studies revealed that once tangential migrating interneurons switch to radial migration, they potentially make use of radial glial fibers (Yokota *et al.,* 2007). It therefore seems that interneurons first migrate tangentially from the MGE, making use of corticofugal fibers, to the MZ or the IZ-SVZ where they switch to glial-guided radial migration in order to be incorporated into the developing neocortex. It is important to note that radial and tangential migration takes place simultaneously.

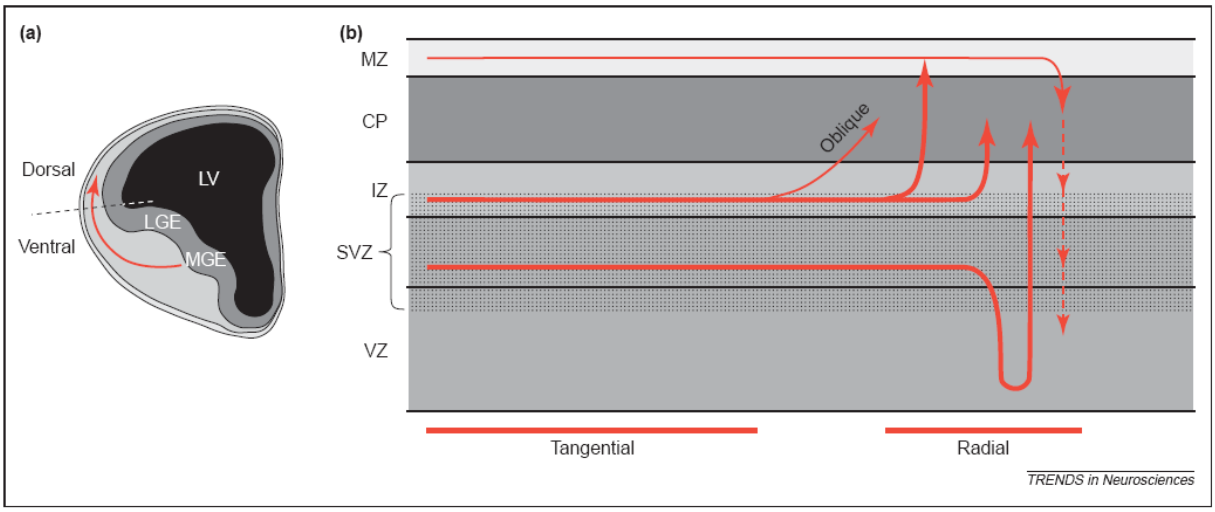

Figure 1.7. Tangential migrating cortical interneurons arising from the medial ganglionic eminence. (a) Cortical interneurons born in the ganglionic emenences migrate tangentially (red arrow) around the cortical notch to the developing cortex. **(b)** Cortical interneurons migrate tangentially within the cortex and subsequently change direction in order to enter the cortical plate. The solid red arrows indicate the path travelled by the cortical interneurons, while the broken red arrow shows that some cortical interneurons have been found to descend radially from the marginal zone into the cortical plate and others continue radially into the deeper cortical layers. Abbreviations: IZ, intermediate zone, LGE, lateral ganglionic eminence, LV, lateral ventricle; MGE, medial ganglionic eminence; MZ, marginal zone; SVZ, subventricular zone, VZ, ventricular zone. (Taken from Kriegstein and Noctor, 2004).

Thus neuronal migration is extremely important in the formation of a complex structure such as the cortex. The correct laminar organization of neurons allows neurons to generate the appropriate synaptic connectivity characteristic of each neuronal layer (Dulabon *et al.,* 2000). Several molecules play essential roles in controlling and regulating neuronal migration, including intracellular and extracellular cues, molecules of the cytoskeleton, and signalling molecules all of which ensure neurons arrive at their proper final positions within the cortex, allowing it to function in all its complexity. Having outlined the basic migratory pathways involved in the development of the neocortex, one now needs to consider the underlying molecular mechanisms that control this process. Several investigations focusing on the molecular control of neuronal migration have uncovered a number of mechanisms that control this process. However, since the present investigation primarily focuses on further unravelling the Reelin signalling pathway, only the Reelin signalling pathway will be reviewed.

1.3.2.3 Reelin signalling pathway and neuronal migration

Unravelling the molecular mechanisms involved in cortical development in humans is very challenging due to the complexity of the cerebral cortex and the numerous genes and their related protein products involved in its regulation. Both of these factors make identifying and understanding genes and proteins involved in the development of the cortex quite a daunting task. This task has been made slightly less arduous by studying neurodevelopmental disorders in naturally occurring and transgenic animal models (D'Arcangelo and Curran, 1998; Gupta *et al.,* 2002). The mouse cerebral cortex lacks gyri, thus serves as the perfect model for studying and examining cortical malformations resulting from aberrant neuronal migration. Several mouse

mutants exhibiting abnormal neuronal migration resulting in cortical malformations have been indentified (D'Arcangelo and Curran, 1998), however, it was the discovery of the naturally occurring *reeler* mouse that has provided researchers with a perfect entry point for studying neuronal migration (Park *et al.,* 2007).

1.3.2.3.1 The spontaneous neurological mutant mouse *reeler* – An animal model for schizophrenia

The *reeler* mouse arose spontaneously in 1948 in a stock of 'snowy-bellied' mice at the Institute of Animal Genetics in Edinburgh, Scotland (D'Aracangelo and Curran, 1998; Rice and Curran, 2001). Since its discovery, the *reeler* mouse has been used for several years as an important experimental model to investigate neurological mutations which affect neuronal migration and hence organisation of the central nervous system (CNS) (Rice and Curran, 1999). This behavioural mutant has characteristic neuroanatomical anomalies in the cerebral cortex, cerebellum and hippocampus; suggesting the genes mutated in the *reeler* phenotype are crucial for regulating neuronal positioning in the developing CNS (Caviness *et al.,* 1988; Rice and Curran, 2001). The *reeler* phenotype is characterized by loss of cellular organisation resulting in severe hypoplasia of the cerebellum, which ultimately causes the ataxic phenotype characterised by tremors, dystonia and a reeling gate (hence the name *reeler* phenotype) (D'Arcangelo, 2006).

Neuroanatomically, the homozygous *reeler* mouse shows an inversion of the normal 'inside-out' lamination of the cerebral cortex, accompanied with an accumulation of neurons in the normally cell sparse marginal zone (Caviness and Rakic 1978; Gleeson and Walsh, 2000) (Figure 1.8). Thus, in the *reeler* mouse cortex, neurons are produced and proliferate normally, but fail to migrate to their correct final positions within the developing neocortex, causing an outside-in manner of lamination (Cooper, 2008; Goffinett, 1979; Nadarajah and Parnavelas, 2002) (Figure 1.8). In addition to the layering and organisational defects of the *reeler* cortex, it was found that postmigratory neurons in the cortex remain closely associated with their radial glia fibers and that during the later stages of corticogenesis, the radial glia scaffold are deployed at oblique angles instead of their normal vertical orientation (Hunter-Schaedle, 1997; Mikoshiba *et al.,* 1983; Pinto-Lord, 1982; Rice and Curran, 2001). Moreover, during the early stages of development, Reelin-deficient neurons are unable to split the preplate, while later during development, glial-guided neurons are unable to migrate past one another (Ayala *et al.,* 2007).

In contrast, the heterozygous *reeler* mouse (HRM) does not show the severe cortical layering defects as the homozygous *reeler* mouse, although they do show subtle neurochemical, neuropathological and behavioural abnormalities that are characteristic in schizophrenia (Ognibene *et al.,* 2007 a, b ; Tueting *et al.,* 1999). Hence, the HRM serves as a good animal model to investigate the complex interactions between genetic vulnerability and environmental factors in the pathogenesis and aetiology of schizophrenia (Lavialo *et al.,* 2008; Tordjman *et al.,* 2007).

In 1995, D' Arcangelo and colleagues identified a mutation in the gene encoding Reelin, an extracellular matrix glycoprotein as being the cause for the *reeler* phenotype in the *reeler* mouse (D'Arcangelo *et al.,* 1995). Since then, several investigations have been undertaken to evaluate the role the Reelin protein plays in neuronal migration.

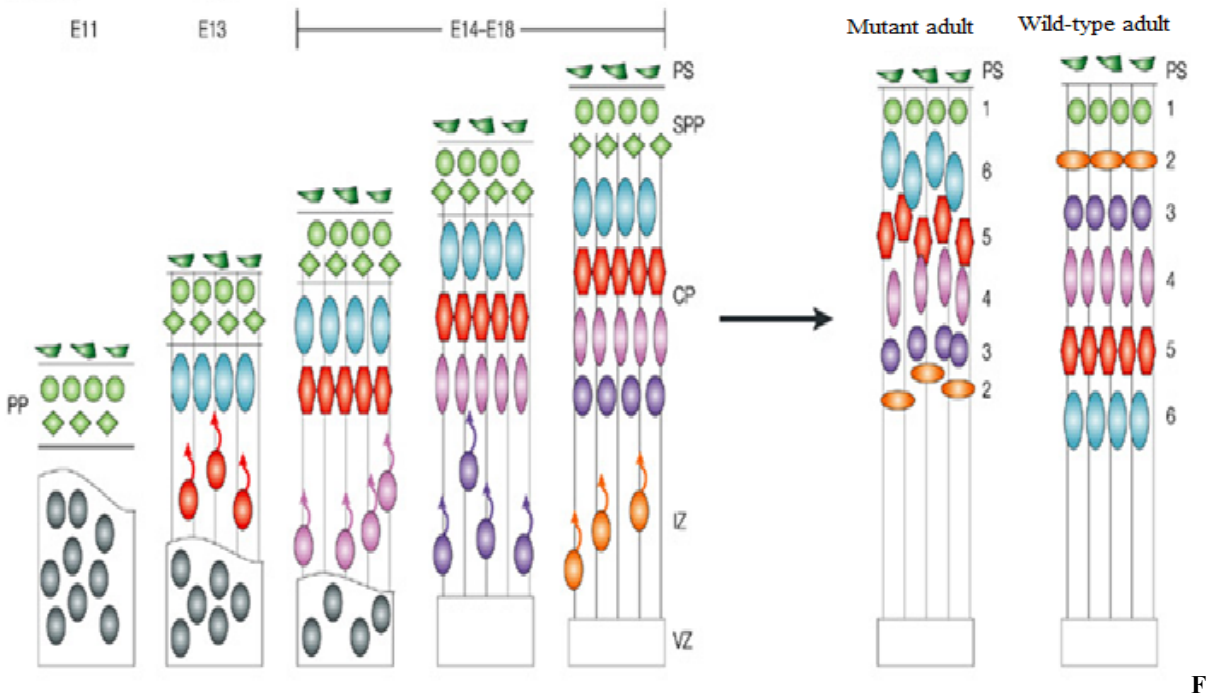

F

Figure 1.8. Cyto-architectural abnormalities in the *reeler* mouse. In the *reeler* cortex, the preplate forms normally with the exception that the first cohort of early-born migrating neurons are unable to split the preplate due to the absence of Reelin; thus the subplate remains adjacent to the marginal zone forming a 'superplate' (SPP, a cell dense area containing the Cajal-Retzius cells, subplate neurons and few cortical plate neurons). The cortical plate then forms underneath the 'superplate', as later generated neurons are not able to migrate past their earlier born predecessors which leads to the formation of a disorganised and inverted (outside-in) cortical plate as neurons are not able to arrange themselves into distinct neuronal layers (Taken from Gupta *et al.,* 2002).

1.3.2.3.2 Reelin glycoprotein

Reelin is a 388kDa extracellular matrix glycoprotein (D' Arcangelo *et al.,* 1995) secreted in the MZ (Ogawa *et al.,* 1995). In humans, the gene encoding Reelin has been localised to chromosome 7 (DeSilva *et al.,* 1997) and is highly conserved in a number of vertebrate species (Rice and Curran 1999).

The Reelin protein is comprised of 3461 amino acid residues that are arranged into a number of domains (Figure 1.9). The amino-terminal domain of Reelin contains a cleavable signal peptide trailed by a small region (reeler domain) which shares similarity with F-spondin (a protein which directs neuronal crest cell migration) (Klar *et al.,* 1992) (Figure 1.9). The carboxy terminus contains a sequence of eight internal Reelin repeats of 350-390 amino acids, followed by 33 positively charged amino acids (Kubo and Nakajima, 2002; Rice and Curran, 2001). Each Reelin repeat is composed of two related sub-repeats which flank a pattern of conserved cysteine residues known as EGF (epidermal growth factor) like motifs (De Bergeyck *et al.,* 1998) (Figure 1.9).

During the development of the cerebral cortex, Reelin is synthesized and secreted primarily by the transient Cajal-Retzius cells found in MZ even before the first wave of postmitotic neurons reach the preplate and is first detected at embryonic day 10 in mice (D'Arcangelo, 1995; Hirotsune *et al.,* 1995; Schiffman *et al.,* 1997). Reelin expression is highest during the early stages of cortical development and can already be detected in humans in the eleventh week of gestation (Deguchi *et al.,* 2003; Meyer and Goffinet, 1998).

The expression of Reelin is maintained in the postnatal and adult cortex, despite the fact that corticogenesis is completed and most of the Cajal-Retzius cells have disappeared (D'Arcangelo 2006). In the postnatal cortex, GABAergic interneurons continue to express Reelin into adulthood, although at significantly lower concentrations (Alcantara *et al.,* 1998; Pesold *et al.,* 1998; Super *et al.,* 1998). It has been shown that the Reelin protein is crucial during neuronal migration, where it is involved in cortical lamination and synapse formation (Guidotti *et al.,* 2000; Toro and Deakin, 2006); while during adulthood it is thought be involved in the adaption and maintenance of neurotransmission, synaptic plasticity, memory formation and neurogenesis (Alcantara *et al.,* 1998; Guidotti *et al.,* 2000; Toro and Deakin 2006).

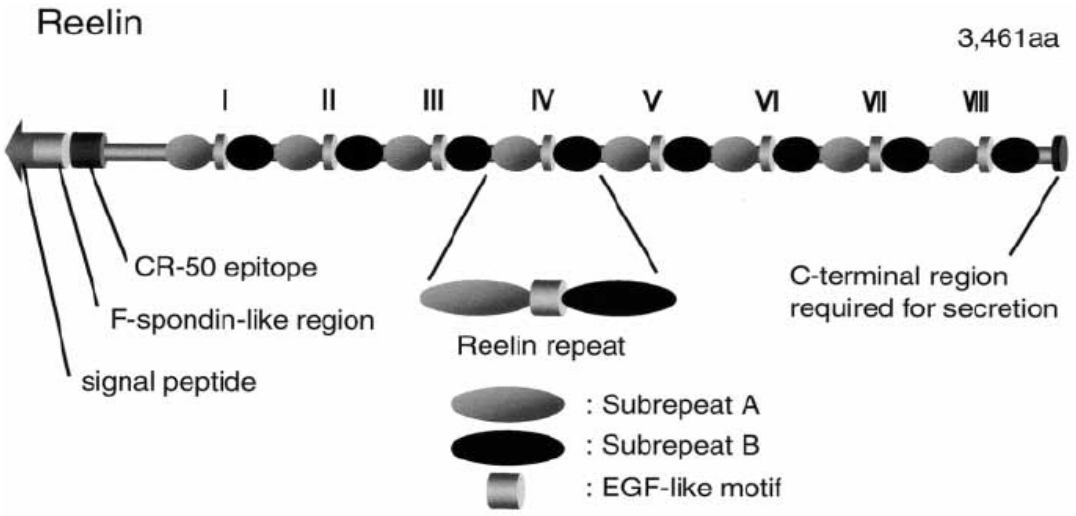

Figure 1.9. Schematic representation of the Reelin structure. The open reading frame predicts a secreted extracellular matrix glycoprotein of 3641 amino acids with a relative molecular mass of 388kDa. At the N terminal Reelin contains a cleavable signal peptide, followed by a region with 25% identity to that of F-spondin (controls cell migration and neurite outgrowth). This is followed by the characteristic presence of a series of eight internal Reelin repeats, each repeat is composed of 350-390 amino acids and is composed of two related subrepeats A and B, which are separated by an EGF-like motif. The epitope for the CR-50 antibody is located upstream of the Reelin repeats; oncebound, this antibody blocks the Reelin-induced kinase cascade both *in vitro* and *in vivo*. The C-terminal is an area rich in arginine residues, which are required for Reelin secretion from the Cajal-Retzius cells during corticogenesis (Taken from Kubo and Nakajima, 2002; Rice and Curran, 2001).

1.3.2.3.3 Reelin signalling pathway

Reelin was the first protein to be identified in the molecular signalling pathway that co-ordinates neuronal migration and cortical lamination. Since Reelin is a secreted extracellular matrix glycoprotein, receptors are crucial for it to relay its guidance effect to migrating neurons. A combination of independent genetic and

biochemical studies (D'Arcangelo *et al.,* 1999; D'Arcangelo *et al.,* 1995; Gotthardt *et al.,* 2000; Heisberger *et al.,* 1999; Hirotsune *et al.,* 1995; Howell *et al.,* 1997; Howell *et al.,* 1999; Trommsdorff *et al.,* 1998; Trommsdorff *et al.,* 1999; Sheldon *et al.,* 1997; Stolt *et al.,* 2003; Yun *et al.,* 2003) from several investigators has established a linear signalling pathway for Reelin (Herz and Chen, 2006) (Figure 1.10).

Reelin binds to the extracellular domains of two high affinity transmembrane receptors which belong to the lipoprotein receptor superfamily. These are the apolipoprotein E receptor 2 (ApoER2) and the very low density lipoprotein receptor (VLDLR) (D'Arcangelo *et al.,* 1999; Heisberger *et al.,* 1999) (Figure 1.10). Both receptors are located on the surface of migrating neurons and are expressed at high levels throughout the brain during cortical development (Kim *et al.,* 1996; Trommsdorff *et al.,* 1999). Interestingly, VLDLR and ApoER2 double knock-out mice were found to exhibit *reeler*-like abnormalities, although each has distinct roles in regulating migration (as each binds to different sets of cytoplasmic proteins): ApoER2 is believed to promote the migration of later born cortical neurons, whereas VLDLR may act as a stop signal for migrating neurons (Hack et al., 2007; Huang, 2009) This observation provided the first concrete evidence for their involvement in the Reelin signalling pathway (Trommsdorff *et al.,* 1999).

The cytoplasmic tails of VLDLR and ApoER2 contain an unphosphorylated NPxY (N, asparagine; P, proline; x, any amino acid; Y, tyrosine) motif which binds to the phosphotyrosine binding (PTB) domain of the intracellular protein Disabled-1 (Dab1) (Howell *et al.,* 1999) (Figure 1.10). Dab 1 is a cytosolic adaptor protein which is highly expressed during development in Reelin target cells (migrating neurons) (Howell *et al.,* 19997a; Sheldon *et al.,* 1997). The importance of Dab1 in the Reelin signalling pathway is highlighted in Dab1 deficient mice, who exhibit a *reeler* phenotype where the preplate does not split into the normal distinct cortical layers (Howell *et al.,* 1997b; Sheldon *et al.,* 1999). In *reeler* mice, Dab1 is expressed normally, but accumulates in a hypophosphorylated state, suggesting that Reelin is crucial for Dab1 phosphorylation, turn over and degradation (Rice *et al.,* 1998; Sheldon *et al.,* 1999).

Even though VLDLR and ApoER2 possess no intrinsic kinase activity, binding of Reelin to these transmembrane receptors results in the tyrosine phosphorylation of Dab1 (Howell *et al.,* 1997a) (Figure 1.10). Several independent investigations have shown that Dab1 phosphorylation is reliant on the clustering of the VLDLR and ApoER2 receptors induced by the binding of oligomeric Reelin. Binding of monomeric Reelin to both these receptors is unable to phosphorylate Dab1 and thus unable to transduce the Reelin signal (Herz and Chen, 2006; Mayer *et al.,* 2006; Riddle *et al.,* 2001; Strasser *et al.,* 2004) (Figure 1.10).

Recent studies have further shown that Dab1 phosphorylation is mediated through the recruitment of SRC family tyrosine kinases (SFKs), such as Fyn and Src (Ballif *et al.,* 2003; Pawson and Scott, 1997; Schillace and Scott, 1999). These investigations found that receptor clustering is crucial for the recruitment of these SFKs (Figure 1.10). Thus, the binding of Reelin to VLDLR and ApoER, triggers receptor clustering, which

recruits SFKs, resulting in the transphoshorylation of Dab1 and subsequent recruitment and activation of additional non-receptor tyrosine kinases (Arnaud *et al.,* 2003; Bock and Herz, 2003). Moreover, Dab1 and SFKs were shown to mutually activate one another upon binding of Reelin to its receptors (Bock and Herz, 2003; Utsunomiya *et al.,* 2000) (Figure 1.10).

The ensuing high concentration of active SFKs initiates the downstream cytosolic kinase cascade which relays the Reelin signal (Herz and Chen, 2006). Phosphorylated Dab1 not only relays the Reelin signal to intracellular effectors, but has also been shown to interact and bind to Lis1 (Assadi *et al.,* 2003), which links the Reelin pathway to microtubule dynamics, as Lis1 interacts with the microtubule-associated cytoplamsic dynein/dynactin-motor complex (Niethammer *et al.,* 2000) (Figure 1.10).

After Reelin binding to its receptors and Dab1 phosphorylation, the Reelin signalling pathway activates phosphatidylinositol 3-kinase (PI3K) and serine/threonine protein kinase B (PKB, also known as Akt), as well as the inactivation and activation of glycogen synthase kinase 3 beta (GSK3β) within neuronal growth cones (Ballif *et al.,* 2003; Beffert *et al.,* 2002; Feng and Cooper, 2008). This Reelin-mediated activation of PI3K is dependent on phosphorylated Dab1 which physically interacts with the regulatory subunit of PI3K, p85 (Bock *et al.,* 2003). The activation of PKB stimulates mammalian target of rapamycin (mTor) (Chiang and Abraham, 2005; Holz and Blenis, 2005; Jossin and Goffinet, 2007).

The effects of Reelin on GSK3β are context-dependent (depending on which microtubule-associated protein is being regulated). Reelin induces the serine phosphorylation of GSK3β, inhibiting its activity, which results in the hypophosphorylation of the microtubule-associated protein tau (Beffert *et al.,* 2004; Hiesberger *et al.,* 1999) (Figure 1.10). Phosphorylation of tau reduces its microtubule assembly-promoting effect, thus phosphorylated tau is unable to stabilize the microtubule network (Dreschel *et al.,* 1992). It has also been observed that tau is hyperphosphorylated in the *reeler* mouse (Beffert *et al.,* 2004; Hiesberger *et al.,* 1999). Moreover, this hyperphosphorylated tau has been found to induce microtubule disassociation (Hardy *et al.,* 1998), which suggests that one function of Reelin is to regulate the phosphorylation (hence activity) of tau and so maintains the microtubule dynamics within neuronal growth cones (Beffert *et al.,* 2004; Heisberger *et al.,* 1999). Additionally, Reelin can also induce the activation of GSK3β (via tyrosine phosphorylation) and cyclin-dependent kinase 5 (cdk5), resulting in the phosphorylation of microtubule-associated protein 1 B (MAP1B). Phosphorylation of MAP1B reduces its ability to bind to the microtubule lattice (Gonzalez-Billault *et al.,* 2005) (Figure 1.10). These studies show that Reelin has opposing phosphorylation effects on MAP1B and tau, suggesting that the cytoskeletal regulation by Reelin through phosphorylation is highly dynamic and depends on the cellular compartment and the needs of the migrating neuron.

In addition to the phosphorylation of Dab1 upon Reelin binding to VLDLR, Reelin is also internalized into intracellular vesicles of neurons (D'Arcangelo *et al.,* 1999) via clatherin-dependent endocytosis (Herz and Bock, 2002). The precise reason for the internalization of Reelin remains unknown.

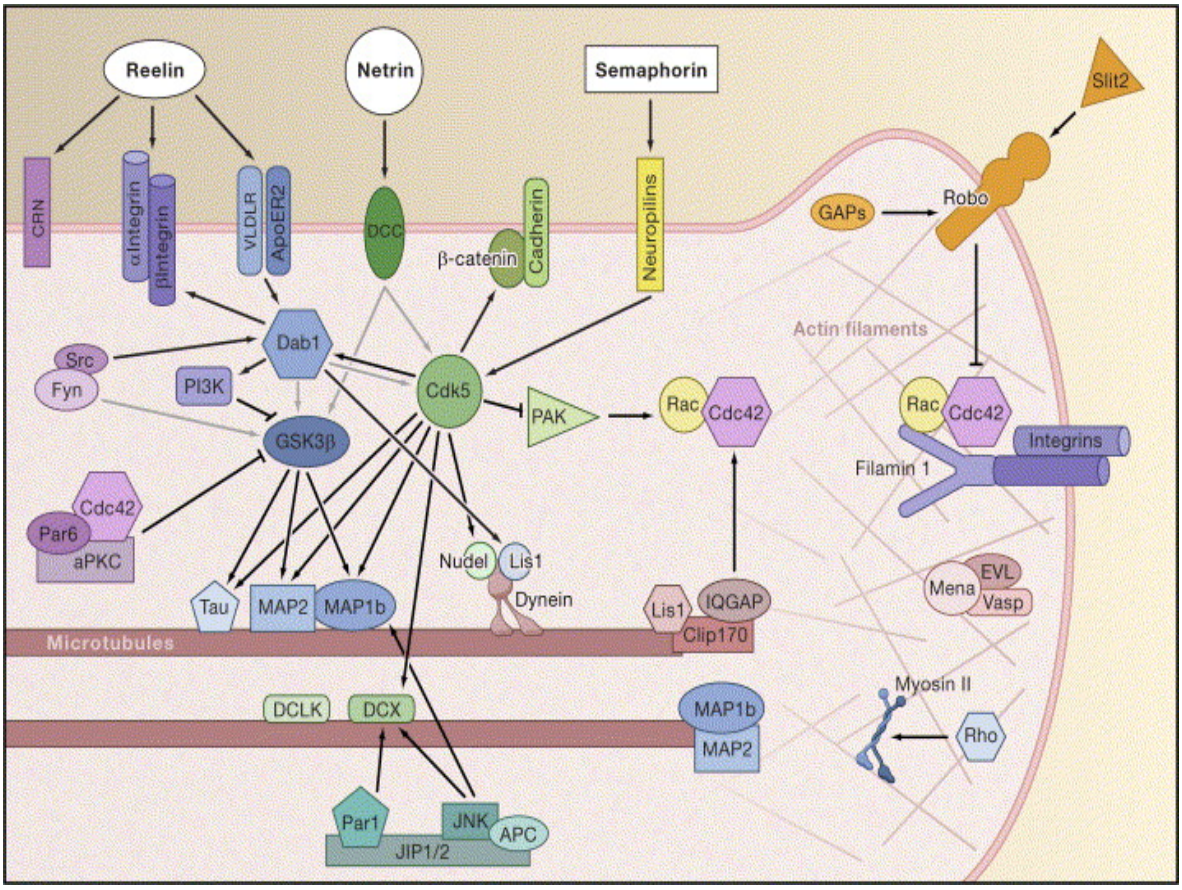

Figure 1.10. Molecular signalling networks regulating neuronal migration. Extracellular guidance cues, growth factors and adhesion molecules trigger a wide range of intracellular signalling cascades which ultimately end in the coordinated regulation of cytoskeletal dynamics. The Reelin signalling pathway is well characterized and explained in the literature above (Taken from Ayala *et al.,* 2007).

Other Reelin receptors have also been identified. These include members of the cadherin-related neuronal receptors (CNRs) (Senzaki *et al.,* 1999) and members of the integrin family of adhesion proteins (Dulabon *et al.,* 2000). The precise role of integrins as coreceptors for Reelin remains highly controversial, as conflicting results have been obtained to date. Integrins are transmembrane receptors which link the extracellular matrix to the cytoskeleton and, in neurons; they play a fundamental role in cell migration and adhesion (Andressen *et al.,* 1998; DeFreitas *et al.,* 1995; Fishman and Hatten, 1993; Georges-Labouesse *et al.,* 1998; Zhang and Galileo, 1998). Dulabon and colleagues demonstrated an interaction between Reelin and α3β1 integrin (Dulabon *et al.,* 2000). This interaction was shown to inhibit the adhesive properties of α3β1 integrin, thereby initiating the detachment of migrating neurons from their radial glial tracts which is believed to stop glial guided neuronal migration (Dulabon *et al.,* 2000). These findings were subsequently confirmed in two further independent investigations (Sanada *et al.,* 2004; Schmid *et al.,* 2004; Schmid *et al.,* 2005).

As appealing as this model for Reelin's action in controlling neuronal migration and cortical lamination may seem, it is not supported by genetic studies on α3β1 integrin (Fassler and Meyer, 1995, Magdaleno and Curran, 2001). In α3β1 integrin null mutant mice, radial glial cells adopt normal and appropriate positions, although complications and defects arise once the fibers reach the basement membrane as the endfeet (anchoring ends of migrating neurons) fail to form normally (Fassler and Meyer, 1995; Magdaleno and Curran, 2001). This has led to an alternative hypothesis in which Reelin exerts its effect, in part, by regulating the development of the radial glial scaffold via the interaction with α3β1 integrin which also regulates interactions among Cajal-Retzius cells, the extracellular matrix and the glial endfeet (Fassler and Meyer, 1995; Forster *et al.,* 2002; Magdaleno and Curran, 2001). More recently Belvindrah and co-workers showed that α3β1 integrins in migrating neurons is not essential for the arrangement of cell layers within the neocortex, although the expression of α3β1 integrins on radial glial themselves are critical for the formation of neocortical layers (Belvindrah *et al.,* 2007). Additionally they also reported that other receptors such as connexins regulate neuronal migration. Elias and colleagues also showed that connexion 26 and 43 are expressed at the contact points between radial glial fibers and migrating neurons providing dynamic adhesion points (Belvindrah *et al.,* 2007; Elias *et al.,* 2007). With all the controversial data surrounding the interaction between Reelin and α3β1 integrin, the precise role of this receptor in neuronal migration remains unclear.

As in any signal transduction pathway, inhibition or down-regulation of the initial stimulus is an essential component of the pathway as this prevents desensitization and allows the system to reset in preparation for the next stimulus (Arnaud *et al.,* 2003, Koshland, 1981). The precise mechanism in which the Reelin signal is down-regulated is still unclear, although inhibition of this signal seems to be important since migrating neurons respond differently to Reelin stimulation at different times during the history of the cell in development (Arnaud *et al.,* 2003).

One mechanism for the down-regulation of Reelin signalling involves the Reelin-dependent down-regulation of Dab1 (Arnaud *et al.,* 2003; Howell *et al.,* 1999; Rice *et al.,* 1998; Sheldon *et al.,* 1997). Arnaud and colleagues reported that tyrosine-phosphorylated Dab1 is targeted for polyubiquitination and degraded via the proteasome pathway (Arnaud *et al.,* 2003). Since Dab1 is the only component of the Reelin pathway to be down regulated (in response to Reelin induced phosphorylation), Dab1 is thus considered the primary mechanism for desensitization of the Reelin pathway in migration neurons (Arnaud *et al.,* 2003; Bock *et al.,* 2004). More recently, Feng and co workers showed that Dab1 down-regulation is mediated by Cullin5 (Cul5 (Feng *et al.,* 2007), a key component of the E3 ubiquitin ligase complex (Ilangumaran *et al.,* 2004; Petroski and Deshaies, 2005). They showed that in Cul5 knockdown mice, phosphorylated Dab1 is up-regulated, resulting in cortical lamination abnormalities (Feng *et al.,* 2007). This study confirms the importance of Dab1 degradation in neuronal migration (Feng *et al.,* 2007).

Another important protein involved the control of neuronal migration and cortical lamination is the cyclin-dependent kinase 5 (Cdk5) (Lew and Wang, 1995; Nikoloc *et al.,* 1998). Cdk5 serine/threonine phosphorylates Dab1 independently of Reelin (D'Arcangelo *et al.,* 1999). Interestingly, mice lacking cdk5 or its activating subunit p35 display abnormalities in cortical lamination and aberrant neuronal migration similar but not identical to *reeler* (Chae *et al.,* 1997; Ohshima *et al.,* 1996; Ohshima *et al.,* 2007; Tanaka *et al.,* 2004). These findings suggest that Reelin and cdk5 are involved in overlapping pathways, which in unison, control normal cortical development and lamination. Ultimately extracellular guidance signals are interpreted by transmembrane receptors that relay the Reelin signal to a network of intracellular signalling pathways, all of which converge onto the cytoskeleton.

Numerous studies to date have sought to unravel the complex Reelin signalling pathway. Upon binding to its receptors the Reelin signal is subsequently removed to maintain sensitivity to further stimulation. Before degradation, Reelin exerts its effects on the cytoskeleton of migrating neurons which ultimately results in the proper formation of neuronal layers. Even though it is well accepted that Reelin is responsible for normal cortical lamination, the precise mechanism by which Reelin controls neuronal migration still remains unresolved.

1.3.2.3.4 How does Reelin control cortical lamination during corticogenesis?

Numerous hypotheses have been proposed to explain the mechanism by which Reelin regulates cortical lamination and how this architectonic structure is disrupted in *reeler* mice. As discussed in section 1.3.2.3.2, Reelin is expressed by Cajal-Retzius cells in the MZ before the first set of postmitotic neurons reaches the PP (Rice and Curran, 2001). Once these neurons leave the VZ they receive guidance cues on where to migrate and settle within the cerebral cortex.

Thus far, all the hypotheses that have been put forward are based on the temporal and spatial expression of Reelin, the proteins which form part of the Reelin signalling pathway, the movement of neurons in the cerebral cortex and cortical lamination in both normal and transgenic mouse brains. In short, these hypotheses can be summed up into three broad categories.

Firstly, Reelin may act as an inhibitory or stop signal that terminates radial migration by inducing detachment from radial glial fibers (Dulabon *et al.,* 2000; Frotscher *et al.,* 2003; Pearlman *et al.,* 1998; Sheppard and Pearlman, 1997). Secondly, Reelin has been postulated to act as a repellent for early neuronal populations (Ogawa *et al.,* 1995; Schiffmann *et al.,* 1997). Lastly, Reelin may act as a chemo-attractant for migrating neurons (Dulabon *et al.,* 2000; Gilmore and Herrup, 2000). The last two categories both encompass the detach and go model for Reelin's actions.

Early evidence suggested that Reelin acts as a 'stop' signal for migrating neurons, providing positional information to migrating neurons by instructing them to detach from their radial glial tracts and to stop migration (Dulabon *et al.,* 2000; Frotscher *et al.,* 2003; Schiffman *et al.,* 1997; Sheppard and Pearlman, 1997). This hypothesis was dubbed the 'detach and stop' model and relied on the fact that most neurons migrate via glial-guided locomotion (Cooper, 2008; Kriegstein and Gotz, 2003). This hypothesis was based on investigations that showed that Reelin causes the detachment of neurons from their glial tracts by binding to α3β1 integrin (Dulabon *et al.,* 2000), resulting in arrested migration (Dulabon *et al.,* 2000; Sanada *et al.,* 2004) (Figure 1.11).

D'Arcangelo proposed that a Reelin concentration gradient is present within the developing cortex and thus Reelin exerts different cellular effects depending on its concentration (D'Aracangelo, 2005). In this model, low concentrations of Reelin (closer to the VZ) induces the upward extension of the leading edge towards the MZ, whereas high concentrations of Reelin (close to the MZ) causes the detachment from radial glial fibers arresting migration (D'Arcangelo, 2005).

Recently, numerous lines of evidence have discredited the 'detach and stop' model. Of these, the most compelling comes from real-time imaging studies which found that during the early stages of corticogenesis many neurons migrate via somal translocation (section 1.3.2.1.1) (Borrel *et al.,* 2006; Cooper, 2008; Kriegstein and Noctor, 2004; Miyata *et al.,* 2001; Nadarajah *et al.,* 2004), while during the later stages, as the cortical distance increases, they migrate via locomotion along radial glial tracts (section 1.3.2.1.2). Once the migrating neurons near the pial surface, they detach from their glial guides and migrate the rest of the cortical via somal translocation until they reach their final positions within the cortical plate (Borrell *et al.,* 2006; Cooper, 2008; Hatanaka *et al.,* 2004; Nadarajah *et al.,* 2001). These data show that glial detachment does not stop migration as previously speculated but may instead be required for neurons to reach the top of the cortical plate and settle within their cortical layers. These observations lead to a new hypothesis, the 'detach and go' hypothesis, being proposed (Figure 1.12). This hypothesis postulated that neurons migrate via glial dependent locomotion until they encounter Reelin near the MZ where they detach from their glial fibers and migrate towards their final positions close to the pial surface via somal translocation (Nadarajah *et al.,* 2001) (Figure 1.12).

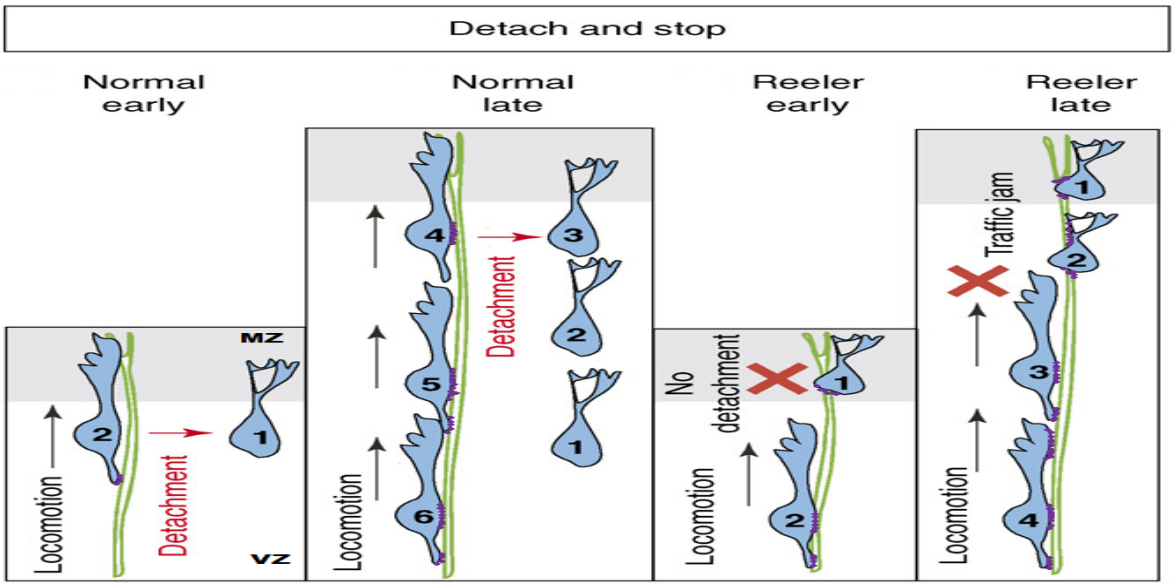

Figure 1.11. 'Detach and stop' model for the role of Reelin in neuronal migration and cortical lamination. Migrating neurons (blue) are numbered in order of birth, radial glial fibers (green), Reelin-dependent actions are in red, the grey area represents the marginal zone (MZ) and the lowest white region the proliferative ventricular zone (VZ). In the normal cortex, layer VI neurons migrate from the VZ along their radial glial guides. As the cell soma enters the MZ, Reelin induces the detachment from glial tracts, arresting migration. In the *reeler* mutant, layer VI neurons do not receive the Reelin detachment signal and fail to detach from their glial guides, these neurons continue to migrate to the MZ. Later born neurons accumulate below earlier born neurons, due to traffic jams created along the glial fibers (Taken from Cooper, 2008).

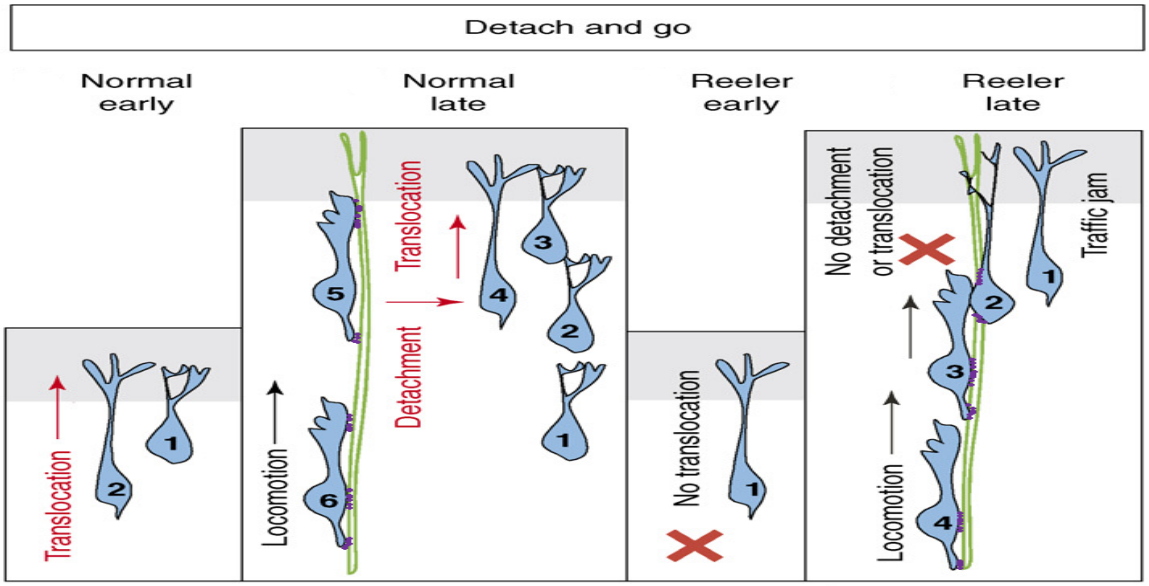

Figure 1.12. 'Detach and go' model for the role of Reelin in neuronal migration and cortical lamination. Migrating neurons (blue) are numbered in order of birth, radial glial fibers (green), Reelin-dependent actions are in red, the grey area represents the marginal zone (MZ) and the lowest white region the proliferative ventricular zone (VZ). Early in development of the normal cortex, Reelin acts on the leading edge of layer VI neurons inducing somal translocation to just beneath the MZ. Later born neurons then migrate by locomotion along radial glial, as the leading edge reaches the MZ Reelin triggers detachment from the glial tracts and induces the anchoring of the leading process to the MZ, the cell body then moves to its correct position by somal translocation. In the *reeler* cortex, layer VI neurons are unable to migrate via somal translocation. Thus later born neurons migrate normally via glial guided locomotion, but fail to detach and move their soma to the top of the cortical plate, resulting in neuronal congestion and causing the inverted cortical layers (Taken from Cooper, 2008).

1.3.3 Cortical organisation

Once migrating neurons reach their final destination within the developing cortex, cortical organisation and terminal differentiation takes place. This allows neurons to mature within their correct final positions and enables the formation of synaptic connections which are important for sensory integration and behavioural output. During this phase of cortical development, programmed cell death or apoptosis of old or damaged neurons also occurs (Guerrini *et al.,* 2006). Little is known about neuronal maturation and specification, although it is known that expression of a proneural (regulators of neurogenesis such as: Neurogenin1, Neurogenin 2 and *Mash1)* is usually adequate to initiate a neuronal differentiation programme in undifferentiated neuronal cells (Ma *et al.,* 1996; Farah *et al.,* 2000; Mizuguchi *et al.,* 2001; Guillemot *et al.,* 2006). This programme regulates the achievement of features common to all neurons, whereas the layer-specific features exhibited by distinct neuronal layers is accomplished by transcription factors belonging to the bHLH class that are expressed by differentiating neurons (Bertrand *et al.,* 2002; Lee, 1997). Further research needs to be done to better understand this stage of cortical development.

Disruption in any of the three stages of cortical development (1.3.1-1.3.3) leads to characteristic morphological disturbances that mostly result in abnormal convolution patterns and manifest as behavioural abnormalities. These neurodevelopmental disruptions have been classed together as a group of disorders known as malformations of cortical development (MCD) each classified according to the first developmental step at which the developmental process was impaired (Barkovich *et al.,* 2001) (Table 1.1, Guerrini *et al.,* 2006). Although MCD are devastating neurological disorders, they do provide researchers with natural models in which to study the molecular pathways involved in the development of the cortex. In addition to MCD, it has been hypothesised that impairment in neurodevelopmental pathways may also contribute to the pathogenesis in complex neuropsychiatric disorders such as schizophrenia (Fatemi *et al.,* 2000; Guidotti *et al.,* 2000; Impagnatiello *et al.,* 1998), major depression (Fatemi *et al.,* 2000), bipolar disorders (Fatemi *et al.,* 2000; Guidotti *et al.,* 2000) and autism (Fatemi *et al.,* 2001; Keller *et al.,* 2000; Persico *et al.,* 2001).

1.4 MALFORMATIONS OF CORTICAL DEVELOPMENT

Many brain or cortical malformations are attributed to defective neuronal migration, in which neurons have failed to migrate in an orchestrated manner. Brain malformations due to abnormal neuronal migration are characterised generally into four pathological groups: agyria/pachygyria, heterotopia, focal cortical dysplasia and lissencephaly (Uher and Golden, 2000), of which lissencephaly is regarded as the most severe or extreme form of aberrant neuronal migration. Due to the fact that neuronal migration occurs in distinct steps or phases, neuronal migration can be affected at numerous levels each resulting in different pathological conditions (Couillard-Despres *et al.,* 2001). The genes believed to play a role in the pathogenesis of neuronal migration and the stages at which the anomalies occur are shown in Table 1.1 (Guerrini *et al.,* 2006). For the purpose of this study defects in ongoing neuronal migration and defects in lamination will be further discussed.

1.4.1 Focal cortical dysplasia

Focal cortical dysplasia (FCD) is a heterogeneous group of lesions characterized by abnormal neurons within a localized region of the neocortex. Focal cortical dysplasia is the term used to describe a spectrum of cortical laminar abnormalities that are associated with cytopathological features which include cytomegalic (giant) neurons, dysmorphic neurons and balloon cells (Tassi *et al*., 2002). The current hypothesis is that FCD's result from abnormalities in the proliferation of neurons which are derived from neuronal progenitor cells within in the ventricular zone (Lamparello *et al.,* 2007). One of the most characteristic symptoms or features of FCD's is drug-resistant epilepsy (Taylor *et al.,* 1971). The cause of this severe form of epilepsy is due to the disorganisation of the abnormal neurons found in patients with FCD, these neurons are unable to form normal synaptic connections and are hence dysfunctional (Guerrini and Fillipi, 2005).

Table 1.1. Genetic malformations of cortical development throughout the stages of development.

Malformation	Gene	Locus	Reference
Malformations due to abnormal proliferation			
Focal cortical dysplasia *- abnormalities of the laminar structure of the cerebral cortex*			
Tuberous sclerosis	TSC1	9q34.13	Dabora *et al.*, 2001
Tuberous sclerosis	TSC2	16p13.3	Dabora *et al.*, 2001
Malformations due to abnormal neuronal migration			
Lissencephaly (X-linked, Autosomal dominant) – *most severe neuronal migration disorder in which neurons are unable to complete migration*			
X-linked lissencephaly with abnormal genitalia	ARX	Xp22.1	Kato *et al.*, 2004
Isolated lissencephaly sequence (ILS) or subcortical band heterotopia (SBH or double cortex - less severe)	DCX	Xq22.3-q23	Matsumoto *et al.*, 2001
ILS or SBH	TUBA1A	12q13.12	Poirier *et al.*, 2007
ILS or SBH	LIS1	17p13.3	Cardosa *et al.*, 2002
Miller- Dieker syndrome	LIS1 + YWHAE	17p13.3	Cardosa *et al.*, 2003
Lissencephaly (Autosomal recessive) *- most severe neuronal migration disorder in which neurons are unable to complete migration*			
Lissencephaly with cerebral hypoplasia (LCH) group b	RELN	7q22.1	Zaki *et al.*, 2007
LCH group b	VLDLR	9p24.2	Boycott *et al.*, 2005
Heterotopia (X-linked, Autosomal dominant) *– clusters of normal neurons in abnormal positions*			
Periventricular nodular heterotopias (PNH)	FLNA	Xq28	Parrini *et al.*, 2006

PNH	-	5p15.1	Sheen *et al.*, 2003
PNH	-	5p15.33	Sheen *et al.*, 2003
PNH	-	7q11.23	Ferland *et al.*, 2006

Heterotopia (Autosomal recessive) *- clusters of normal neurons in abnormal positions*

Microcephaly and PNH	ARFGEF2	20p13	Sheen *et al.*, 2004

Cobblestone cortical malformations (Autosomal recessive)

Fukuyama congenital muscular dystrophy or Walker-Warburg syndrome (WWS)	FCMD	9q31.2	Kondo-Iida *et al.*, 1999
Muscle-eye-brain disease (MEB) or WWS	FKRP	19q13.32	Beltran-Valero de Barnabe *et al.*, 2004
MEB	LARGE	22q12.3	Longman *et al.*, 2003
MEB	POMGnT1	1p34.1	Beltran-Valero de Barnabe *et al.*, 2002
MEB or WWS	POMT1	9q34.13	van Reeuwijk *et al.*, 2006
MEB or WWS	POMT2	14q24.3	van Reeuwijk *et al.*, 2005
Bilateral fronto-parietal cobblestone malformation (polymicrogyria)	GPR56	16q13	Piao *et al.*, 2005
CEDNIK syndrome	SNAP29	22q11.2	Sprecher *et al.*, 2005

Malformations due to abnormal cortical organization

Polymicrogyria (X-linked, Autosomal dominant) *- excessive number of abnormally small gyri presenting as an irregular cortical surface*

Rolandic seizures, oromotor dyspraxia	SRPX2	Xq22	Roll *et al.,* 2006
Agenesis of the corpus callosum (ACC), microcephaly and polymicrogyria (PMG)	TBR2	3p21	Baala *et al.,* 2007
Aniridia plus	PAX6	11p13	Glaser *et al.,* 1994
PMG	-	11p36.3-pter	Ribeiro *et al.,* 2007
Microcephaly, PMG	-	1q44-qter	Zollino *et al.,* 2003
ACC, PNH and PMG	-	6q26-qter	Eash *et al.,* 2005
PMG	-	21q2	Yao *et al.,* 2006
DiGeorge syndrome	-	22q11.2	Robin *et al.,* 2006
Polymicogyria (Autosomal recessive) *- excessive number of abnormally small gyri presenting as an irregular cortical surface*			
Goldberg-Shprintzen syndrome	KIAA1279	10q21.3	Brooks *et al.,* 2005
Micro syndrome	RAB3GAP1	2q21.3	Aligianis *et al.,* 2005

(Adapted from Guerrini *et al.,* 2006).

Table 1.2. Human migration disorders and respective mouse mutants resulting from abnormal neuronal migration. Tabulating the different stages of migration at which these anomalies occur in light of the causative genes.

Stage of migration	Gene name	Human disorder	Mouse mutant	Putative function
Initiation	*filamin*	PVNH	-	Actin binding protein
	Arfgef2	PVH/microcephaly	-	Vesicle trafficking
Ongoing migration	*Dcx*	DC/XLIS	Hippocampal malformation	MAP
	Lis1	LIS/DC	Disrupted cortex and hippocampus	MAP and dynein regulator
	14-3-3epsilon	-	Migration defect	Phosphatase inhibitor
	kif2A	-	Migration defect	+ end motor protein
	Map1b/Map2	-	Migration defect	MAP
	Map1b/Tau	-	Migration defect	MAP
Lamination	*Reelin*	LCH	*reeler*	Glycoprotein
	dab1	-	*scrambler, yotari*	Adaptor protein
	Apoer2	-	Inverted cortex	Reelin receptor
	Vldlr	-	Inverted cortex	Reelin receptor
	P35	-	Inverted cortex	Activator of cdk5
	cdk5	-	Inverted cortex	Serine-threonine kinase
	Brn1/Brn2	-	Inverted cortex	Transcriptional activation of cdk5 and dab1
Termination	*Fak*	-	Disrupted migration	Focal-adhesion kinase
	POMT1	Walker-Warburg syndromome	-	A-dystroglucan *O*-linked glycosylation
	POMGnT1	Muscle-eye-brain disease	-	A-dystroglucan *O*-linked glycosylation
	fukutin	Fukuyamu MD	Disrupted migration	Phospholigand transferase

Abbreviations: PVNH, periventricular nodular heterotopias; PVH, periventricular heterotopias; DC/XLIS, double cortex /X-linked lissencephaly; LIS, lissencephaly; LCH, lissencephaly cerebral hypoplasia; MAP, microtubule associated protein; MD, muscular dystrophy; - not known or previously described (Taken from Beilas *et al.*, 2004).

1.4.2 Anomalies in ongoing neuronal migration: lissencephaly and double cortex

Lissencephaly, which means smooth brain, is characterized by absent (agyria) and decreased (pachygyria) convolutions, resulting in a smooth cerebral cortex (Barkovich *et al.*, 2005; Uher and Golden, 2000). Two forms of lissencephaly have been identified, classical or type I lissencephaly and cobblestone complex or type II lissencephaly, each classified according to anatomical differences observed in the formation of the

cortex (Kanatani *et al.,* 2005). In both these forms of lissencephalies neurons fail to migrate to their proper cortical destinations which disrupts the normal six layered organisation of the cortex (Guerrini and Marini, 2006).

1.4.2.1 Classical or type I lissencephaly

Type I lissencephaly (LIS) is regarded as the most severe neuronal migration disorder, with symptoms ranging from epilepsy to mental retardation (Kubo and Nakajima 2002). The lissencephalic brain is abnormally enlarged and is characterized by a thicker than normal four-layered cortex (Kubo and Nakajima, 2002; Kuchelmeister *et al.,* 1993), which is comprised of a molecular layer (marginal zone, layer 1), an outer cellular layer (layer 2), a cell sparse layer (layer 3) and a deep cellular layer which contains the majority of misguided cortical plate neurons (Barkovich *et al.,* 1991; Dobyns *et al.,* 1996; Kubi and Nakajima, 2002). Interestingly, despite the loss of distinctive neuronal layers, the lissencephalic brain retains the proper inside-out lamination of healthy individuals.

Investigations into the molecular causes of lissencephaly in humans and in mice, have identified several mutations in a number of genes. These include mutations in the *LIS1* gene (also known as the β subunit of platelet activating factor acetylhydrolase gene, PAFAH1B1) (Hattori *et al.,* 1994; Reiner *et al.,* 1993; Reiner *et al.,* 2000) and in the X-linked doublecortin gene (*DCX*, also known as *XLIS*). Both these genes encode proteins that are considered microtubule-associated proteins (MAP) and exert their regulatory function by controlling microtubule dynamics within migrating neurons (Bielas, 2004; Reiner *et al.,* 1995). The protein products of these two genes are structurally unrelated and it is not known whether they physically interact with one another (Gleeson and Walsh, 2000), yet they are believed to act in an overlapping manner to control neuronal migration (Kubo and Nakajima, 2002). More recently, Keays and colleagues showed that humans with type I lissencephaly may also carry heterozygous mutations in *TUBA1A*, the α-tubulin gene, which encodes a crucial microtubule protein (Keays *et al.,* 2007).

1.4.2.2 Double cortex or type 2 lissencephaly

X-linked lissencephaly results from mutations within the X-linked gene doublecortin (*DCX*). Mutations within this gene cause two distinct disease phenotypes: in males the neuronal migration disorder type I lissencephaly, whereas in females doublecortin mutations causes a syndrome known as double cortex. This mosaic effect is most probably due to the X-inactivation of *DCX* in certain cells in females (Ayala *et al.,* 2007; des Portes *et al.,* 1998; Gleeson *et al.,* 1998).

Recently, it was shown that the mutations in *DCX* responsible for the lissencephalic phenotype are found within the protein's tubulin-binding domains (Sapir *et al.,* 2000; Taylor *et al.,* 2000). Gleeson and co-workers postulated that doublecortin has a strong microtubule-bundling effect, causing microtubules to

reorganise into large bundles which are more resistant to depolymerisation thus over stabilizing the microtubule network (Gleeson *et al.,* 1999).

Both Lis1 and DCX regulate microtubule dynamics by stabilizing microtubules enabling microtubule polymerization. Thus it has been suggested that Lis1 and DCX act in similar pathways to regulate microtubules in migrating neurons (Gupta *et al.,* 2002). Caspi and colleagues showed that Lis1 and DCX interact both *in vitro* as well as in mouse embryonic slices to maintain the pool of polymerized microtubules, essential for neuronal migration and the extension of the leading process (Caspi *et al.,* 2000).

1.5. NEURODEVELOPMENT IN COMPLEX DISORDERS

The pathogenesis of numerous more complex neuropsychiatric disorders have also been attributed to abnormalities in neurodevelopment; a few of these are discussed briefly below.

1.5.1. Schizophrenia

The notion that schizophrenia may have a neurodevelopmental component first gained prominence in the 1970's when studies by Watt and co-workers and Fish and co-workers showed that the behavioural and neurological abnormalities seen in schizophrenic patients dated back to childhood (Fish, 1957; Watt, 1972). Over the years this theory has gained widespread popularity in the literature which is supported by numerous studies (Marenco and Weinberger, 2000; Weinberger, 1986). The neurodevelopmental hypothesis of schizophrenia poses that disease process affect critical brain circuits during embryonic development (lesion forming). These brain lesions or insults are able to remain clinically dormant until triggered later during adolescence when several developmental changes occur (Achte *et al.,* 1969; Hyde *et al.,* 1992; Weinberger, 1987).

By the end of the 1980s a more comprehensive neurodevelopmental hypothesis for the pathogenesis of schizophrenia had emerged (Weinberger, 1986; 1987), which is supported by more recent epidemiological and neuropathological studies. These studies mostly implicate changes within the schizophrenic brain. Firstly, numerous studies have shown that there is an increase in the size of the ventricles in the brains of schizophrenic patients, this enlargement of the ventricles was found to be present prior to the onset or at the onset of schizophrenia (Johnstone *et al.,* 1976; Weinberger, 1979; 1982). Not only were the ventricles enlarged before the development of schizophrenia, the enlargement did not progress with the progression of the illness and its associated symptoms nor did the degree of enlargement correlate to the severity of the illness (Johnstone *et al.,* 1976; Weinberger, 1979; 1982). These findings disprove the previously postulated neurodegenerative hypothesis for the development of schizophrenia (Illowsky *et al.,* 1988). It should however be noted that several studies have shown no ventricular enlargement during or prior to schizophrenia (De Lisi *et al.,* 1992; Degreef *et al.,* 1991; Illowsky *et al.,* 1988; Jaskiw *et al.,* 1994). Thus it

seems that in a subset of schizophrenia patients the pathogenesis of schizophrenia may be attributed to factors other than neurodevelopmental insults.

Secondly, cyto-architectural abnormalities found within the brains of certain schizophrenic patients provided evidence to support the neurodevelopmental hypothesis. Harrison and colleagues showed that within the schizophrenic brain neurons are abnormal in size and they are incorrectly positioned, causing neuronal disarray and displacement, heterotopias and disorganisation of laminar structures (Harrison *et al.,* 1997). These abnormalities are all caused by disruptions in neuronal proliferation and migration. In parallel, schizophrenic patients have a reduction in Reelin protein levels by up to 50% (Impagnatiello *et al.,* 1998; Fatemi *et al.,* 2000). Reelin is extracellular matrix glycoprotein secreted by the Cajal-retzius cells of the developing marginal zone and is required for neuronal migration and normal cortical lamination (D'Arcangelo and Curran, 1998) (section 1.3.2.3.2),

Lastly, post mortem studies have shown no indication of gliosis (Harrison *et al.,* 1997). Gliosis (neuronal scarring) is an indicator of neuronal damage or injury after the second trimester of gestation, and is also used as a histopathological marker for neurodegeneration (Kreutzberg *et al.,* 1997). The absence of neuronal scarring indicates that the changes in the schizophrenic brain occurred before the third trimester of gestation (Kreutzberg *et al.,* 1997), further supporting the neurodevelopmental hypothesis for schizophrenia. Neurodevelopmental insults caused before the second trimester would ultimately result in gross abnormalities in the cerebral cortex suggesting that neurodevelopmental abnormalities in schizophrenic patients are caused by insults or disruptions during the second trimester (Bloom *et al.,*1993; Roberts *et al.,* 1991).

All these studies provide a significant amount of evidence to support the neurodevelopmental hypothesis of schizophrenia, in which this polygenic disorder is accompanied by early neuropathological insults occurring during embryonic development. These morbidity risks which begin to be expressed during embryonic neurodevelopment remain dormant until activated later during adulthood in which they manifest into schizophrenia. In spite of all the evidence supporting this hypothesis, other factors (such as environment and other susceptibility genes) occurring later in life beyond the neurodevelopmental stages also remain plausible risk factors for the pathogenesis of schizophrenia (Marenco and Weinberger, 2000).

1.5.2. Obsessive-compulsive disorder

Despite the high prevalence of OCD, the precise pathophysiology of this distressing and debilitating disorder remains unclear. One theory that is gaining momentum, is that the aetiology of OCD has neurodevelopmental origins (Rosenberg and Keshavan, 1998). The manifestation of OCD in children is similar to its presentation in adulthood, the most cases of OCD have their onset during early childhood and adolescence (Pauls *et al.,* 1995; Bolton, 1996). These and numerous other studies have suggested that the

risk for OCD emerges during early childhood brain development (Bolton, 1996; Castillo *et al*., 2005; Venkatasubramanian *et al*., 2009). Further support for the neurodevelopmental hypothesis of OCD is its comorbidity with the well known neurodevelopmental disorder, Tourette's syndrome (Lenane *et al.,* 1990; Paul *et al.,* 1995). In addition, patients with OCD demonstrate severe impairments in neurological functions in comparison to healthy controls (Behar *et al.,* 1984; Conde Lopez *et al.,* 1990; Hollander *et al.,* 1990). Several neurological soft sign abnormalities (such as sensorimotor abnormalities, poor sensory and motor integration) observed at the onset of OCD in the absence of deterioration as the disorder progresses, further support the hypothesis that neurodevelopmental abnormalities contribute to the pathogenesis of OCD (Rosenberg and Keshavan, 1998).

1.5.3. Autism spectrum disorders

Autism spectrum disorders (ASD) is a group of complex and heterogeneous conditions including autism, Rett and Asperger syndromes and pervasive developmental disorders (American Psychiatric Association 1994, DSM-IV). The stereotypic behaviours and delay or disruption in communication and social behaviour characteristic of ASDs, indicate that these spectrum of disorders have abnormal brain structures (Pardo and Eberhart, 2007). It is thought that abnormalities could arise in neurodevelopmental pathways during intra-uterine development and/or during early postnatal brain development (Pardo and Eberhart, 2007). Several clinical assessments, neuroimaging and neuropathological studies have been used to link aberrant neurodevelopment to the pathogenesis of ASDs (Pardo and Eberhert, 2007). One of the most striking features in ASDs is altered brain growth, in which overgrowth occurs in areas of the frontal lobe, cerebellum and limbic structures; this pattern of overgrowth is followed by abnormal slowness in brain growth (Courchesne *et al.,* 2004; Courchesne and Peirce, 2005). Additionally neuroimaging studies have shown an enlargement of brain volume and abnormal patterns of growth in the cerebral cortex (Herbert, 2005). Moreover, post mortem neuropathological studies have also shown disturbances in neuronal and cortical organization of the cerebellum and cerebral cortex (Bailey *et al.,* 1998; Kemper and Bauman, 1998). Taken together, all the clinical, neuroimaging and neuropathological studies support the hypothesis that ASDs are disorders of neuronal-cortical organization which cause alterations in neurodevelopment and in information processing.

Bipolar disorders have also been attributed to abnormal neurodevelopment; these disorders most commonly have cognitive impairments within the domains of attention, memory and executive function (Bearden *et al.,* 2001; Quraishi and Frangou, 2002). Despite several lines of evidence linking the aetiology of bipolar to impaired neurodevelopment (such as neurocognitive deficits, and superior to average cognitive ability), there is still no conclusive hypothesis as evidence suggest that bipolar may be linked more to neurodegeneration rather than neurodevelopment (Goodwin *et al.,* 2008).

In summary, embryonic cortical development is a highly complex process which is regulated by numerous pathways and proteins, each playing a crucial role in the development of the cerebral cortex. The importance of normal cortical development is highlighted by the vast amount of cortical malformation disorders caused by abnormal neuronal proliferation, migration and differentiation. Normal neuronal migration (both radial and tangential) is fundamental to the development of an organised six layered neocortex. Neuronal migration disorders and mutant mice such as reeler have shed light on the processes involved in controlling neuronal migration during corticogenesis. Despite the vast amount of evidence on the Reelin signalling pathway and it's pivotal role in neuronal migration and cortical lamination, the precise mechanism by which Reelin instructs migrating neurons remains a mystery. More recently, aberrant embryonic neuronal development has also been linked to more complex neuropsychiatric disorders such as schizophrenia and OCD.

1.6 THE PRESENT STUDY

The literature reviewed above highlights the importance of normal cortical development, with particular emphasis on the role of the Reelin signalling pathway in normal neuronal migration. The present investigation was conducted in an effort to further unravel the components of the Reelin signalling pathway which may shed more light on the molecular processes involved in cortical development.

In a previous investigation conducted in our laboratory, the amino (N)-terminal domain (reeler domain) of Reelin was used in a yeast-two hybrid (Y2H) screen to identify novel interacting proteins (Kinnear, 2007). In this study, the reeler domain was found to bind to C-terminal domain of WDR47 (WD-repeat domain), a protein of unknown function belonging to the WD-repeat family of proteins. In an effort to determine the function of WDR47 and what role it may play in cortical development, the present study sought to identify proteins which interact with WDR47.

1.6.1 WDR47

WDR47 is a seven WD-repeat containing protein belonging to the WD-repeat protein family (Figure 1.13). Despite the fact that the function of this protein being largely unknown, we hypothesised that it may play a crucial role based on its domain structure which bears a striking resemblance to that of LIS1,a protein involved in the Reelin signalling pathway (Figure 1.13). Besides having seven WD repeats in common, both WDR47 and Lis1 contain a Lis homology domain (LisH) at their N-termini (Figure 1.13). Moreover, WDR47 contains a C-terminal to LisH domain (CTLH), a domain also found in RAN-binding protein 9, a protein shown to be involved in microtubule assembly (Nishitani *et al*, 2001).

1.6.1.1 WD- repeat family

WD-repeats are minimally conserved domains of approximately 40-60 amino acids which typically contain a glycine-histidine (GH) dipeptide 11- 24 residues from the proteins N-terminus and end with a tryptophan-

aspartic acid (WD) dipeptide at the C-terminus (Li and Roberts, 2001; Smith *et al.,* 1999). The repeating unit was first recognised in the β subunit of the GTP-binding protein transducin, and have since been found in approximately 140 human proteins (Vander and Ploegh, 1992).

WD-repeat proteins perform a wide variety of functions which include RNA synthesis and processing, chromatin assembly, vesicular trafficking, cytoskeletal assembly, cell cycle regulation and programmed cell death (Li and Roberts, 2001; Neer *et al.,* 1994; Smith *et al.,* 1999; Vander and Ploegh, 1992). Despite the diverse functions, all members of the WD-repeat family have an underlying common function in coordinating multi-protein complex assemblies (Li and Roberts, 2001; Smith *et al.,* 1999). It is thought that these repeating units may serve as a scaffold for protein interactions, which can occur simultaneously with several different proteins (Li and Roberts, 2001; Smith *et al.,* 1999). This notion is supported by structure-function analysis which suggested that the repeats act as a rigid platform or scaffold regardless of the proteins involved, and that the specificity of the proteins involved is determined not by the repeating WD motif but rather by the sequences flanking the repeating units (Li and Roberts, 2001; Smith *et al.,* 1999).

Of particular relevance to the present study is the fact that some of the identified WD-repeat containing proteins have been found to play crucial roles in the signal transduction and cytoskeletal assembly, two processes that are vital for neuronal migration and neurodevelopment. Furthermore, mutations in WD-repeat containing proteins have been identified that cause disorders of neuronal migration. For example, mutations or deletion in the WD-repeat gene, Lis1, causes Type 1 Lissencephaly in humans (Lo *et al.,* 1997; Neer *et al.,* 1993) (section1.4.2.1) while Cockayne syndrome (CS), an autosomal recessive disorder neuronal migration disorder, is caused by mutations within the WD-repeat protein CSA (Henning *et al.,* 2005; Troelstra *et al.,* 1992).

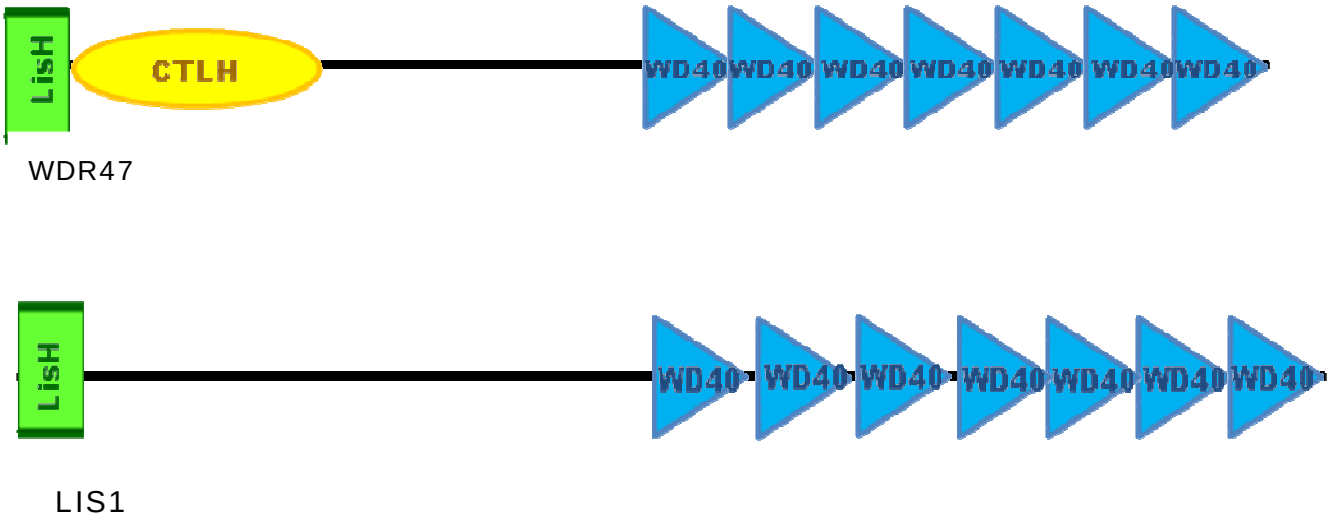

Figure 1.13. Domain structures of WDR47 and LIS1. A comparison of the domain structures of WDR47 and LIS1, showing that WDR47 and LIS1 have similar domain structures namely the Lis homology domain (LisH, green rectangle) and the same number of WD40 repeating units (blue triangles). Additionally, WDR47 also contains a C-terminal Lis homology domain (CTLH, yellow oval).

1.6.1.2 *LIS1* homology domain

The LIS1 homology domain was first described as a novel sequence motif in the products of genes mutated in Miller-Dieker Lissenecephaly, Treacher Collins and oral-digital type 1 syndromes, three disorders associated with defects in cell migration (Emes and Ponting, 2001). As mentioned in the previous section, mutations in LIS1 are associated with Miller-Dieker lissencephaly, which is a consequence of abnormal neuronal migration. Interestingly, in mice heterozygous for a LIS1 mutation, in which the LISH domain was removed, aberrant morphology of the developing cortex was found, which is consistent with defects in neuronal migration (Cahan *et al.,* 2001). Furthermore, in a patient with low severity lissencephaly, a mutation was found within the LISH domain of the LIS1 gene (Cahan *et al.,* 2001). This suggests that the LISH domain may play a vital role in mediating neuronal migration during neurodevelopment. Additionally, LISH domains have also been suggested to contribute to the regulation of microtubule dynamics, either by mediating dimerisation, or by binding cytoplasmic dynein heavy chain or microtubules directly (Emes and Ponting, 2001; Gerlitz *et al.,* 2005). Microtubule rearrangement has been shown to play an important role in neuronal migration (reviewed by Jossin, 2004). Based on the functions of both WD40-repeat domains and LISH domains in neuronal migration, it is quite reasonable to assume that the WDR47 protein, which contains both of these domains, may also play a critical role in the process of neuronal migration.

Therefore, we hypothesized that this protein plays a crucial role in neocortical development via its participation in the Reelin pathway, and that the subsequent protein-protein interactions may also be implicated in neurological disorders. To further understand the function of this novel protein, a human foetal brain cDNA library was screened to identify its binding partners. In this experiment, the region of WDR47

corresponding to the LisH and the CTLH domains was used as ‘bait’ in a Y2H analysis; this region was chosen as it is likely that this region of WDR47 (rather than the WD repeat domains) is responsible for the interactions specific to WDR47. Plausible WDR47-interactions indentified in the Y2H screen were then verified in a mammalian system via 3D-colocalisation.

CHAPTER TWO: MATERIALS AND METHODS

CHAPTER TWO: MATERIALS AND METHODS

2.1. POLYMERASE CHAIN REACTION (PCR)

2.1.1. Oligonucleotide primer design

Oligonucleotide primers were designed according to the sequence of the pEYFP-WDR47 (clone IOH26831, protein ref sequence: gi | 55960048 | emb | CAI14353.1 |), which encodes the full length WDR47 (Imagenes, Berlin, Germany). Before the primers were synthesized, the sequences were analysed for both self-complimentarity and primer-primer complimentarity as well as melting temperature compatibility using DNAman™ version 4 software (Lynnion Biosoft Corp©). The primers were synthesized according to standard phosphoramidite techniques at the Department of Molecular and Cell Biology, University of Cape Town (UCT), South Africa.

2.1.1.1. Primer design for WDR47 bait construct used in Y2H

Oligonucleotide primers were designed to PCR-amplify the cDNA region encoding the two N-terminal domains (LisH and CTLH) of the WD-repeat 47 protein (WDR47). The primers were designed according to the sequence of the pEYFP-WDR47 (clone IOH26831), which encodes the full length WDR47 (Imagenes, Berlin, Germany).

The primers were engineered to incorporate restriction enzyme sequences on both the forward (*Nde*I) and reverse (*Sal*I) primers in order to facilitate the insertion of the amplified product into the pGBKT7 shuttling vector. In addition, the primers were also designed to incorporate a universal enzyme seat, which allows the restriction enzyme to digest at the specific engineered restriction sites, and a stop codon. The sequences of the N-terminal WDR47 bait-insert primers are shown in Table 2.1.

Table 2.1. Primer sequences used for PCR amplification and engineering of WDR47

Name	Sequence	Ta (°C)
WDR47- F	5'- act gca gaa cat atg aaa gag gtt gaa atc att aag- 3'	51
WDR47-R	5' –act gca gaa gtc gac cta tga cat cgc gtt gtt a-3'	51

Blue: universal enzyme seat, Purple: *Nde*I restriction site, Green: *Sal*I restriction site, Red: stop codon, Black gene specific sequences. Abbreviations: Ta, annealing temperature

2.1.1.2. Vector- specific primer design

In order to amplify inserts cloned into the pACT2 library vector, and for subsequent sequence analysis, primers were also designed to amplify vector-specific sequences flanking the multiple cloning site of the pACT2 vector (BD Bioscience, Clontech, Paulo Alto, CA, U.S.A). The primers were designed according to

vector sequences obtained from the Clonetech MATCHMAKER™ handbook (www.clonetech.com). Similarly vector-specific primers were also designed for pGBKT7, these primers were used to amplify and sequence the pGBKT7-WDR47 bait construct. Table 2.2 shows the sequences for both the vector-specific primers.

Table 2.2 Primer sequences and annealing temperatures used for the amplification of inserts from cloning vectors.

Name	Sequence	Ta (°C)
pGBKT7-F	5' TCA TCG GAA GAG AGT AG 3'	50
pGBKT7-R	5' TCA CTT TAA AAT TTG TAT ACA 3'	51
pACT2-F	5' CTA TTC GAT GAT GAA GAT ACC CCA CCA AAC C 3'	68
pACT2-R	5' GTG AAC TTG CGG GGT TTT TCA GTA TCT ACG A 3'	68

Abbreviations: °C, degrees Celsius; Ta, Annealing temperature

2.1.2. PCR-amplification to generate WDR47 bait-insert fragment

PCR reactions were performed in 50 µl reactions and consisted of 1 µl of 150 ng plasmid DNA (WDR47-EYFP), 150 ng/µl forward and reverse primer, 1.5 µl of an equimolar dNTP solution (2.5 mM of each dATP, dCTP, dGTP, dTTP) (TaKaRa Shuzo Co. Ltd, Shiga, Japan), 5 µl of 10X Ex Taq™ Mg^{2+}-containing reaction buffer (TaKaRa Shuzo Co. Ltd, Shiga, Japan), 1.5 U Ex Taq™ (TaKaRa Shuzo Co. Ltd, Shiga, Japan) and sterile water (ddH_2O) to a final volume of 50 µl.

Amplification was performed on a GeneAmp® PCR System 2720 thermal cycler (Applied Biosystems, Foster City, CA, U.S.A) using the following cycling parameters: initial denaturation at 94°C for 5 min, followed by 30 cycles of denaturation at 94°C for 30 seconds, annealing at 51°C for 30 seconds and extension at 72°C for 30 seconds, a final extension step followed at 72°C for 7 minutes.

2.1.3. Bacterial colony PCR

Bacterial colony PCR was performed in order to rapidly identify bacterial colonies harbouring the desired recombinant plasmid, as the vectors used in the Y2H analysis do not support blue-white colour selection. In these PCR reactions, a tiny amount from an individual bacterial colony was picked from an agar plate containing the appropriate antibiotic, and used as a template. Y2H vector-specific primers (Table 2.2) were used in conjunction with the appropriate primers and the 2X Kapa Ready mix (Kapa, Woburn, U.S.A), a pre-made reaction mixture containing all the reagents required for a standard PCR reaction under the abovementioned PCR conditions (section 2.1.2). PCR amplified products were subsequently electrophoresed on a 1% agarose gel, and visualisized under UV light for verification (section 2.2).

2.2. GEL ELECTROPHORESIS

In the present study, agarose gel electrophoresis was used to visualise PCR-amplified fragments, to identify recombinant plasmids harbouring the correct insert and to identify DNA fragments for purification.

2.2.1. Agarose gel electrophoresis for visualisation of PCR-amplified products

In order to verify if the PCR-amplification of the products was successful, the amplified products were subjected to agarose gel electrophoresis as follows: 10 µl of product was initially mixed with 5 µl bromophenol blue (Appendix I) loading dye. Each mixed sample was loaded into separate wells of a 1% agarose gel containing EtBr submerged in 1x SB buffer (Appendix I). A 100bp marker (Promega, Madison WI, USA) was co-electrophoresed with the amplified products to give an indication of relevant sizes. The DNA fragments were then visualised on a long wave 3UV trans-illuminator (UVP, Inc. Upland, CA, USA).

2.3. AUTOMATED DNA SEQUENCING

Bidirectional automated DNA sequencing of PCR-amplified products, as well as cloned inserts, was performed at the Core Sequencing Facility at the Department of Genetics of the University of Stellenbosch, RSA, either on an ABI Prism™ 377 or an ABI Prism™ 3100 automated sequencer (P.E. Applied Biosystems, Forster City, CA, U.S.A). The primers used for the sequencing reactions for PCR-amplified products were identical to the initial PCR primers (Table 2.1), while for the sequencing of Y2H constructs, the vector-specific primers were used (Table 2.2).

2.4. SEQUENCE ANALYSIS

2.4.1. DNA sequence analysis

Sequence analysis was done using the ChromasPro computer program (Techelysium Pty Lmt, Helensvale, Queensland, Australia) and DNAman™ version 4 (Lynnion Biosoft Corp©) to verify that the sequence integrity and frame of the WDR47 fragment generated by PCR-amplification (section 2.1.2.) were intact, as well as to identify Y2H possible interacting prey clones isolated during Y2H library screening. The nucleotide sequence of the amplified WDR47 was compared to the WDR47 reference sequence obtained from the Genbank database (www.ncbi.nlm.nih.gov/Entrez) and the Ensembl database (www.ensembl.org). The Y2H prey constructs were identified by BLASTn comparison of the nucleotide sequences against the Genbank database (www.ncbi.nlm.nih.gov/Entrez) and the Ensembl database (www.ensembl.org). The insert sequences of the prey clones were also translated in the frame dictated by the preceding GAL4AD reading frame (i.e. reading frame 1), and this deduced protein sequence was compared to proteins in the Swissprot database by BLASTp analyses.

2.4.2. Protein sequence analysis

Following the identification of the protein encoded by each of the clones obtained from the Y2H screen, the protein sequence was analysed using Proteome Analyst (http://www.cs.ualberta.ca/%7Ebioinfo/PA/Sub/index.html) and ESLpred (http://www.imtech.res.in/raghava/eslpred/) to determine protein domain structure of the putative interactors of WDR47.

2.5 GENERATION OF CONSTRUCTS

2.5.1. Y2H constructs

To generate the pGBKT7-WDR47 bait construct for the Y2H screen, the engineered WDR47 bait-insert was cloned into the pGBKT7 cloning vector (Appendix V). This was achieved by sequential double-digestion of the amplified cDNA fragment and pGBKT7 vector with appropriate enzymes (section 2.5.2) followed by the ligation of the digested amplified product (WDR47 bait construct) to digested pGBKT7 vector (section 2.7), to form the pGBKT7-WDR47 bait construct. The bait construct was transformed into a competent DH5α *E.Coli* strain (section 2.8.1), single bacterial colonies were subjected to bacterial colony PCR to detect or identify colonies harbouring the recombinant plasmid.

Colonies containing the correct insert were then grown overnight in Luria-Bertani Broth (LB) supplemented with 10 µl of a 50 mg/ml stock of Kanamycin (Appendix I). The following day the plasmids were purified using Zippy™ Plasmid miniprep kit (Inqaba Biotec, Pretoria, South Africa) according to manufacturer's instructions (section 2.12.2). The purified plasmids were then sequenced to determine the integrity of the sequence and conservation of the GAL4 DNA-BD reading frame. The purified pGBKT7-WDR4 bait construct was then transformed into the *S.cerevisiae* yeast strain YH109, thus generating the bait yeast strain which was used to screen a Clonetech MATCHMAKER™ pre-transformed foetal- brain cDNA library (section 2.14.2) (Clonetech, Paulo Alto, CA, U.S.A). The library consisted of foetal brain cDNA which were cloned into the pACT2 prey vector (Figure 2, Appendix V) and pretransformed into the *S.cerevisiae* yeast strain Y187.

2.5.2. Restriction enzyme digestion for cloning of WDR47 bait-insert into pGBKT7

In order to generate the pGBKT7-WDR47 bait construct, both the insert (WDR47) and the vector (pGBKT7) were sequentially double-digested with *Nde*I and *Sal*I (Promega, Madison WI, USA). The digests were prepared in a 50µl reaction volume as follows: 30 µl PCR amplified insert DNA or 20 µl vector DNA (100 ng/µl) was mixed with 2 µl restriction enzyme (5 U/µl), 5 µl restriction enzyme buffer and the appropriate volume of ddH_2O (insert, 13 µl; 23 vector, µl). The mixtures were incubated at 37 °C for 3h. Following this, the samples were purified using the Wizard™ kit (Wizard® Purefection Plasmid DNA purification kit,

Promega Corp. Madison Wisconsin, USA) (section 2.12.1), with the exception that instead of gel electrophoresis and excision of DNA from the gel for purification, the samples were purified directly.

The samples were subsequently eluted in 50 µl ddH_2O and mixed with 5µl of the second restriction enzyme (5 U/µl), 10 µl restriction buffer and 35 µl ddH_2O. These samples were incubated at 37°C for 3 hours, after which they were again purified using the Wizard™ kit (Wizard® Purefection Plasmid DNA purification kit, Promega Corp. Madison Wisconsin, USA).

2.6. CALF INTESTINAL ALKALINE PHOSPHATASE (CIAP) TREATMENT OF VECTOR

To prevent the vector re-circularising by self-ligation, the ends of the linearised plasmid were CIAP-treated to remove any phosphate groups after the final restriction enzyme digestion step. This was accomplished by mixing 50 µl of the digested vector with 1 µl CIP (Promega, Madison WI, USA), 10 ul CIAP buffer and 38µl ddH_2O. The sample was incubated at 37 °C for 30 min, after which another 2 µl CIAP was added and the mixture incubated for a further 30min. Following this, 2 µl 0.5 M EDTA (Appendix I) was added and the sample was incubated at 65 °C for 20 min to inactivate the enzyme. The vector was subsequently purified using the Wizard™ kit (Promega Corp. Madison Wisconsin, USA) (section 2.12).

2.7. DNA LIGATION

DNA ligations were performed in order to generate the Y2H bait constructs to be used in Y2H analysis. Ligations were performed in 10 µl reactions as follows: 1 µl double-digested CIAP-treated vector, 2 µl double-digested insert (section 2.6), 5 µl T4 DNA ligase buffer (Promega, Madison WI, USA), 5U T4 DNA ligase and ddH_2O, to a final volume. The sample was then incubated for 16 hours at 4 °C. Following incubation, 5 µl of the sample was transformed into the bacterial strain DH5α (section 2.11.1) which was plated onto LB agar plates containing the appropriate antibiotic. After incubation of the plates, successful ligation reactions were confirmed by bacterial colony PCR (section 2.1.3).

2.8. BACTERIAL STRAINS, YEAST STRAINS AND CELL LINES

2.8.1. Bacterial strains- *E.coli* DH5α strain

To facilitate the selection and purification of Y2H constructs, ligation reactions were transformed into the *E.coli* DH5α strain. Transformed bacterial colonies were selected on the basis of their ability to grow on LB agar plates (Appendix I) containing selection antibiotics. Kanamycin (Kan) was used when selecting for pGBKT7 recombinant plasmids, and Ampicillin (Amp) was used when selecting for pACT2 recombinant plasmids. Recombinant plasmids were identified by colony PCR (section 2.1.3).

2.8.2. *S.cerevisiae* yeast strains

The pGBKT7 bait construct was transformed into the yeast strain AH109, while all the clones present in the pre-transformed CLONTECH foetal cDNA library (section 2.14.2) used in the Y2H analysis had been transformed into the yeast strain Y187 by the manufacturer.

2.8.3. Mammalian neuronal cells

GT-17 hypothalamus cells (kindly provided by Dr Pamela Mellon, University of California, San Diego, USA), were used to verify the results obtained from the Y2H analysis by co-immunoprecipitation using polyclonal antibodies specifically directed towards the positive prey proteins identified.

2.9. GENERATION OF *E.Coli* DH5α COMPETENT CELLS USED FOR BACTERIAL TRANSFORMATIONS

A scrape of an *E.coli* DH5α frozen (-70°C) glycerol stock was inoculated into 10ml LB-media (Appendix I). The culture was then incubated overnight at 37 °C in a YIH DER model LM-530 shaking incubator (SCILAB Instrument CO. Ltd, Taipei, Taiwan) at approximately 3000 rpm. Following incubation, a 1 ml aliquot of this culture was inoculated into a 2l Ehrlenmeyer flask (with cotton-wool plug and tinfoil lid) containing 200 ml LB media (Appendix I). This culture was incubated at room temperature for 24 hours, while shaking at 3000 rpm, to mid-log phase (OD_{600nm}=0.6) on a Labcon orbital shaker (Labcon Pty, Ltd, Maraisburg, RSA). At this point the culture was decanted into 4x 50 ml polypropylene tubes, which were centrifuged at 3000 rpm for 15 min at 4 °C in a Multitex centrifuge (MSE instruments, England). The supernatant was removed and 8ml of ice-cold CAP buffer (Appendix I) was used to resuspend the pellet. The cells were re-pelleted by centrifugation at 3000 rpm for 15 min at 4 °C in a Multitex centrifuge. The supernatant was discarded and the pellet was resuspended in 4 ml of ice-cold CAP buffer. The suspended cells were subsequently transferred into 1.5 ml microfuge tubes in 500 µl aliquots and snap frozen by immersion in liquid nitrogen. The cells were then stored at -70 °C until they were needed.

2.10. CULTURING OF THE GT-17 CELL LINE

2.10.1. Culturing of GT-17 cells from frozen stocks

2.10.1.1 Thawing the GT-17 cells

Frozen GT-17 cells (provided by Dr Pamela Mellon, University of California, San Diego, USA) were rapidly thawed by immersing the vial containing the frozen stock in a waterbath at 37°C (Memmert®, Schwabach, Germany) for 10 minutes. Once the cells were thawed, the outside of the vial was sterilized using 70% ethanol.

2.10.1.2. Removing DMSO from the GT-17 frozen stocks and culturing the neuronal cells

The frozen cell stocks contained DMSO, which needed to be removed for maximum viability of the cells once they were plated. DMSO was removed as follows: One millilitre of growth media (Appendix I), pre-warmed to 37°C was added to the thawed stock and mixed by gently pipetting the mixture. The mixture was transferred to a 12ml Greiner tube (Greiner Bio-one, Frickenhaussen, Germany) and another 5ml growth media was added. The cells were then pelleted by centrifugation at 10000rpm for 1 minute using a Sorval ® GLC-4 General Laboratory centrifuge (Separations Scientific, Johannesburg, South Africa), followed by removal of the supernatant. The pellet was resuspended in 5ml growth media and once again centrifuged at 10000rpm for 1 minute. The cells were then once again resuspended in 10ml growth media and transferred into a T25 culture flask. The flask was then incubated at 37°C in a Farma termosteri-cycle 5% carbon dioxide humidified incubator (Farma International, Miami, Florida).

2.10.2. Splitting the cell cultures

Cell cultures were split every 2-4 days when they reached approximately 80% confluency (to ensure efficient transformation). Briefly, the growth media was removed from the flask and the cells were washed with sterile phosphate buffered saline (PBS) containing no magnesium or calcium, to this 2ml of trypsin (Highveld Biological, Lyndhurst, South Africa) was added to aid in detaching the cells from the growth surface of the flask. After 3min, 5ml growth media was added and the cells were gently resuspended. The cells were then transferred into four flasks, each containing 10ml growth media.

2.11. TRANSFORMATIONS AND TRANSFECTION OF PLASMIDS INTO PROKARYOTIC (*E.Coli*) AND EUKARYOTIC (*S.cerevisiae*) CELLS

2.11.1. Bacterial plasmid transformations

Prior to the transformation, an aliquot of competent *E.coli* DH5α was removed from the -70°C freezer and allowed to thawed on ice for 15-20 min. One tube which contained 200µl competent cells was used per transformation. Once the cells had thawed, 1µl plasmid preparation (section 2.12.3), or 3-5µl of the ligation reaction (section 2.7), was added to the 200µl cells and gently mixed. The mixture was then incubated on ice for 20-30 min after which they were placed in a Lasec 102 circulating water-bath (Lasec Laboratory and Scientific Company Pty Ltd, Cape Town, R.S.A) at 42°C for exactly 45s. The sample was then removed from the water bath and left at room temperature for 2min. Subsequently, 1ml of LB media was added to the mixture and the sample was incubated for 1h at 37°C, while shaking at 200rpm in a YIH DER model LM-530 shaking incubator.

Following the incubation step, 200µl of the sample was plated onto LB agar plates containing the appropriate selection antibiotic (Appendix I). The remaining transformation reaction mixture was centrifuged at 13000rpm for 2min in a Beckman Microfuge Lite, the supernatant discarded and the pellet resuspended in

200µl LB media. This was then also plated onto the appropriate LB-agar plates. All the plates were incubated overnight, inverted, at 37°C in a model 329 stationary CO_2 incubator (Former Scientific, Marieta, Ohio, U.S.A).

2.11.2. Yeast Plasmid transformations

The yeast strain to be transformed (either AH109 or Y187) was streaked from frozen stocks onto YPDA agar plates (Appendix I). These plates were then incubated at 30°C for 2-3 days in a Sanyo MIR262 stationary ventilated incubator (Sanyo, Electronic Company Ltd, Ora-Gun, Japan). Following incubation, a volume representing 20-50µl of yeast cells was picked and resuspended in 1ml sterile ddH_2O in a sterile 2ml tube. The cells were then re-pelleted by centrifugation at 13000rpm for 30sec in a Beckman Microfuge Lite (Beckman Instruments Inc, CA, USA). The supernatant was removed and the pellet was resuspended in 1ml 100mM lithium acetate (LiAc) (Appendix I) and incubated for 5 min at 30°C in a MIR262 stationary ventilated incubator. Thereafter, the cells were pelleted by centrifugation at 13000 rpm for 20s in a Beckman Microfuge Lite and all the LiAc was removed.

Next, the following were added in this specific order onto the pellet: 240µl of 50% polyethylene glycol (PEG) (Appendix I), 36µl 1M LiAc (Appendix I), 25µl of 2mg/ml heat-denatured and snap-cooled sonicated herring sperm DNA (Promega, Madison WI, USA),10-20µl plasmid preparation and ddH_2O to a final volume of 350µl.The samples were then mixed by vortexing for at least 1 min and incubated at 42°C for 20-30min in a Lasec 102 circulating water-bath. Following incubation, the cells were pelleted by centrifugation at 13000rpm in a Beckman Microfuge Lite and all the supernatant was removed. The cells were resuspended in 150µl sterile Millipore ddH_2O and plated (using sterile glass beads) onto the appropriate selection plates (Appendix I) and incubated inverted at 30°C for 2-5 days in a Sanyo MIR262 stationary ventilated incubator.

2.11.3. Transfection of GT-17 cells

Two days before the cells were transfected, approximately 1-3 x 10^4 cells per well were plated in sterile complete growth media (Appendix I) in 6-well tissue culture plates, each containing a coverslip, and incubated at 37°C in a 5% Farma-thermosteri-cycle carbon dioxide humidified incubator (Farma, International , Miami, Florida, U.S.A). Forty-eight hours later, the cells were visualised under a Nikon TMS light microscope (Nikon, Tokyo, Japan) to determine the level of confluence. The cells were only transfected once an 80% level of confluence had been reached, to ensure optimum transfection efficiency. For each transfection, 100µl of serum-free media was aliquoted into a sterile 1.5ml eppendorf tube. To each tube containing serum-free media, 4µl of GeneJuice® (EMD Biosciences, Darmstadt, Germany) was added. This mixture was inverted a few times and incubated at room temperature for 5min. One microgram of WDR47-EYFP (clone IOH26831, Imagenes, Berlin, Germany) plasmid was added to each tube, which was then

inverted gently. The GeneJuice®/plasmid/media was incubated at room temperature for 15 minutes. Additionally, one tube was set aside and used as a GeneJuice® control, in which GeneJuice® was added to the serum-free media but no plasmid was added. The entire volume of the mixture of both the controls and plasmid tubes were added drop-wise to the cells in the growth media, making sure the drops fell over the coverslip. The cells were incubated at 37°C in a 5% Farma-thermosteri-cycle carbon dioxide humidified incubator (Farma, International, Miami, Florida, U.S.A) for 48 hours. Not all the wells containing cells were transfected, the remaining untransfected cells were used as controls for transfection efficiency, and as controls for both primary and secondary antibodies during the co-localisation experiments (section 2.15).

2.12. DNA AND PLASMID PURIFICATION

2.12.1. Gel purification of PCR-amplified products

Purification of PCR-amplified DNA products from agarose gels was performed to obtain DNA products suitable for sequencing reactions and cloning. The relevant PCR-amplified DNA product was electrophoresed in a 1% agarose gel (section 2.2.) and subsequently viewed under ultraviolet (UV) light. The segment of the gel containing the DNA to be purified was excised using a sterile blade, and the DNA extracted from the agarose gel was purified using the Wizard® Clean-Up System (Wizard® Purefection Plasmid DNA purification kit, Promega Corp. Madison Wisconsin, USA). As per manufacturer's instructions, the excised gel band (containing amplified product) was dissolved in 10 µl per 10 mg membrane binding solution and incubated at 50°C until completely dissolved, this mixture was then transferred to a mini-column assembly and centrifuged at 14000rpm in a Beckman Microfuge Lite (Beckman Instruments Inc., CA, USA) for 1 min and the flow through was discarded; subsequently 700 µl of membrane washing solution was added to the column and centrifuged for 1min, the flow-through was discarded and the column washed again with 500µl membrane washing solution and centrifuged for 5mins. Fifty microlitres nuclease-free water was then used to elute the purified PCR-product.

2.12.2. Bacterial plasmid purification

One *E.coli* colony containing the plasmid of interest was picked from an appropriate selection plate and inoculated into 10 ml LB (Appendix I), containing the correct antibiotic, in a 50ml polypropylene tube. The culture was then incubated at 37°C overnight, while shaking at 250rpm in a YIH DER model LM-530 shaking incubator (SCILAB instrument Co LTD., Taipei, Taiwan).

The following morning, the culture was centrifuged for 10min at 3000rpm in a Beckman model TJ-6 centrifuge (Beckman Coulter, Scotland, UK), after which the supernatant was discarded and the pellet was resuspended in 600µl LB. The plasmid DNA was then extracted from the pellet using the Zippy™ Plasmid Miniprep kit (Promega Corp. Madison Wisconsin, U.S.A). As per manufacturer's instructions, 100µl of 7X

lysis buffer was added to the 600µl resuspended bacterial culture and gently inverted, 350µl of cold neutralization buffer was added and gently mixed, this mixture was then centrifuged for 2min, the supernatant was then transferred to a Zymo-Spin™ II column and centrifuged for 15s, the flow through was discarded and 200µl Endo-Wash buffer was added to the column. The column was then centrifuged for 15s, the flow through was then discarded and 400µl of Zippy™ wash buffer was added to the column, which was again centrifuged for 30 seconds. Thirty microlitres of Zippy™ elution buffer was used to elute the purified plasmids.

2.12.3. Bacterial plasmid purification using Wizard® Purefection Plasmid DNA purification kit

The Wizard® Purefection Plasmid DNA purification kit (Wizard® Purefection Plasmid DNA purification kit, Promega Corp. Madison Wisconsin, USA) was used to isolate plasmid DNA, free of endotoxins, which was used to transfect GT-17 cells for 3D *in vivo* co-localisation assays (section 2.15).

Twenty microlitres of a bacterial glycerol stock, of the appropriate vector, was inoculated into 10ml LB media (supplemented with the appropriate antibiotic) in separate 50ml polypropylene tubes. The cultures were incubated at 37^{o}C overnight, while shaking at 250rpm in a YIH DER model LM-530 incubator. The next day, the cultures were centrifuged for 10min at 3000rpm in a Beckman model TJ-6 centrifuge. The supernatant was then discarded and the plasmid DNA was extracted using the Wizard® kit, as per manufacturer's instructions. Following extraction, the DNA was resuspended in 50µl sterile water and the concentration determined.

2.12.4. Yeast plasmid purification

A yeast colony containing the plasmid of interest was inoculated into 1ml synthetic dropout (SD) medium containing the appropriate dropout supplement (BD Bioscience, Clontech, Paulo Alto, CA, U.S.A) and incubated overnight at 30°C in a shaking incubator at 250rpm. The following morning, 4ml YPDA (Appendix I) was added to the culture, which was incubated for an additional 4 hrs at 30°C. Thereafter, the samples were centrifuged at 14000rpm for 10min in a Beckman model TJ-6 centrifuge (Beckman Coulter, Scotland, UK), and the supernatant was discarded. The pellet was resuspended in the remaining supernatant and then transferred to 2ml Eppendorf microfuge tubes.

The 'Smash and Grab' plasmid isolation method was used in order to purify *S.cerevisiae* plasmids, thus the following were added to the suspension: 200µl 'Smash and Grab' buffer (Appendix 1), 200µl Phenol:Chloroform:Isoamylalcohol (25:24:1 [PCI]) (Sigma, St Louis, MO, USA), and 0.3g sterile 450-600µm glass beads. This mixture was then vortexed using a Snijders model 34524 (Snijders Scientific, Tilburg, Holland) for 2.5min and then centrifuged for 5min at top speed in a Beckman Microfuge Lite

(Beckman Instruments Inc, CA, USA) centrifuge, to allow phase separation. Subsequently, the aqueous phase was transferred to a 1.5ml Eppendorf microfuge tube. The plasmids were then purified from this phase using the Wizard™ Clean-Up System (Wizard® Purefection Plasmid DNA purification kit, Promega Corp. Madison Wisconsin, USA) according to the manufacturer's instructions.

2.13. ASSESMENT OF Y2H CONSTRUCTS

2.13.1. Phenotypic assessment of yeast strains

Both of the yeast strains (AH109 and Y187) to be used in the Y2H analysis were assessed phenotypically before being transformed. Both these yeast strains have been engineered to have defects in genes crucial for production of adenine (-Ade), histidine (-His), leucine (-Leu) and tryptophan (-Trp) amino acid, but neither have a deficiency in the uracil (-Ura) amino acid-producing pathway (as indicated by Appendix V). Therefore, it was possible to assess the phenotype of the strains by plating them onto agar plates lacking essential amino acids. Non-transformed yeast cells that were unable to grow on SD^{-Ade}, SD^{-His}, SD^{-Leu}, SD^{-Trp} but were able to grow on SD^{-Ura} were used for transformations with bait vector and subsequent Y2H analysis.

2.13.2. Autonomous reporter gene activation

The AH109 yeast strain that was transformed successfully with the pGBKT7-WDR47 bait construct was tested for its ability to autonomously activate the *ADE2* and *HIS3* reporter genes (activation of which is crucial for identification of interactions between bait and preys in the Y2H screen) by streaking transformed and un-transformed AH109 onto agar plates lacking essential amino acids namely SD^{-Ade}, SD^{-His}, SD^{-Leu}, SD^{-Trp} and SD^{-Ura}.

2.13.3. Toxicity test for transformed AH109 yeast strain

In order to test whether the bait-construct had any noticeable toxic effects on the AH109 host strain, growth curves of three categories of the AH109 host strain were compared: 1. AH109 transformed with WDR47-pGBKT7 bait construct, 2. AH109 transformed with empty pGBKT7 (non-recombinant vector control) and 3. Untransformed AH109. The growth tests were conducted concurrently and under the same experimental conditions for each category.

The growth curves were generated by growing each of the yeast strains to stationary phase in SD^{-Trp} in a 50ml polypropylene tube at 30°C in a YIH DER model LM-530 shaking incubator shaking at 200rpm. Following this incubation, a 1:10 dilution of each primary culture was made in SD^{-Trp} and incubated for an additional 24h in a 50ml polypropylene tube at 30°C in a YIH DER model LM-530 shaking incubator shaking at 200rpm. Every 2 hours, over a period of 8h during this incubation, a 1ml aliquot of the culture was taken and its OD_{600nm} was measured. An overnight (24h) reading was also taken. A linearised graph of

the log of these OD_{600nm} readings versus time was constructed and the slopes of the graphs generated for the recombinant and non-recombinant transformants were compared.

2.13.4. Mating efficiency test

As decreased mating efficiency would result in a reduced number of interacting clones in the Y2H screen using the WDR47 bait construct, the effect that the bait construct had on the mating efficiency of AH109, was determined using small scale yeast matings. In these mating experiments, the AH109 transformed with pGBKT7-WDR47 bait construct was mated with the prey host strain, Y187 transformed with the non-recombinant prey vector pACT2 or the control prey vector, pTD1.1, supplied by the manufacturer (BD Bioscience, Clontech, Paulo Alto, CA, U.S.A). Concurrently, control matings were also performed in which the yeast strain AH109 transformed with non-recombinant pGBKT7 or the control pGBKT7-53 vector supplied by the manufacturer (BD Bioscience, Clontech, Paulo Alto, CA, U.S.A) was mated with the prey host strain, Y187 transformed with the non-recombinant prey vectors pACT2 or the Clontech pTD1.1 control vector. The experimental procedures were as follows:

Each of the yeast strains used in the mating efficiency experiments was plated onto the appropriate nutritional selection plates (AH109 pGBKT7-WDR47, AH109 pGBKT7 and AH109 pGBKT7-53 on SD^{-Trp} plates; Y187 pACT2 and Y187 pTD.1.1 on SD^{-Leu} plates). These plates were incubated for 2-5 days in a Sanyo MIR262 stationary gravity-ventilated incubator. A single colony from these agar plates was used for each the mating experiments; which was performed in 1ml YPDA media (Appendix I) in a 2ml microfuge tube. The matings were incubated overnight at 30°C, shaking at 200rpm, in a YIH DER model LM-530 shaking incubator. Following the overnight incubation, serial dilutions (1:10; 1:100; 1:1000 and 1:10000) of the mating cultures were plated onto SD^{-Leu}, SD^{-Trp} and $SD^{-Leu/-Trp}$ agar plates and incubated for 4-5 days at 30° in a Sanyo MIR262 stationary ventilated incubator. After the incubation period, the colonies on each plate were counted and used to calculate the mating efficiency (Appendix II).

2.14 Y2H ANALYSIS

2.14.1. Principles of the Y2H

The Y2H assay analyses protein-protein interactions in yeast cells, this is achieved by cloning the genes for the proteins of interest into relevant vectors. Each of these vectors contains either the DNA binding domain (BD) or the activation domain (AD) of the GAL4 transcription activator complex. Normal transcription in yeast requires the interaction of the GAL4 DNA-BD and the GAL4 AD to form a functional and active transcription complex (Figure 1). This complex then binds to recognition sequences within the promoter regions and activates the transcription of downstream reporter genes cloned into relevant vectors (Figure 2.1). In the Y2H screen, unlike in the intact yeast GAL4 transcription factor, the two engineered domains do

not physically interact, thus downstream reporter genes will only be transcribed if the bait and prey proteins interact, hence bringing the two domains into close proximity to form the transcription complex. The transcription of reporter genes is crucial to identify whether proteins have interacted.

In the present Y2H analysis the *ADE2, HIS3* and *MEL1* reporter genes were used as indicators of protein interactions. The N-terminus of WDR47 was fused to the GAL4 DNA-BD and used as the bait once transformed into the AH109 yeast strain, whereas the GAL4 DNA-AD were fused to the proteins within the human foetal cDNA library to form the preys pre-transformed into Y187. These two strains were then mated in the Y2H screen and produced diploid yeast cells in which transcription of reporter genes was activated due to the interaction of the bait and prey fusion constructs. These diploid cells were then subjected to selection assays including nutritional selection, X-α- galactosidase assays and heterologous matings to select for positive prey clones in which a putative protein-protein interaction activated the transcription complex and hence activated downstream reporter genes. After the prey clones were selected, their inserts were sequenced and subjected to further analysis (*in vivo* 3D co-localisation) to identify novel ligands interacting with the N-terminus of WDR47.

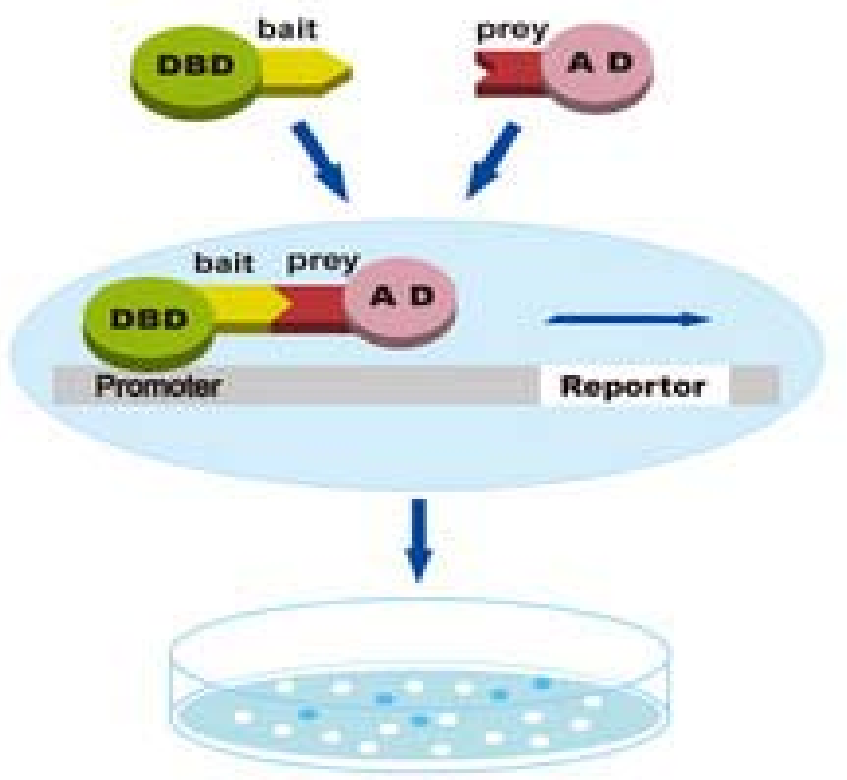

Figure 2.1. **The basis of the Yeast 2- Hybrid technique.** The bait construct will only activate the transcription of the downstream reporter genes, if the bait fusion protein and prey fusion protein interact, bringing together the DNA binding domain and the activation domain of the Gal4 transcription complex. The transcription of reporter genes allows for the detection of putative interactions.

Yeast two-hybrid analysis

↓

Library screen using pre-transformed foetal brain cDNA library and N-terminal WDR47 as 'bait' protein

↓

Detection of activation of nutritional reporter genes:

- Growth on TDO- activation of *HIS3*
- Growth on QDO- activation of both *HIS3* and *ADE2*

↓

Detection of activation of colorimetric reporter genes:

- X-α-Galactosidase assay- intensity of blue colour product, indicates activation of *MEL1*

↓

Interaction specificity test:

- Heterologous mating

↓

Verification studies:

- 3D *in vivo* co-localisation

Figure 2.2. Schematic flow diagram of the Y2H analysis and verification studies.

2.14.2. The foetal brain cDNA library

A pre-transformed human MATCHMAKER foetal brain cDNA Library (BD Bioscience, Clontech, Paulo Alto, CA, U.S.A) consisting of *S.cerevisiae* Y187 transformed with a foetal brain cDNA library, constructed in pACT2, was used in the Y2H library assay (Figure 2.1).

This library had been constructed from a pool of nine male and female Caucasian foetuses aged between 20-25 weeks. The library was *Xho*I-(dT)15 primed and contains approximately $3.5x10^6$ independent clones inserted into pACT2 through *EcoR*I and *Xho*I sites. The average insert size for this library was reported by the manufacturer as 2.0kb, with a range of between 0.5 and 4.0kb.

2.14.3. Establishment of bait culture

A colony of AH109 transformed with the WDR47 bait construct was streaked out onto SD^{-Trp} plates and allowed to grow at 30°C for 4 days. Yeast colonies were inoculated into four separate 500 ml Erlenmeyer flasks, each containing 50ml SD^{-Trp} media. This was done in order to facilitate the generation

of a final bait culture with a titre of at least $1x10^{10}$, i.e. 100-fold excess of bait to prey, to facilitate high mating efficiency.

The four initial cultures were incubated at 30°C overnight, while shaking at 200rpm in a YIH DER model LM-530 shaking incubator (SCILAB instrument CO. Ltd, Taipei, Taiwan). Following overnight incubation, the cultures were transferred into individual 50ml polypropylene tubes and the cells pelleted by centrifugation at 3000rpm for 10min at room temperature in a Beckman Microfuge Lite (Beckman Instruments Inc., CA, USA). The supernatants were discarded and the four pellets were resuspended together in 50ml SD^{-Trp} following which, the suspension was transferred to a single 500ml Erlenmeyer flask and incubated for a further 16h in a YIH DER model LM-530 shaking incubator (SCILAB instrument CO. Ltd, Taipei, Taiwan), shaking at 200 rpm. After incubation, the titre of the bait culture was estimated by measuring the OD_{600nm} of a 1ml aliquot of the bait culture. This estimation was subsequently confirmed by means of a haemocytometric cell count (using a Neubauer Haemocytometer which determines the number of cells per millilitre).

The bait culture was centrifuged at 3000rpm at room temperature for 10min in a Beckman Microfuge Lite to pellet the cells; the supernatant was removed and the pellet resuspended in ml SD^{-Trp} media. An appropriate number of 10µl aliquots of this culture were removed for control mating experiments.

2.14.4. Library mating

A 1ml aliquot of the pre-transformed foetal brain cDNA library was removed from the -70°C freezer and thawed at room temperature (BD Bioscience, Clontech, Paulo Alto, CA, U.S.A). Once thawed, the library aliquot was vortexed and 10µl aliquoted into a sterile 1.5µl microfuge tube for library titering. The pGBKT7-WDR47 transformed AH109 pellet (section 2.11.2) was resuspended in 45ml 2x YPDA media (Appendix I) supplemented with 10µg/ml kanamycin (Kan) in a 2L Erlenmeyer flask, the remaining 990µl of the library culture was added to the Erlenmeyer flask (thus mixing the bait and prey cultures). This mating culture was incubated at 30°C overnight, while shaking at 200rpm in a YIH DER model LM-530.

After the overnight incubation, the entire mating culture was transferred into a sterile 50ml polypropylene centrifuge tube and the cells pelleted by centrifugation at 3000rpm for 5min in a Multex centrifuge (MSE Instrumentation, England, UK), and the supernatant subsequently removed. The Erlenmeyer flask in which the library mating was performed was rinsed twice with 40ml 2x YPDA containing 10µg/ml Kan. Each time the flask was rinsed, the 2x YPDA medium was used to resuspend the cell pellet and the cells then re-pelleted by centrifugation at 3000rpm for 10min at room temperature in Multex centrifuge. Following the

final centrifugation step, the supernatant was removed and the pellet resuspended in 15ml 0.5x YPDA containing 10µg/ml Kan (Appendix I).

Serial dilutions of 100µl aliquots (1:10; 1:100; 1:1000; and 1:10000) of this cell-suspension were plated onto 90mm SD^{-Leu}, SD^{-Trp} and $SD^{-Leu/-Trp}$ agar plates, in order to determine bait:library mating efficiency. Two hundred and fifty microlitres aliquots of the remainder of the culture was plated onto each of 60 140mm diameter TDO (media lacking leucine, trytophan and histidine) plates (Appendix I). The TDO plates were incubated, inverted, at 30°C for 2 weeks in a Sanyo MIR262 stationary ventilated incubator.

2.14.5. Establishing a library titre

The serial dilutions of the mating culture plated onto the 90mm SD^{-Leu}, SD^{-Trp} and $SD^{-Leu/-Trp}$ agar plates were inverted and incubated in a Sanyo MIR262 stationary ventilated incubator for 4 days. Colony counts were performed on the SD^{-Leu}, SD^{-Trp} and $SD^{-Leu/-Trp}$ plates after the 4 day incubation in order to calculate the mating efficiency of the library mating and the number of library plasmids screened (section 2.13.4).

2.14.6. Control matings

Control matings were set up concurrently with library matings, in order to determine whether the recombinant WDR47 bait construct (transformed into AH109) had any negative effect on the ability of the transformed AH109 strain to mate with the library strain (Y187). A 10µl aliquot of the bait culture and a single test prey- (yeast strain Y187 transformed with pTD 1.1 control vector) colony were co-inoculated in 1ml 0.5x YPDA containing 10µg/ml kanamycin (Appendix I) in a 2ml centrifuge tube. This culture was subsequently incubated for 24h at 30°C in a YIH DER model LM-530 shaking incubator, shaking at 200 rpm. Following incubation, serial dilutions (1:10; 1:100; 1:1000; 1:10000) were plated onto SD^{-Leu}, SD^{-Trp} and $SD^{-Leu/-Trp}$ agar plates and incubated for 4 days in a Sanyo MIR262 stationary ventilated incubator. Following this, colony counts were done and the mating efficiency was calculated. Control preys included non-recombinant pACT2 transformed into Y187 and the pTD1.1 control vector supplied by Clontech.

2.14.7. Detection of activation of nutritional reporter genes

2.14.7.1. Selection of transformant yeast colonies

Yeast transformed with the bait construct to be used in Y2H analysis was plated onto SD^{-Trp} agar plates. Following incubation of these plates for 4-6 days in a Sanyo MIR262 stationary gravity-ventilated incubator, transformant yeast colonies were picked and used in small and large scale bait cultures (section 2.14.2) and library matings (section 2.14.5).

2.14.7.2. Selection of diploid yeast colonies containing putative interacting peptides

In order to identify yeast colonies in which an interaction between the bait- and prey-fusion peptides had taken place, yeast colonies were plated onto TDO plates (Appendix I) as well as QDO (media lacking leucine, histidine, tryptophan and adenine) plates (Appendix I). Growth of the yeast cells on TDO plates indicated the transcriptional activation of the *HIS3* nutritional reporter gene, while growth on the QDO plates indicated that both the *HIS3* and *ADE2* nutritional reporter genes had been transcriptionally activated. The activation of these genes in the diploid yeast cells is an indication of the interaction between the bait and prey peptides.

Briefly, the library mating culture was plated directly onto 60 140mm TDO agar plates (Appendix I) (section 2.14.3) and incubated in a Sanyo MIR262 stationary ventilated incubator for 2 weeks. The growth of these colonies on the TDO plates were monitored every 2 days and colonies were picked and re-streaked onto TDO and QDO plates in order to test for the activation of *HIS3* and *ADE2* nutritional reporter genes. These plates were incubated for 3-6 days at 30°. Colonies growing on TDO plates after incubation were picked and plated onto QDO plates containing X-α-galactose, to assess activation of the *MEL1* gene, and incubated at 30°C in a stationary gravity-ventilated incubator for a further 3-5 days.

2.14.8. Detection of activation of colourimetric reporter genes

2.14.8.1. X-α-galactosidase assay

X-α-galactosidase assays were performed in order to test for the activation of the *MEL1* reporter gene by the specific interaction between specific bait and prey peptides. The *MEL1* gene encodes for the yeast secreted enzyme α-galactosidase, thus when the bait protein and the prey protein interact the *MEL1* gene is transcribed and the enzyme product is secreted into the culture media where it catalyses melibiose and subsequently produces a notable blue yeast colony containing the interacting proteins.

Briefly, yeast colonies in which the *HIS3* and *ADE2* reporter genes were activated, as determined by their growth on QDO agar plates, were replicated from QDO plates onto Hybond N^+ nylon membranes (Amersham pharmacia biotech Ltd, England). These membranes were subsequently placed colony-side up onto a QDO plate impregnated with 20mg/ml X-α-gal solution (BD Biosciences, Clontech, Palo Alto, CA, U.S.A). The plates were then incubated at 30°C in a Sanyo MIR262 stationary ventilated incubator. Following incubation, the intensity of the blue colour of yeast colonies that had activated the *MEL1* reporter gene was assessed visually.

2.14.9. Rescuing/extracting prey plasmids from diploid colonies

In order to identify the novel interacting proteins, each individual prey needed to be isolated from the diploid yeast colonies, containing both the WDR47 bait plasmid as well as the prey plasmid. To enable this, plasmid DNA, comprised of a mixture of bait and prey plasmids, was isolated from each of the diploid cells following the protocol discussed in section 2.12.3 and transformed into *E.coli* strain DH5α as described in section 2.11.1. The transformants were plated onto LB ampicillin (20μg/ml) plates which only allows for the growth of transformants containing the prey constructs. These prey constructs were prepared from the *E.coli* (section 2.11.1) and subsequently transformed into the yeast strain Y187 (section 2.11.2).

2.14.10. Interaction specificity test i.e. heterologous mating

To test whether the interactions detected by Y2H analysis, through the activation of nutritional and colourimetric reporter genes represented specific interactions between the pGBKT7-WDR47 bait and a particular prey peptide, interaction-specificity tests were used. Y187 colonies expressing the specific prey peptide were individually mated with the yeast strain AH109 (transformed with different plasmids): 1. transformed with the pGBKT7-WDR47 construct, 2. AH109 transformed with non-recombinant pGBKT7, 3. AH109 transformed with the pGBKT7-53 control bait-plasmid supplied by the manufacturer (BD Biosciences, Clontech, Palo Alto, CA, U.S.A) and 4. transformed with a heterologous bait, encoding a cytosolic cardiac myosin binding protein C (MyBPC) C5C10 domain. The first round of matings was done on $SD^{-Leu-Trp}$ plates and incubated for four days at 30°C, these clones were subsequently streaked onto TDO and incubated four days at 30°C. Finally, the heterologous matings were transferred to QDO selection plates and incubated for four days at 30°C. Clones that interacted specifically with the WDR47 bait (thus only grew once mated with WDR47 and not with any of the other transformed AH109) were considered putative true interactors. The inserts of these putative interactor plasmids were then nucleotide sequenced to determine their identities and subjected to further analysis.

2.15. *IN VIVO* CO- LOCALISATION

To verify the positive interactions identified in the present Y2H screen (after numerous stringency tests) *in vivo* co-immunoprecipitation was utilized to analyse whether the indentified prey proteins co-localised with WDR47 in GT-17 hypothalamus cells. The mammalian GT-17 cells were transfected with WDR47 tagged with yellow fluorescent protein (YFP), primary antibodies directed against the individual prey proteins were detected by a secondary antibody labelled with Texas Red (TxRed) fluorescent dye.

2.15.1. Culture and transfection of GT-17 cells

Human GT-17 hypothalamus cells (provided by Dr Pamela Mellon, University of California, San Diego, USA) used in the immunoflourescence co-localisation, were maintained at 37°C and 5% CO_2 in Dulbecco's

modified Eagle's medium supplemented with 10% fetal calf serum, 4% glutamine and 1% penicillin/streptomycin. Cells were grown on sterile cover slips which were placed inside 30-mm culture dishes, allowing the GT-17 cells to grow and adhere onto the cover slips submerged in growth media.

2.15.2. Immunocytochemistry

Twenty-four hours after transfection with pEYFP-WDR47 (section 2.11.3), GT-17 cells grown on cover slips were washed with phosphate buffered saline (PBS) (Appendix I). The cells were then fixed with a 1:1 methanol/acetone solution and incubated for 10min on ice at 4°C. The fixative was then removed and the cover slips were air dried for 20min. Cover slips were then incubated at room temperature in 5% serum (depending on which secondary antibody was used, refer to Table 2.3) for 20min. Following this, the cover slips were incubated for 90min at room temperature with the appropriate prey primary antibodies (Table 2.3). The cover slips were then rinsed with PBS, and subsequently incubated at room temperature for 30min with respective Texas red-labelled secondary antibodies (Table 2.3). Thereafter, Hoescht 33342 (10mg/ml; Sigma, St Louis, MO, USA) was added in a 1:200 dilution and allowed to incubate at room temperature for 10min. This dye stains the nuclear material blue and is required for orientation purposes during the acquisition of images for the z-stack. Cover slips were then washed three times with PBS and transferred to glass microscope slides, mounted with fluorescent mounting media (Dako Cytomation, Glostrup, Denmark) and sealed with clear nail polish.

Table 2.3. Prey proteins and respective antibodies used for immunprecipitation.

Prey	Primary antibody	Dilution	Serum	Secondary antibody	Dilution
Cul7	Cul7 rabbit polyclonal	1:200	Goat	Goat anti-rabbit TxRed	1:200
Guk1	Guk1 mouse polyclonal	1:200	Donkey	Donkey anti-mouse TxRed	1:200
SCG10	SCG10 goat polyclonal	1:200	Donkey	Donkey anti-goat TxRed	1:200
SNAPIN	SNAPIN goat polyclonal	1:200	Donkey	Donkey anti-goat TxRed	1:200

Abbreviations: Cullin 7 (Cul7); Guanylate kinase 1 (Guk1); Stathmin like 2 (SCG10), SNARE associated protein (SNAPIN); Texas Red (TxRed). **Suppliers:** Cul7 rabbit polyclonal antibody – Bethyl Laboratories, INC, Montgomery, TX, USA. Guk1 mouse polyclonal antibody – Abnova Corporation, Taiwan. SCG10 goat polyclonal antibody and SNAPIN goat polyclonal antibody – Santa Cruz Biotechnology, INC. Secondary antibodies - Santa Cruz Biotechnology, INC.

2.15.3 Fluorescence microscopy and co-localisation

Cells were observed through an Olympus Cell^R system attached to an IX-81 inverted fluorescence microscope equipped with a Z-motor, a cooled CCD camera (F-view-II Soft Imaging Systems) and automated excitation and emission filter wheel controlled by MT20 Cell^R (Olympus Biosystems GMBH, Tokyo, Japan). Cell^R imaging software was used for the image acquisition and analysis.

Fluorescence was excited through an excitation filter for the each of the fluorescent tags and labels (Table 2.4). Emission was collected using Ultraviolet, blue, green (UBG) bandpass and YFP emission filter cubes, using an oil immersion 60X objective. Three-dimensional (3D) co-localised images were produced from an average of 13 Z-stacked images at 0.26µm increments. Based on the 3D images data, co-localisation was calculated using the Cell^R co-localisation analysis tool. The two fluorescence signals (bait and prey) to be measured were activated, the threshold was set and co-localisation was displayed as a new false colour image.

Table 2.4. Excitation and emission spectra, and filter requirements of fluorescent proteins used in *in vivo* co-localisation

Fluorescent protein	Excitation	Emission	Filter set
EYFP	500nm	527nm	YFP
TexasRed	557nm	585nm	TxRed
Hoechst H-33342*	360nm	460nm	DAPI

* Nuclear stain, not a fluorescent protein tag.

CHAPTER THREE: RESULTS

CHAPTER THREE: RESULTS

3.1. YEAST-TWO HYBRID ANALYSIS OF N-TERMINAL DOMAIN OF WDR47

3.1.1 Y2H bait constructs

3.1.1.1. PCR amplification to generate the bait-insert fragment

The WDR47 bait-insert fragment was obtained by PCR-amplification of the N-terminus domain of WDR47 from the commercially available clone (Imagenes, Berlin, Germany clone IOH26831). The primers used in the amplification allowed for the incorporation of restriction enzyme recognition sites and universal enzyme seats (section 2.1.1.1, Table2.1). Amplification with this primer set generated a WDR47 bait fragment of 279 bp suitable for cloning into the pGBKT7 shuttle vector.

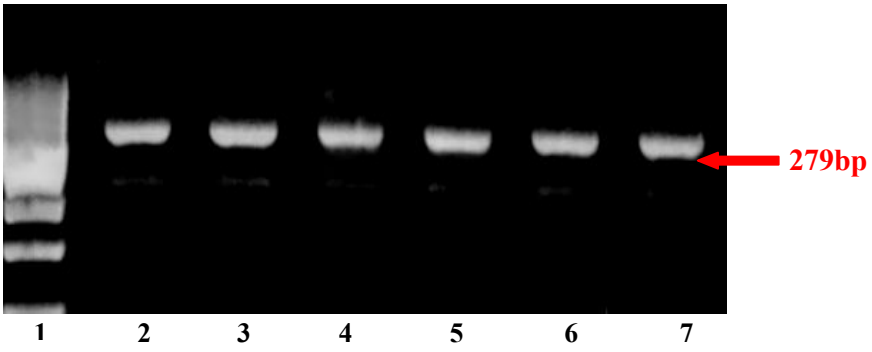

Figure 3.1. Image of the PCR amplified N-terminal domain of WDR47, representing a product of 279bp. Lane 1 contains the 100bp marker, Lanes 2-7 contain the PCR amplified product.

3.1.1.2. Restriction enzyme digestion and ligation

Both the PCR amplified WDR47 bait fragment and the pGBKT7 cloning vector were successfully double-digested with *Nde*I and *Sal*I (section2.6.1). After CIP- treatment of the vector, a ligation reaction (section 2.7) generated the pGBKT7- WDR47 bait construct.

3.1.1.3. Selection for successful cloning via bacterial colony PCR

Bacterial colony PCR reactions were done in order to select for recombinant pGBKT7 plasmids, confirming successful cloning of the bait insert into the bait vector. PCR reactions were done using primers flanking the multiple cloning site of pGBKT7 cloning vector (section 2.1.3, Table 2.2). This PCR amplification generated either non recombinant pGBKT7 plasmid (333bp) products or recombinant pGBKT7-WDR47 products. These recombinant plasmids were then used as the bait protein in the Y2H analysis.

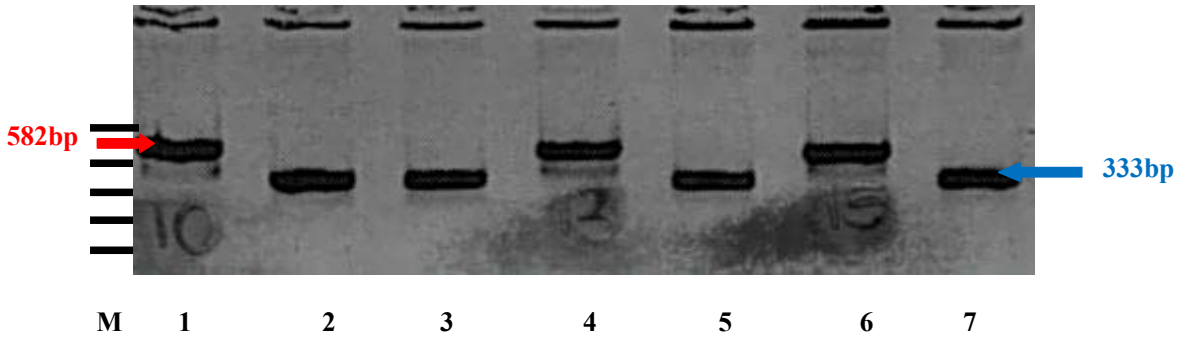

Figure 3.2. Image of the bacterial colony PCR, to identify which clones carried N-terminal domain of WDR47 (red arrow, lanes 1, 4, 6) and clones with no WDR47 inserts (blue arrow, lanes 2, 3, 5, 7), M 100bp molecular marker).

3.1.1.4. Sequence analysis of pGBKT7 - WDR47 bait construct

The generated bait construct was sequenced to verify the integrity of the coding sequence and to confirm that the integrity of the reading frame had been preserved. Sequence analysis revealed that the pGBKT7 - WDR47 bait construct was in the correct reading frame and proved that the integrity of the nucleotide sequence of the WDR47 insert had been conserved (even after the multiple cloning steps used in the generation of the bait construct) (Chromatogram in Appendix V).

3.1.2. Verification of the integrity of the Y2H construct

3.1.2.1. Auto- activation test

The yeast strain AH109 transformed with the bait construct was unable to grow on selection media lacking essential amino acids (SD^{-Ade}, SD^{-His} and SD^{-Leu}) indicating that the pGBKT7 - WDR47 bait construct did not autonomously activate the expression of the endogenous reporter genes. The lack of growth on these plates also indicated that the phenotype of the AH109 yeast strain was maintained after transformations with the generated bait construct. The transformant was, however, able to grow on SD^{-Trp} and SD^{-Ura} as expected.

3.1.2.2. Toxicity test

In order to determine whether the pGBKT7 - WDR47 bait construct had any toxic effects on the AH109 yeast cells, linear growth curves of AH109 transformed with empty pGBKT7 vector and AH109 transformed with pGBKT7 - WDR47 were constructed and compared. The slopes of these curves, which did not differ significantly from each other, indicated that the WDR47 bait construct had no toxic effect on the growth of the yeast strain (Figure3.3).

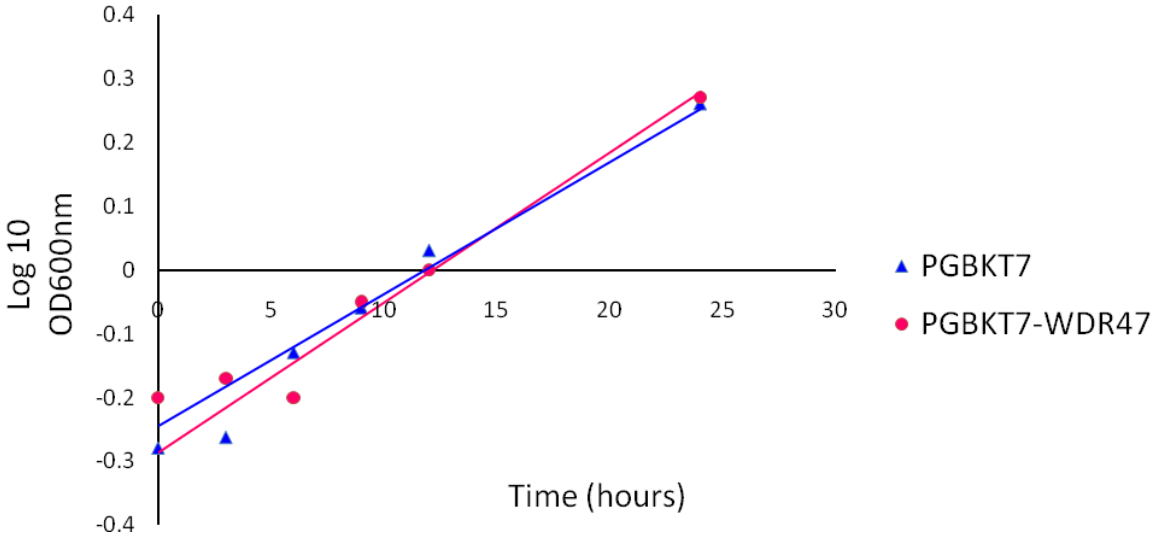

Figure 3.3. Linear growth curve of yeast strain AH109 transformed with non-recombinant pGBKT7 and pGBKT7-WDR47 bait constructs. In order to determine whether the bait constructs had toxic effects on the AH109 strain, the growth rate of the pGBKT7-bait transformants were compared to the non-recombinant pGBKT7. The growth rate was determined by calculating the slope of each of the curves. The slopes were comparable indicating that the bait constructs had no toxic effect on the growth of the host yeast strain.

3.1.2.3. Mating efficiency of AH109 transformed with WDR47 bait construct

Small scale yeast matings were performed to assess whether the WDR47 bait construct affected the mating efficiency of the host yeast strain AH109. These mating experiments allowed for the calculation (AppendixII) and the comparison of mating efficiency of the WDR47 bait construct with the mating efficiency of AH109 yeast strains transformed with control plasmids (pGBKT7 and pGBK53) and standard prey transformants (pACT2 and pTD1.1).

Table 3.1 show the mating efficiency results, and indicate that pGBKT7 - WDR47 did not hinder the mating efficiency of the AH109 yeast strain. The calculated mating efficiency (63.6%) of the pGBKT7 - WDR47 transformant with the empty library vector, pACT2, was notably higher than the minimum of 2% recommended by the manufacturer of the MATCHMAKER Y2H system (BD BioScience, Paulo Alto, CA, U.S.A). This proved that the pGBKT7 - WDR47 construct did not decrease the mating efficiency of the AH109 yeast strain, and would result in screening of 10^6 individual prey clones if mated at a 100-fold excess against the commercial pretransformed foetal brain cDNA (titre= 3 x 10^8).

Table 3.1. Effect of WDR47 bait construct on AH109 mating efficiency.

Mating	Mating efficiency (%)
pGBKT7-WDR47 (AH109) x pACT2 (Y187)	**63.60**
pGBKT7 (AH109) x pACT2 (Y187)	2.22
pGBK53 (AH109) x pACT2 (Y187)	64.20
pGBKT7-WDR47 (AH109) x pTD1.1 (Y187)	**1.33**
pGBKT7 (AH109) x pTD1.1 (Y187)	23.00
pGBK53 (AH109) x pTD1.1	0.41

Control matings indicated in black, blue indicates matings of pGBKT7-WDR47 transformants. Yeast strains indicated in brackets.

3.1.3. Y2H screening of pretransformed foetal brain cDNA library

Following the verification tests performed in section 3.1.2, the pGBKT7 - WDR47 bait construct was used in the Y2H analysis. Library mating-efficiency calculations indicated that approximately 8.4 x 10^5 pretransformed foetal brain cDNA library clones were screened with the pGBKT7 -WDR47 construct. The screen yielded 817 clones which were able to activate the *HIS3* reporter gene as determined by growth on TDO plates. Successive nutritional selection stages reduced the initial number of diploid colonies to 704 clones, which were also able to activate the *ADE2* reporter gene, as they grew on QDO plates (Table 3.2). These 704 clones were then assessed for their ability to activate the colourimetric reporter gene *MEL1*. Activation of this gene was detected by the presence of the blue end product of the x- α- galactosidase assay (section 2.14.8). Of the 704 assessed, 198 were found to activate the *MEL1* reporter gene of which 37 were classified as primary clones and 161 as secondary clones based on the amount of growth and the intensity of the blue colour produced in the x-α-galactosidase assay. Table 3.2 shows only the clones that were able to activate the *MEL1* reporter gene.

Table 3.2. Activation only of *ADE2* (nutritional) and *MEL1* (colorimetric) reporter genes by prey-WDR47 interactions

Colony #	Growth on TDO (*HIS3 activation*)	Growth on QDO (*ADE2 activation*)	X-α-galactosidase (colour, *MEL1 activation*)
8		+	+ (very light blue)
9		++	++ (blue- grey)
10		++	++ (light blue)
11		+	+ (very light blue)
16		+++	+++ (blue-green)
20		+	+ (very light blue)
24		++	+ (very light blue)
25		+	+ (light blue, pink spots)
26		+	+ (very light blue)
32		+	++ (small, but blue)
34		++++	++++ (bright blue)
37		++	++ (light blue)
42		++	+ (light blue)
44		++	++ (light blue)
46		+++	+++ (darker blue)
50		++++	++++ (bright blue)
51		++++	++++ (bright blue)
52		+++	++ (light blue)
54		++	+ (very light blue)
64		+	+ (very light blue)
76		++++	++ (light blue)
86		++++	++++ (bright blue)
87		++	++ (light blue)
91		++++	+ (very light blue)
93		++	+ (very light blue)
97		++++	+++ (bright blue brown)
103		++++	+ (very light blue)
105		++++	++++ (bright blue)

Colony #	Growth on TDO (*HIS3 activation*)	Growth on QDO (*ADE2 activation*)	X-α-galactosidase (colour, *MEL1 activation*)
110		++	++ (light blue)
113		++++	++++ (bright blue)
114		++++	+++ (darker blue)
115		++++	+++ (blue grey)
119		++++	++++ (bright blue)
121		++++	++++ (bright blue)
122		++	++++ (bright blue)
126		++++	++ (brown blue)
127		++++	+ (very light blue)
129		++++	+ (very little blue)
130		+++	++ (light blue)
135		++	++++ (bright blue)
142		++	+ (brown blue)
143		++++	++++ (bright blue)
144		++++	+ (brown blue)
145		++++	+++ (dark light blue)
146		++++	++ (light blue)
155		++	+ (very light blue)
160		++++	++++ (bright blue)
172		++	++ (light blue)
182		+++	++ (light brown/blue)
188		+++	++ (light blue white)
203		+++	+ (brownish blue)
206		++	++ (light blue)
213		+	+ (very light blue)
217		+	+ (very light blue)
218		++++	++ (whitish blue)
221		+++	++++ (bright blue)
228		++	++ (light blue)

Colony #	Growth on TDO (*HIS3 activation*)	Growth on QDO (*ADE2 activation*)	X-α-galactosidase (colour, *MEL1 activation*)
236		++++	++++ (bright blue)
239		++	+ (brown blue)
241		++	++ (light blue)
243		+++	++ (brown blue)
244		++++	+++ (darker light blue)
249		+	++++ (bright blue)
251		+++	++ (light blue)
252		+++	++ (blue yellow)
264		++	+ (very light blue)
268		+++	++ (very light blue)
277		++	++ (light blue)
279		++	++ (light blue)
281		++	+ (yellowy blue)
282		++	+ (brown blue)
291		++	++ (light blue)
293		++	++ (very light blue)
294		++	+ (yellow light blue)
295		+	+ (brown blue)
297		++	+ (very light blue)
303		+++	++ (light blue)
305		++	+ (very light blue)
315		++	+ (brown blue)
319		+++	++++ (bright blue)
320		+++	++ (light blue)
326		+	+ (very light blue)
334		++	++ (light blue)
336		+++	++ (light blue)
342		+++	++ (light blue)
348		++	+ (brown blue)

Colony #	Growth on TDO (*HIS3 activation*)	Growth on QDO (*ADE2 activation*)	X-α-galactosidase (colour, *MEL1 activation*)
350		+	++ (cream blue)
361		++++	++ (brown light blue)
367		++	+++ (darker blue)
373		+++	++++ (bright blue)
374		+++	++ (creamy yellow blue)
375		++	++ (cream blue)
376		+	++++ (very blue)
380		+	+ (very light blue)
388		++++	++ (light cream blue)
390		++++	++++ (bright blue)
393		++	++ (cream blue)
396		++	++ (cream blue)
402		+	++++ (bright blue)
405		++	++ (blue white)
407		+	+ (brownish blue)
410		++++	++ (blue, mostly yellow)
417		+	++++ (bright blue)
418		+++	++++ (bright blue)
423		+	+++ (dull blue)
424		++	+++ (dull blue)
425		++	+++ (yellowish blue)
437		++++	+ (blue, mostly cream brown)
438		++++	++ (blue, mostly cream brown)
441		++	++ (light blue)
446		+	+ (brownish blue)
447		+	++++ (bright blue)
449		+	++ (whitish light blue)
459		+++	+++ (darker blue)

Colony #	Growth on TDO (*HIS3 activation*)	Growth on QDO (*ADE2 activation*)	X-α-galactosidase (colour, *MEL1 activation*)
460		+	+ (light blue, more white)
462		++	++ (light blue)
463		++	++ (cream light blue)
464		++++	++ (brownish blue)
467		++	++ (light blue)
472		+	+ (dark brown blue)
476		+++	++++ (bright blue)
477		+++	+ (very light blue)
486		++	+ (very light blue)
489		+	++ (light blue)
490		+++	+ (creamy yellow blue)
493		++	++ (light blue)
500		+++	+ (creamy yellow blue)
502		++	++ (light blue)
512		+	+ (very light blue)
516		++	+ (whitish cream blue)
530		+++	+++ (blue, dark brown area)
532		++	++ (light blue)
533		+++	+ (cream brown blue)
541		++	+ (very light blue)
545		+++	+ (creamy yellow blue)
552		++	++ (light blue)
553		++++	++++ (bright blue)
554		++	++ (light blue)
556		++	+ (brown blue)
557		++++	+ (brown blue)
558		++	++ (green blue, white areas)
560		++	+ (light blue, mostly brown & pink)
563		++	++ (light blue, mostly pink)

Colony #	Growth on TDO (*HIS3 activation*)	Growth on QDO (*ADE2 activation*)	X-α-galactosidase (colour, *MEL1 activation*)
564		+	+ (very light yellow blue)
576		++	++ (creamy light blue)
584		+++	++++ (bright blue)
585		+++	++ (creamy blue green)
586		+++	++++ (bright blue)
587		+++	++ (creamy blue green)
589		++	++ (creamy blue green, more white)
590		+	++ (creamy blue green)
596		++	++ (creamy blue green)
598		++	++ (creamy light blue)
614		++	+ (very light blue)
615		+	+ (yellow cream blue)
619		++	+ (creamy yellow blue)
625		+++	+ (very light blue, yellow patches)
626		+++	+ (dark brown blue)
640		++++	++ (creamy light blue)
652		+	++ (light blue)
657		+++	+ (very light blue)
668		++++	++ (light blue, brown patches)
670		+	+++ (darker blue)
673		++	++ (creamy light blue)
682		+	+ (very light blue green)
683		+	+ (very light blue green)
694		+	+++ (darker blue)
696		++++	+ (very light blue green)
702		++	++++ (bright blue)
704		+++	++ (creamy blue green)
719		++++	++ (creamy yellow blue green)
724		++++	++ (creamy blue green)

Colony #	Growth on TDO (*HIS3 activation*)	Growth on QDO (*ADE2 activation*)	X-α-galactosidase (colour, *MEL1 activation*)
728		++++	++++ (bright blue)
729		+	++ (creamy blue green)
733		++	++ (creamy blue green)
734		++++	++ (creamy blue green)
735		++++	++ (creamy blue green)
736		+	++ (creamy blue green)
746		++	+++ (darker bright blue)
747		++	+ (light brown blue)
764		++	+ (very light blue)
767		+++	++ (light cream blue)
770		++	+++ (darker bright blue)
781		++	+ (very light blue)
791		++	+++ (bright light blue)
793		++	+ (creamy brown blue)
796		+++	+++ (very dark cream blue)
798		+	+ (very light blue)
801		++	+ (light brown blue)
806		++	+++ (dark light blue)
807		++++	++ (creamy blue green)
808		+++	++ (creamy blue green)
813		++	++ (creamy brown blue)
817		++	+++ (dark blue)

TDO= solid media lacking Leu, Trp and His, QDO= solid media lacking Leu, Trp, His and Ade. Growth of clones on solid media: ++++ = very good; +++ = good; ++ = weak; +=very weak, - = no growth

3.1.3.1. Heterologous mating

Primary clones, viz. prey clones that lead to strong activation of the *MEL1* gene, clones that produced bright blue colonies during the x-α-galactosidase assay in addition to activation of the *ADE2* and *HIS3* reporter genes were subjected to heterologous matings (section 2.14.10). Due to time constraints and the vast number of clones able to activate both ADE2 and HIS3 reporter genes, only primary prey clones and not secondary

prey clones were subjected to heterologous bait matings. The results of these heterologous mating experiments are shown in Table 3.3.Following heterologous mating experiments, only 21 of the 37 primary clones showed binding specificity for the WDR47 bait protein (Table 3.3). The inserts of these prey constructs were subsequently analysed by automated nucleotide sequence analysis.

Table 3.3. Interaction of preys with heterologous baits in specificity tests as assessed by *HIS3* and *ADE2* reporter gene activation- Primary clones

Clone #	x pGBK-WDR47 TDO	x pGBK-WDR47 QDO	x pGBKT7 TDO	x pGBKT7 QDO	x pGBK53 TDO	x pGBK53 QDO	x pGBK-C5C10 TDO	x pGBK-C5C10 QDO
16	++++	++++	++++	+	++++	-	++++	-
34	++++	++++	+++	-	+++	-	++++	-
46	++++	++++	++++	++	+++	+	+++	+
50	++++	++++	+++	-	++++	-	++++	-
52	++++	-	++++	-	+++	-	++++	-
76	++++	++++	+++	++	+++	-	+++	-
86	++++	+++	+++	+	+++	-	+++	-
87	++++	-	+++	-	+++	+	+++	+
97	++++	++++	+++	++	+++	-	+++	-
105	++++	++++	+++	-	++	-	+++	-
113	++++	++++	+++	+	+++	-	+++	-
114	++++	+++	+++	-	+++	-	+++	-
115	++++	++++	+++	-	++	-	++++	+
119	++++	++++	+++	-	+++	-	+++	+
121	++++	++++	+++	-	+++	-	+++	+
122	++++	++++	++++	-	++++	-	++++	-
135	++++	++++	++++	++	++++	++	++++	++
143	++++	++++	++++	-	++++	+	++++	+

145	++++	++++	++++	-	++++	-	++++	-
160	++++	++++	++++	-	++++	-	++++	++
221	++++	-	++++	-	++++	-	++++	-
236	++++	+	++++	-	++++	-	++++	+
244	++++	++++	++++	++	++++	++	+++	++
268	++++	++	++++	+	+++	+	+++	-
293	++++	+++	+++	++	++++	++	++++	+
319	++++	+++	++++	+++	++++	++	++++	+
336	++++	-	++++	-	++++	-	++++	-
373	++++	-	++++	-	++++	-	++++	+
417	++++	-	++++	-	++++	-	++++	-
418	++++	-	++++	-	++++	-	++++	-
476	++++	-	++++	+	++++	-	++++	-
553	++++	-	+++	-	++++	++	++++	-
584	++++	-	+++	+	+++	-	+++	-
586	++++	-	++++	-	++++	-	++++	-
668	++++	-	++++	-	++++	-	++++	+
702	++++	-	++++	-	++++	-	++++	-
806	++++	-	++++	-	+++	-	++++	-

Pink font denotes clones that were selected based on their ability to activate reporter genes in the absence of heterologous baits, hence used in further analysis. TDO= solid media lacking Leu, Trp and His, QDO= solid media lacking Leu, Trp, His and Ade. Growth of clones on solid media: ++++ = very good; +++ = good; ++ = weak; +=very weak, - = no growth.

3.1.3.2. Sequence analysis

The 21 prey clones were sequenced and their identity determined by searching nucleotide and protein databases. The identities of these interacting clones are shown in Table 3.4. The frame and integrity of the prey sequences were analysed using ChromasPro computer software and DNAman™ version 4 software, and subsequently subjected to Genbank BLAST database using both BLASTN (nucleotide sequences) and BLASTP (in frame protein sequences) (http://www.ncbi.nlm.nih.gov/Entrez). Eight of the 21 sequenced clones contained prey insert sequences which were rejected as their open reading frames (ORFs), fused to the GAL4-AD ORF, did not match the ORF predicted from the gene locus in the NCBI Genbank (http://www.ncbi.nlm.nih.gov) protein database. This is not unusual, as only one sixth of the clones represented within the Matchmaker™ pretransformed cDNA libraries are predicted to be in the correct reading frame (Clonetech MATCHMAKER Two-Hybrid Assay Kit User Manual).

Of the in-frame clones, one primary clones were discarded as positive interactors due to their cellular localisation, as the identified cellular compartment was incompatible with WDR47's cytosolic cellular localisation (Kinnear, 2007). Two of the identified protein sequences, for SNAPIN and SCG10, were represented by multiple clones. The identities of the clones are shown in Table 3.4.

Table 3.4. Identification of plausible WDR47 interacting clones from the Y2H screen.

Clone	Genomic		Protein		Cellular localisation and Function
	Blastn acc (e-value)	**ID**	**Blastp acc (e-value)**	**ID**	
34, 86, 114, 115, 122, 143*	NM_007029.2 (0.0)	Homo sapiens stathmin-like 2 (STMN2)	gb | AAB36428.1 | (9e-90)	SCG10 [Homo sapiens]*	**Cytoplasm (soluble or membrane bound) -** Member of the Stathmin gene family of microtubule destabilising phosphoproteins. Involved in the regulation of neurite outgrowth by controlling dynamic properties of neuronal microtubules. Neuronal specific, and developmentally regulated.
97, 244, 293*	NM_012437.3 (0.0)	Homo sapiens SNAP-associated protein (SNAPIN)	sp | O95295 | S25BP_HUMAN (7e-37)	SNARE-associated protein Snapin *	**Cytoplasm or transmembrane, cytoplasmic vesicle or cytoplasmic vesicle membrane** – forms part of the SNARE complex essential for synaptic vesicle docking and fusion
46	NM_005493.2 (0.0)	Homo sapiens RAN binding protein 9 (RANBP9)	sp | Q96S59 | RANB9_HUMAN (1e-163)	Ran-binding protein9 (RanBP9)	Extracellular matrix
160*	NM_000858.4 (0.0)	Homo sapiens guanylate kinase 1 (GUK1)	gb | AAH07369.2 | (4e-84)	GUK1 protein [Homo sapiens]*	**Cytoplasm** – involved in GMP recycling
319*	NM_014780.3 (0.0)	Homo sapiens cullin 7 (CUL7)	sp | Q14999.2 | CUL7_HUMAN (4e-139)	Cullin-7 (CUL7)*	**Cytoplasm (by function)** – component of the ubiquitin ligase complex, involved in the ubiquitination pathway targeting proteins for proteosomal degradation
16	NM_018241.1 (0.0)	Homo sapiens transmemebrane protein 34 (TMEM34)	*No significant similarity*		N/A
50	NM_001838430 .2 (0.0)	Homo sapiens chromosome 17 genomic contig	*No significant similarity*		N/A

76	NT_007299.12 (0.0)	Homo sapiens chromosome 6 genomic contig	*No significant similarity*		N/A
113	NM_002509.2	Homo sapiens NK2 homeobox 2 (NKX2-2), mRNA	*No significant similarity*		N/A
119	NT_007299.12 (0.0)	Homo sapiens chromosome 6 genomic contig, ref assembly	*No significant similarity*		N/A
121	NM_018183.2 (0.0)	Homo sapiens strawberry notch homolog 1 (Drosophila) (SBNO1)	*No significant similarity*		N/A
135	NM_006387.5 (0.0)	Homo sapiens calcium homeostasis endoplasmic reticulum protein	*No significant similarity*		N/A
145	NM_001013839 .1	Homo sapiens exocyst complex component 7 (EXOC7)	*No significant similarity*		N/A
268	NW_001838952 .2 (0.0)	Homo sapiens chromosome 5 contig, alternate assembly	*No significant similarity*		N/A

*- represent the clones that will further be investigated using 3D co-localisation

3.2. Ligands used for further analysis

Of the 21 putative prey clones identified by sequence analysis nine were discarded due to out of frame nucleotide sequences, while one was discarded based on incompatible cellular locations. Therefore 11 clones (four multiply represented proteins- Guk1, Cul7, SNAPIN and SCG10) were identified as putative WDR47 ligands. These clones were then subjected to further analysis to verify if the interactions with WDR47 occurred in a mammalian system. To test for such *in vivo* interaction, *in vivo* three-dimensional co-localisation using fluorescence microscopy was performed.

3.2.1. Three-dimensional *in vivo* co-localisation using fluorescence microscopy

In vivo co-localisation using fluorescence microscopy was employed to assess the interaction of WDR47 with SCG10, SNAPIN, Cul7 and Guk1 (Figures 3.4-3.6). The panels of images presented represent a single frame of the 13 images that were captured for the Z-stack (images taken at 0.3 microns right through the cell, thus the co-localised images are a collection of images at different depths throughout the cell). In all these figures, images A-C shows a single colour channel with, A representing the yellow channel for localization of the WDR47-YFP, B representing the red channel for localization of the respective preys with Texas Red-labelled secondary antibody, and C representing the co-localised image of both the bait and prey proteins, while image D shows an over!ay of the four colour channels used including the nuclear stain. In all the samples, the proteins investigated showed no nuclear localisation and appeared to be localised to the cytoplasm, yet only SCG10 co-localised with WDR47 (Figure 3.6 C). These results confirm that neuronal specific SCG10 interacts with WDR47 in GT-17 hypothalamus cells. However, it appears as if SNAPIN co-localises with WDR47 (Figure 3.6 C), although these results are inconclusive as this image represents the maximal image projections, and the area of co-localisation is not above the background for that seen in image B of the secondary antibody. Thus, the WDR47-SNAPIN interaction needs to be further investigated, yet due to time constraints this was not possible for the present study and only the definite WDR47-SCG10 interaction will further be discussed.

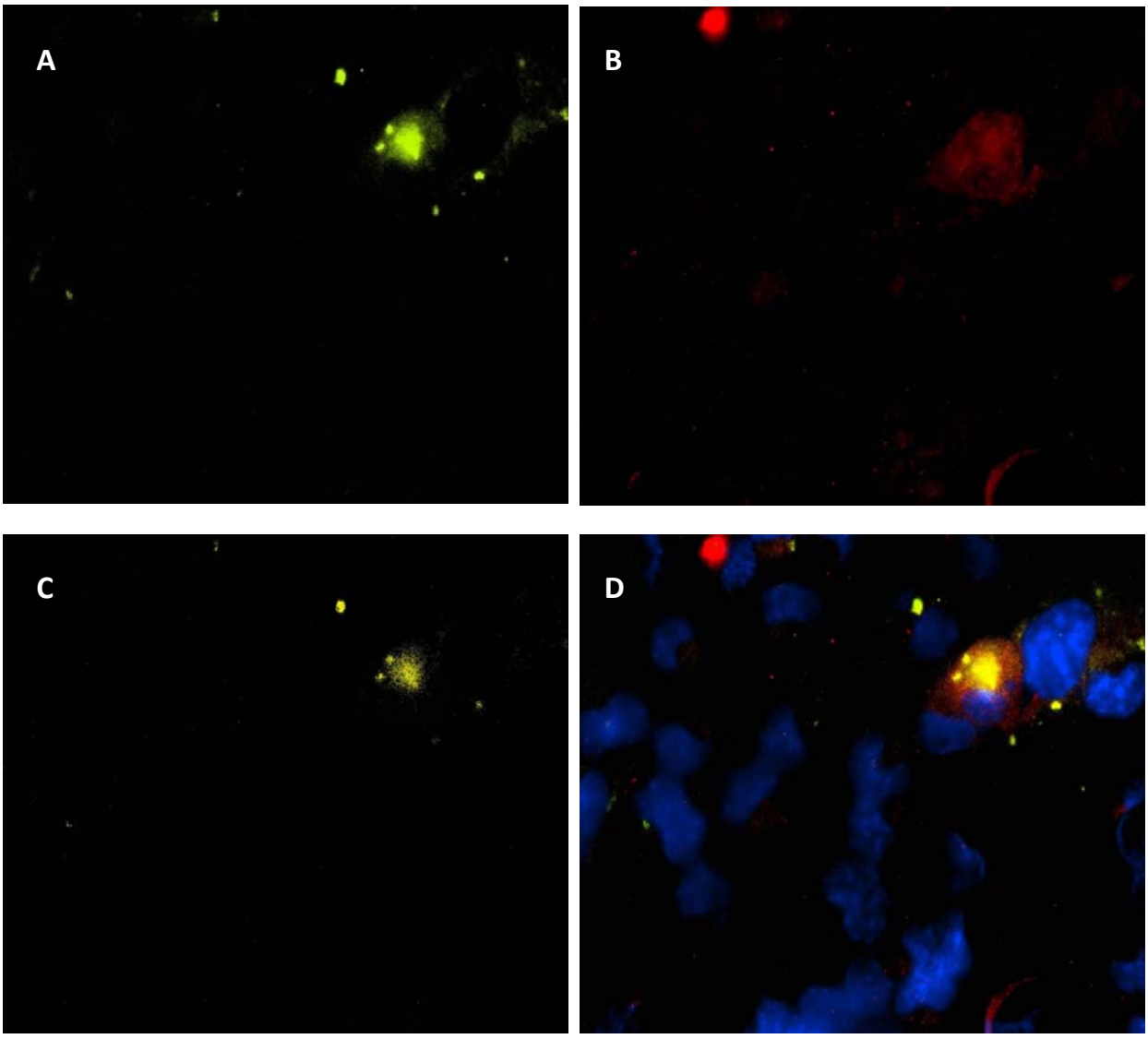

Figure 3.4. Fluorescence imaging of Cul7 and WDR47 in GT-17 cells. (A) YFP-tagged WDR47 (yellow). (B) Cullin7 TxRed labelled (red). (C) Co-localisation of WDR47 and Cul7 generated from Z-stack (yellow). (D) Overlay of images A-C with Hoechst H-33342 labelling of the nuclei (blue). Magnification: 60X oil immersion before 70% reduction.

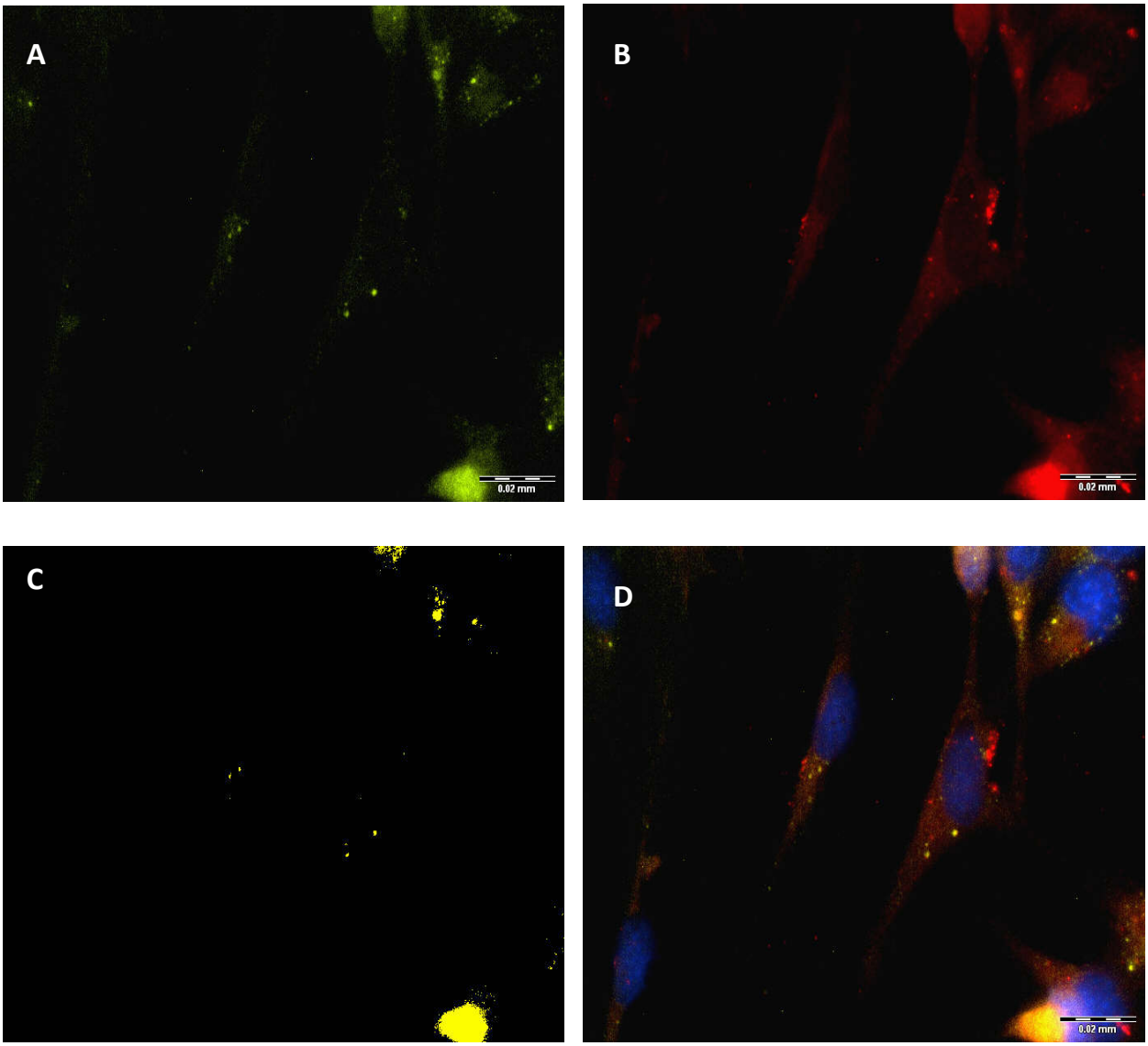

Figure 3.5. Fluorescence imaging of Guk1 and WDR47 in GT-17 cells. (A) YFP-tagged WDR47 (yellow). (B) Guanylate Kinase 1 TxRed labelled (red). (C) Co-localisation of WDR47 and Guk1 generated from Z-stack (yellow). (D) Overlay of images A-C with Hoechst H-33342 labelling of the nuclei (blue). Magnification: 60X oil immersion before 70% reduction.

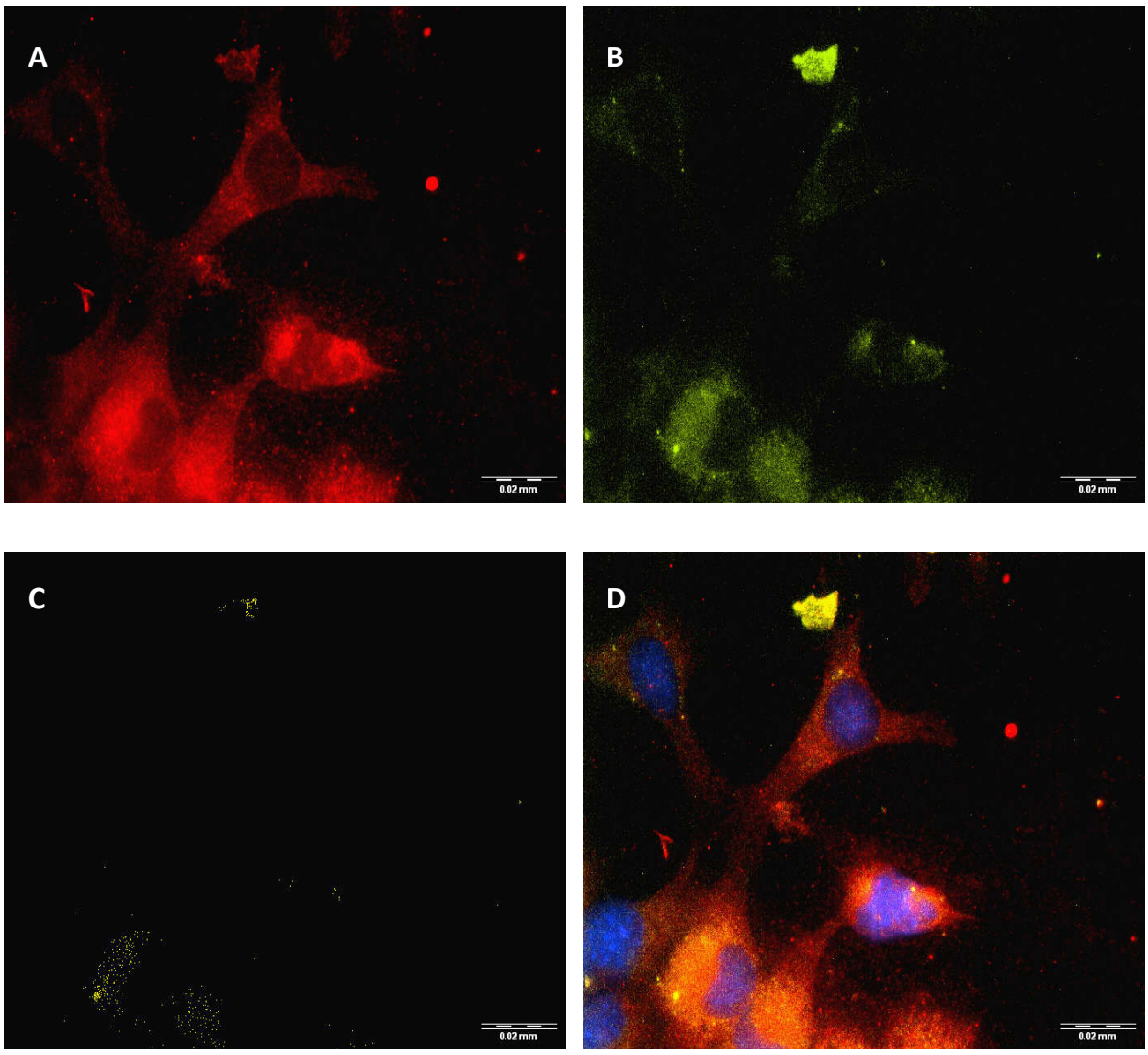

Figure 3.6. Fluorescence imaging of SNAPIN and WDR47 in GT-17 cells. (A) YFP-tagged WDR47 (yellow). (B) SNARE-associated protein (SNAPIN) TxRed labelled (red). (C) Co-localisation of WDR47 and SNAPIN generated from Z-stack (yellow). (D) Overlay of images A-C with Hoechst H-33342 labelling of the nuclei (blue). Magnification: 60X oil immersion before 70% reduction.

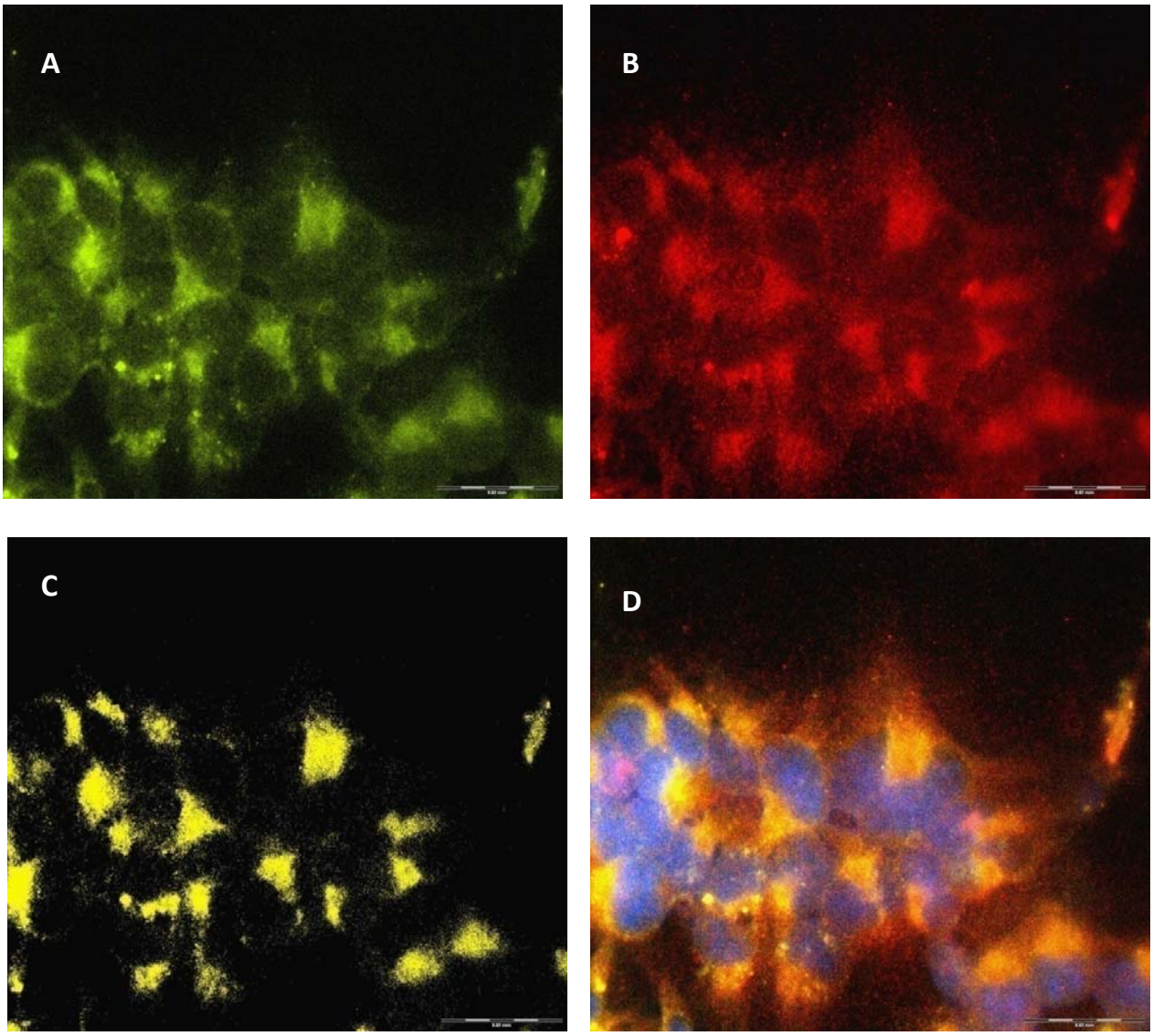

Figure 3.7. Fluorescence imaging of SCG10 and WDR47 in GT-17 cells. (A) YFP-tagged WDR47 (yellow). (B) Stathmin-like 2 (SCG10) TxRed labelled (red). (C) Co-localisation of WDR47 and SCG10 generated from Z-stack (yellow). (D) Overlay of images A-C with Hoechst H-33342 labelling of the nuclei (blue). Magnification: 60X oil immersion before 70% reduction.

CHAPTER FOUR: DISCUSSION

INDEX **PAGE**

CHAPTER FOUR: DISCUSSION

Cortical development is an intricately regulated process resulting in the proper lamination and organisation of the neocortex. This complicated process relies on the ordered migration of neurons from their place of birth to their proper final destination within the six-layered neocortex. The proper migration of neurons is crucial for the organisation and the function of the neocortex, which is responsible for numerous tasks, most notably, in humans, higher cognition and memory (Kaas, 2000; Kaas, 2007; Douglas and Martin, 2007).

One of the key regulators of neuronal migration during neocortical development is Reelin, an extracellular matrix glycoprotein.Despite the vast amount of research on Reelin and the Reelin signalling pathway, the precise mechanism in which Reelin controls cortical lamination is still largely unknown. To date numerous Reelin interacting proteins have been identified, and more recently Kinnear and colleagues (Kinnear, 2007) identified a novel interaction between the N-terminal reeler domain of Reelin and WDR47, a protein of unknown function.

The WDR47 protein belongs to a family of highly conserved proteins, of which the tryptophan-aspartic acid (WD) dipeptide at the C-terminus is characteristic to each protein at variable lengths (section 1.6.1). This family of proteins have been implicated in several cellular functions from signal transduction to cytoskeletal rearrangements (section 1.6.1). In the present study, the N-terminal domain of WDR47 (section 1.6) was used as bait in a Y2H screen to identify interacting proteins. Identification of its binding partners will ultimately aid in a better understanding not only of the function of WDR47, but also in further elucidating the function of the Reelin signalling pathway in regulating cortical lamination.

The results of the Y2H screen yielded 21 putative WDR47-interacting clones based on their ability to activate all reporter genes within the system. However, only four clones were deemed plausible as nine clones were not in the correct reading frame and a further one clone encoded proteins that reside in cellular compartments that renders them inaccessible to interact with cytosolic WDR47.

4.1. YEAST TWO-HYBRID ANALYSIS TO IDENTIFY INTERACTORS OF THE N-TERMINAL DOMAIN OF WDR47

4.1.1. Number of independent clones screened

The library mating efficiency calculations indicated that approximately 8.4 x 10^5 pre-transformed foetal brain cDNA library clones were screened (section 3.1.2.4). Therefore, since the pre-transformed

foetal brain cDNA library used contained approximately 3.5 x 10^6 independent clones, a number of library clones were not tested as plausible WDR47 interactors. It may therefore be possible that some putative WDR47-interacting proteins could have been missed in the current screen.

4.1.2. Preys excluded from further analysis

Upon completion of the Y2H and subsequent stringency experiments which tested for the activation of both nutritional and colorimetric reporter genes, 21 clones were identified. However, sequence analysis of the 21 putative interacting clones showed that ten were unlikely to encode biologically relevant WDR47 interacting proteins for the following reason, and were thus excluded:

4.1.2.1. No significant protein matches

Although several insert sequences had significant DNA matches in the NCBI Genbank (http://www.ncbi.nlm.nih.gov) or Ensemble (http://www.ensembl.org) databases, many of these inserts were either not in-frame in accordance with the reading frame dictated by the upstream GAL4 domain and/or once translated had no significant protein matches in the database. One reason for the lack of significant protein matches in spite of significant DNA matches, is due to the limitations of the commercially available cDNA libraries used in a classical Y2H screen. The CLONETECH library used in the present investigation is derived from oligo-dT primed cDNA [generated from mRNA using a oligo(dT)15 primer containing a degenerate nucleotide site which positions the primer to the proper transcript at the poly-A tail (Borson *et al.,* 1992). This method enhances the representation of full-length clones and 3' ends in the engineered library (Chenchik *et al.,* 1994; Borson *et al.,* 1992; Moqadam & Siebert, 1994), which means that only one out of six of all cloned inserts are in-frame with the transcription factor activation domain (van Criekinge and Beyaert, 1999).

4.1.2.2. Incompatible cellular compartments

The sub-cellular localisation of proteins is helpful in understanding their functions. It is also not possible for proteins in different sub-cellular compartments to interact with one another. Therefore, proteins localised to sub-cellular compartments incompatible with WDR47 (cytosolic) localisation were excluded from further analysis. However, for some proteins, the sub-cellular localisation has not yet been experimentally determined. To overcome this obstacle several online sub-cellular localisation tools have been developed which predicts a proteins sub-cellular localisation based on amino acid sequence information (Hua and Sun, 2001; Emanuelssen *et al*., 2001; Nair and Rost, 2002). These prediction tools are somewhat restricted in their function as they have a limited accuracy for predicting sub-cellular localisation and they have limited coverage of the number of sub-cellular regions (Lu *et al*., 2003).

The accuracy of the publically available sub-cellular localisation prediction programmes vary rather substantially. Thus, the present study used two prediction programmes, namely "Proteome Analyst" and "ESLpred" which have a reported prediction accuracy of 92% (Lu *et al.,* 2003) and 88% respectively. In spite of the several other programmes available to predict sub-cellular localisation, these two programmes were used as they have the highest accuracy and cover nine cellular compartments (cytoplasm, endoplasmic reticulum, extracellular, golgi, lysosome, mitochondria, nucleus, peroxisome and plasma membrane).

Using these prediction programmes, only four in frame clones were found to encode proteins that localised to the cytoplasm a cellular compartment compatible with WDR47 localisation. However, as the automated prediction programmes are not 100% accurate, it remains possible that some preys identified may have been assigned to incorrect cellular compartments, but due to project constraints, the predicted sub-cellular localisation of each prey was not verified experimentally.

4.1.3. Preys identified as putative WDR47 ligands

Four in-frame prey proteins, encoding Cul7, Guk1, SNAPIN and SCG10, were identified as plausible WDR47 interacting proteins by their compatible cytoplasmic comparmentalization. Due to the limitations of Y2H analysis, further *in vivo* studies were employed to verify these interactions.

4.2. VERIFICATION STUDIES

Due to the various limitations of Y2H (section 4.5), three-dimensional *in vivo* co-localisation was used to verify the putative WDR47-interactors in the present investigation. Of the four putative interactions detected by Y2H, the *in vivo* co-localisation only verified the WDR47-SCG10 interaction. It should however be noted that the co-localisation of SNAPIN and WDR47 needs to be further verified, as the images obtained were inconclusive due to the fact that the area of co-localisation seen was not above the background for that seen in image B (Figure 3.6. B) of the secondary antibody. Therefore, the co-localisation between WDR47 and SNAPIN needs to be re-investigated however; due to time constraints this was not possible for the present study. So, in the present investigation, only the interaction between WDR47 and SCG10 was deemed conclusive and therefore, only this interaction will be discussed further although SNAPIN will be briefly discussed.

4.3. SNAPIN

Neurons release neurotransmitters by excocytosis of synaptic vesicles (Vites *et al.,* 2004). The process of neurotransmitter release is dependent on synaptic vesicle docking and fusion via the association of neuronal proteins on the vesicle and plasma membranes. This interaction ensures the docking of the

vesicle to the plasma membrane and fusion of the two membranes releasing the neurotransmitters contained within the vesicles (Ilardi *et al.,* 1999). The formation of the soluble *N*-ethyl maleimide sensitive factor adaptor protein receptor (SNARE) core complex is essential for vesicular transport and in the docking and fusion process (Ilardi *et al.,* 1999). The assembly of a stable SNARE complex consists of the vesicle-associated protein synaptobrevin (VAMP), which interacts with two plasma-membrane associated proteins syntaxin and the 25kDa synaptosomal associated protein SNAP-25 (Trimble *et al.,* 1988; Oyler *et al.,* 1989; Bennett *et al.,* 1992; Söllner *et al.,* 1993; Calakos *et al.,* 1994; Fasshauer *et al.,* 1998; Hilfiker *et al.,* 1999). The assembly of this complex is thought to pull together the vesicle and the plasma membrane, initiating the docking/fusion reaction (Chen and Scheller, 2001; Vites *et al.,* 2004).

SNAPIN, a 15kDa protein, was first identified as a SNAP-25 binding partner that associates with the SNARE complex and increases the binding of synaptotagmin to the SNARE complex (Ilardi *et al.,* 1999). Synaptotagmins are integral Ca^{2+} binding proteins located on the membranes of synaptic vesicles, providing Ca^{2+} dependent regulation of the fusion process and neurotransmitter release (Augustine, 2001; Chapman, 2002). SNAPIN is a ubiquitously expressed soluble phospho-protein, present in both the cytosol and peripheral membranes (due to transmembrane domain located at the N-terminal) (Buxton *et al.,* 2003; Vites *et al.,* 2004; Ruder *et al.,* 2005). The synaptotagmin-SNARE binding activity of SNAPIN is further enhanced by the protein kinase A (PKA) phosphorylation of SNAPIN at Ser50, ultimately increasing the excocytosis of neurotransmitters (Chheda *et al.,* 2001). Thus, SNAPIN provides a direct molecular link between the fusion/docking machinery and second messenger pathways (Tian *et al.,* 2005).

It seems as if SNAPIN could be a possible interactor of WDR47, based on SNAPINs role in excocytosis and vesicular content release. It could serve as a mechanism by which excess WDR47 is removed from neuronal cells. WDR47 could possibly facilitate the attachment of vesicles for release to the plasma membrane via the interaction with SNAPIN. The results from the current study regarding SNAPIN need to be re-investigated and confirmed using additional biochemical assays. However, due to time constraints this did not form part of the present study.

4.4. SCG10-WDR47 INTERACTION AND NEURONAL MIGRATION

The data presented in the present study revealed a novel and exciting interaction between WDR47 and SCG10, however to fully appreciate the significance of this interaction one needs to understand the role of microtubules in migrating neurons. Therefore, the sections that follow will give a brief overview on microtubules, and microtubule dynamics during neuronal migration.

4.4.1. Neuronal migration and the neuronal cytoskeleton

Neuronal migration involves many aspects of intrinsic cytoskeletal regulation and reorganisation (Feng and Walsh, 2001). Therefore, several proteins involved in neuronal migration ultimately function by regulating the neuronal cytoskeleton (Feng and Walsh, 2001). The cytoskeleton of most eukaryotic cells is composed of both actin filaments and microtubule (MIT) arrays, each of which is regulated by associated proteins to control migration and also to confer structural support to non-migrating neurons (Desai and Mitchison, 1997; Nogales and Wang, 2006).

Whereas mature neurons are highly polarised cells that typically have one thin, long axon (to transmit information) and several shorter, branched dendrites (to receive information) (Craig and Banker, 1994; Witte *et al.,* 2008), developing neurons begin their journey as simple, symmetric spheres in the proliferative layers (Witte and Bradke, 2008). The formation of the leading edge (axon) is the first step in neuronal migration and in the establishment of neuronal polarity (Witte and Bradke, 2008). The extension of axons, and ultimately neuronal migration, is controlled by extracellular guidance cues which are temporally and spatially distributed within the developing neocortex (Gordon-Weeks, 2003; Tessier-Lavigne and Goodman, 1996). These guidance cues are detected by highly motile and dynamic structures known as growth cones, situated at the tips of growing neurites, which guide axons towards their target regions (Dickson, 2002; Gordon-Weeks, 2003; Kalil and Dent, 2005). Growth cones have both sensory and motor capabilities, allowing them to integrate the information relayed by the guidance cues into appropriate behaviours (Gordon-Weeks, 2003). These behaviours are most commonly a steering movement either towards (attraction) or away (repulsion) from the guidance cues, followed by vectorial growth towards the pial surface (Gordon-Weeks, 2003).

The movement of the growth cone in response to guidance cues is controlled by the organisation and dynamics of both the actin and microtubule cytoskeleton (Dent and Gertler, 2003; Kalil and Dent, 2005). The growth cone can be divided into two main domains or regions, the central domain (C) which is dominated by microtubule arrays, and the peripheral domain (P) which is dominated by actin filaments that form both a meshwork in the veil-like lamellipodia and bundles in the finger-like filopodia (Gordon-Weeks, 2003; Kalil and Dent, 2000; Smith, 1988). Filopodia are the structures responsible for pathfinding via the detection of guidance cues and the steering of the growth cone in response to these cues (Gordon-Weeks, 2000; Gordon-Weeks, 2003; Kalil and Dent, 2005).

The role of the actin cytoskeleton in neuronal migration and neurite outgrowth has been extensively studied, and it is well known that actin dynamics plays a crucial role in cell motility (Kalil and Dent 2005). More recently, emphasis has been on the role of MITS and MIT dynamics during neuronal and cellular elongation and/or migration. Of particular interest to the present study is the fact that the

identified WDR47-interacting protein, SCG10, is a key regulator of microtubule dynamics during neuronal migration (Lutjens *et al.,* 2000; Mori and Morri, 2002; Stein *et al.,* 1988; Sugiura and Mori, 1995).

4.4.2. Superior Cervical Ganglion10 (SCG10)

Superior Cervical Ganglion10 is a developmentally regulated neuron-specific protein that is abundantly expressed in the growth cones of developing neurons (Curmi *et al.,* 1997; Di Paolo *et al.,* 1997; Lutjens *et al.,* 2000; Mori and Morri, 2002; Stein *et al.,* 1988; Sugiura and Mori, 1995). SCG10 belongs to the family of phosphoproteins known as stathmins, which include stathmin, SCG10, SCLIP, RB3, and its splice variants RB3' and RB3'' (Schubart *et al.,* 1989). Structural and biochemical studies have shown that each stathmin protein can bind two tubulin heterodimers and that each contributes to the regulation of MIT dynamics by inhibiting MIT polymerization (favouring depolymerization) thereby negatively regulating MIT stability (Charbaut *et al.*,2001;Curmi *et al.*,1999; Horwitz *et al.*,1997; Ravelli *et al.,* 2004,). The MIT destabilising activity of the stathmin family of proteins is regulated by phosphorylation, i.e. phosphorylation of these proteins inhibit their MIT destabilising activity (Mori and Morri, 2002).

Each member of the stathmin family contains a conserved C-terminal stathmin-like domain, which is composed of a regulatory domain, a tubulin binding domain and an N-terminal domain (Maucuer *et al.,* 1993; Ozon *et al.,* 1997, 1998; Stein *et al.,* 1988; Schubart *et al.,* 1989; Togano *et al.,* 2005) (Figure 4.1). For SCG10 (179 amino acids), the N-terminal includes sites for palmitoylation (a dynamic type of acetylation) which enables the attachment of SCG10 to growth cone vesicles and Golgi localisation (Di Paolo, 1997b; Grenningloh *et al.*,2004; Lutjens *et al.*,2000) (Figure 4.1). Essentially, when palmitoylation is inhibited SCG10 is no longer targeted to the growth cone where it is associated with vesicular structures (Grenningloh *et al.,* 2004). The SCG10-bound growth cone vesicles associate with labile MITs in the growth cone, suggesting that SCG10 could possibly bind directly to MITs (Di Paolo *et al.,* 1997b, Riderer *et al.,* 1997). In SCG10, the stathmin-like domain is organised into two overlapping sub-domains, the regulatory domain which contains four serine phosphorylation sites (S50, S62, S73 and S97), each phosphorylated by distinct kinases (such as cdk5, Protein kinase A and MAP kinase) (Antonsson et al.,1997) (Figure 4.1) and the interacting domain which forms the α-helical structure responsible for the coiled-coil interactions with other proteins such as tubulin (Curmi *et al.*,1994; Doye *et al.*,1989; Mauceur *et al.*,1990) (Figure 4.1).

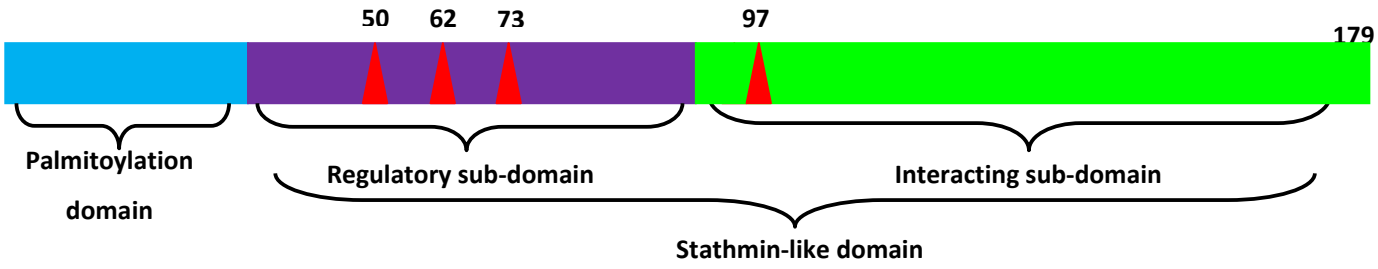

Figure 4.1. Schematic representation of the microtubule destabilising protein SCG10. The N-terminal blue represents the palmitoylation domain responsible for membrane anchoring of SCG10 to growth cone vesicles. The purple represents the regulatory sub-domain of the conserved stathmin-like domain, while the red triangles represent the serine phosphorylation sites. The green represents the interacting sub-domain of the stathmin-like domain, which is responsible for the tubulin interaction and MIT destabilising activity of SCG10 (adapted from Curmi *et al.,* 1997).

Although SCG10 shares similar characteristic features to stathmin, small distinctive features separate these two proteins. One such characteristic is that SCG10 is a potent MIT destabilising factor, which promotes catastrophe (growth to shrinkage) of MITs. Unlike stathmin which is present in developing neurons and neuronal glial tracts, SCG10 is exclusively expressed in developing neurons, with the highest level of expression during development, but with drastically decreased expression in the adult brain. However, some expression of SCG10 persists in areas associated with synaptic plasticity (Himi *et al.,* 1994; Ozon *et al.,* 1993; Sugiura and Mori 1996).

To better understand SCG10 and the crucial role it plays in neuronal migration via its actions on MITs, one needs to understand MITs themselves and the dynamic properties they exhibit which allow them to respond to guidance cues such as Reelin.

4.4.2.1. Microtubules

Microtubules are non-covalent, polarised polymers of composed of tubulin dimers assembled into linear arrays (Dent and Gertler, 2003; Desai and Mitchison, 1997). Tubulin dimers are composed of one α-tubulin subunit and one β-tubulin subunit, forming an α/β heterodimer (Dent and Gertler, 2003; Desai and Mitchison, 1997; Gordon-Weeks, 2003). Microtubule polymerization, the head-to-tail association of α/β heterodimers forms a protofilament. In neuronal cells thirteen protofilaments associate laterally to form a long, hollow, cylindrical microtubule structure (Dammermann *et al.,* 2003; Dent and Gertler, 2003; Desai and Mitchison, 1997). Due to the head-to-tail configuration of the heterodimers, MITs are inherently polarised, with the N-terminal of the β-tubulin subunit directed to the faster polymerizing 'plus' end, and the α-tubulin subunit facing the slower polymerizing 'minus' end (Dammermann *et al.,*2003; Dent and Gertler, 2003). This intrinsic polarity of microtubules is critical to their function (Dammermann *et al.,* 2003). As a rule of thumb, the plus end

of the MIT is considered the most dynamic i.e. it has the ability to grow and shrink, whereas the minus end is inherently unstable and shrinks unless stabilized by minus end capping proteins or via attachment to the microtubule organization centre (MITOC) (Dent and Gertler, 2003; Gordon-Weeks, 2003).

In neuronal cells, MITs in the axonal growth cones are arranged so that their plus ends are orientated distally, towards the actin rich peripheral domain (Baas *et al.,* 1987, 1988; Heidemann *et al.,* 1981). This polarity is of importance as studies have shown that individual MITs elongate at their distal plus ends towards the actin rich P domain. These studies also showed that depolymerization of actin filaments (via the actin depolymerizing drug cytochalasin) allowed MITs to move even further into the P domain, linking actin dynamics to the MIT cytoskeleton (Dent and Kalil, 2001; Forscher and Smith, 1988; Lin and Forscher, 1993; Zhou *et al.,* 2002).

4.4.2.2. Microtubule dynamics

Both *in vitro* and *in vivo* studies have revealed a unique polymerization property of tubulin, termed dynamic instability, a behaviour which allows MITs to alternate between prolonged periods of polymerization and depolymerization (Mitchison and Kirschner, 1984; Schulze and Kirschner, 1986). Thus, even though a population of MITs are in a bulk steady state within a migrating cell, a single MIT never reaches a steady-state length due to in frequent inter-conversions between prolonged states of polymerization and depolymerization (Mitchison and Kirschner, 1984). This behaviour is most prominent at the MIT plus end, where they cycle between phases of growth and shrinkage interspersed by occasional pauses (Dent and Gertler, 2003; Mitchison and Kirschner, 1984). In short, after a period of growth, a MIT can begin to shrink (known as catastrophe= transition from growth to shrinkage), and a shrinking MIT can resume growth (known as rescue= transition from shrinkage to growth) (Dent and Gertler, 2003; Mitchison and Kirschner, 1984; Schulze and Kirschner, 1986; Tanaka *et al.,* 1995).

The dynamic behaviour of tubulin and MITs results in the rapid exchange between tubulin pools, and a swift turnover of the MIT array. This dynamic character of the MIT array is crucial to neuronal migration as it allows for rapid changes in cell shape, i.e. dynamic instability allows MITs to explore three-dimensional space more effectively than non-dynamic equilibrium polymerization (Desai and Mitchison, 1997; Dreschel *et al.,* 1992; Schulze and Kirschner, 1986). The dynamic instability of MITs, allows MITs to dynamically explore the growth cone and ensures that MITs can interconvert between arrays from looped arrays, bundled arrays and splayed out arrays depending on the need of the developing neuron (Sabry *et al.,* 1992; Tanaka *et al.,* 1993). More recently the importance of MIT dynamics has been implicated as an essential component in axonal outgrowth and in axonal guidance.

These studies show that inhibition of MIT dynamics abolishes directional growth cone movement and axonal elongation (Tanaka *et al.,* 1995), suggesting that proper regulation of the transition frequencies is required for normal neuronal migration (Kawauchi *et al.,* 2005).

Not surprisingly, microtubules are abundant in the leading processes of migrating neurons (Tanaka *et al.,* 1995). These MITs are selectively stabilized in dense arrays to maintain the morphology of the leading process. Stability is decreased at the tips of the growth cones, allowing MIT arrays to splay out into single, dynamic pioneer MITs (Bunge, 1973; Bray and Bunge, 1981; Tanaka *et al.,* 1995; Yamada, 1971). Accordingly, there is a gradient of MIT stability in migrating neurons so that MITs turn over more rapidly and frequently the further distal they are along the migrating neuron (the closer MITs are to the P domain of growth cones, the more MIT instability and dynamics increase) (Bamburg *et al.,* 1986; Gordon-Weeks, 2003; Lim *et al.,* 1989). Microtubule dynamics is critical to growth cone steering. It has been shown that MIT stabilization on the one side of the growth induces a growth cone turn in the direction of the MIT stabilization, and conversely MIT destabilization steers the growth cone away towards the more stabilized MIT region (Buck and Zheng, 2002). Thus, although instability is crucial for growth cone turning and steering, simultaneous stabilization in the direction of growth is required to form stable structural MIT bundles which are more resilient to depolymerization (Bondallaz *et al.,* 2006; Mimori-Kiyosue and Tsukita, 2003). Recently fluorescent studies have shown that MITs rapidly extend and retract from the actin-rich P-domain of growth cones. Over a period of only a few minutes MITs can explore almost the entire P domain of the growth cone via the dynamic polymerization and depolymerization abilities of single pioneer MITs (Dent *et al.,* 1999; Dent and Kalil, 2001; Kabir *et al.,* 2001; Schaefer *et al.,* 2002; Tanaka and Kirschner, 1991, 1995).

Microtubule stability is conferred or enhanced by microtubule associated proteins (MAPs) and decreased by microtubule destabilising proteins such as stathmin and SCG10 (Tararuk *et al.,* 2006). Thus, neurite elongation and axonal outgrowth requires a fine balance between MIT stability and instability, as too much or too little stabilization hinders neuronal migration (Chuckowree and Vickers, 2003; Tararuk *et al.,* 2006). Stability is essential in the shaft where in addition to MAPs MITs are stabilised by numerous post-translational modifications, whereas instability is crucial for MITs present in the growth cone. Activity of both stabilizing and destabilising factors (such as SCG10) is tightly regulated by phosphorylation, thus regulating the dynamic state required for neurite extension (Stoothoff and Johnson, 2005; Walter-Yohrling *et al.,* 2003). Importantly, inappropriate expression or phosphorylation of these MIT regulatory proteins result in numerous forms of cancer and neurodegenerative diseases, such as Alzheimer's disease (hyperphosphorylated tau, a MAP) (Stoothoff and Johnson, 2005; Walter-Yohrling *et al.,* 2003). Okazaki and colleagues showed that

patients with Alzheimer's disease had altered SCG10 compartmentalization and inadequate degradation (Okazaki *et al.,* 1995). Additionally, patients with Down's syndrome had almost undetectable amounts of SCG10 in neuronal precursor cells (Bahn *et al.,* 2002). These cells exhibited reduced neurogenesis, abnormal neuronal morphology and reduced neurite lengths (Bahn *et al.,* 2002). More recently it has been shown that the MIT destabilising protein stathmin is hyperphosphorylated in patients with schizophrenia, suggesting that MIT dynamics and regulation need to be investigated in neurodevelopmental disorders such as schizophrenia and OCD (Hayashi *et al.,* 2006).

4.4.2.3. SCG10 and growth cone microtubule dynamics

It is well known that SCG10 acts as a potent MIT destabilising factor, although the precise mechanism by which it regulates neurite extension via the regulation of MIT stability still remains unclear. The MIT destabilising activity of SCG10 can be explained by two molecular mechanisms. Firstly, SCG10 has the ability to sequester free tubulin dimers into a ternary T2S complex (2 tubulin molecules: 1 SCG10) which prevents assembly into an MIT lattice (Curmi *et al.,* 1997; Jourdain *et al.,* 1997; Morii *et al.,* 2006) (Figure 4.2).

Secondly, SCG10 has the ability to promote catastrophe at the MIT plus end (Belmont and Mitchison, 1996) (Figure 4.2). It is this feature that allows SCG10 to play a pivotal role in regulating MIT dynamics in migrating neurons, a property unique to tubulin heterodimers (Gavet *et al.,* 1998; Riederer *et al.,* 1997). Moreover, investigations by Li and colleagues and Manna and colleagues have shown that SCG10 has a dual activity. It has the potential to partially stabilize the plus end by increasing the extent and rate of growth, while also having the potential to destabilize free minus ends by sequestering free tubulin and slightly increasing the catastrophe rate (Li *et al.,* 2008; Manna *et al.,* 2007). However, *in vivo* studies have shown that the main function, known to date, of SCG10 is to act as a catastrophe promoting factor (Morri *et al.,* 2006).

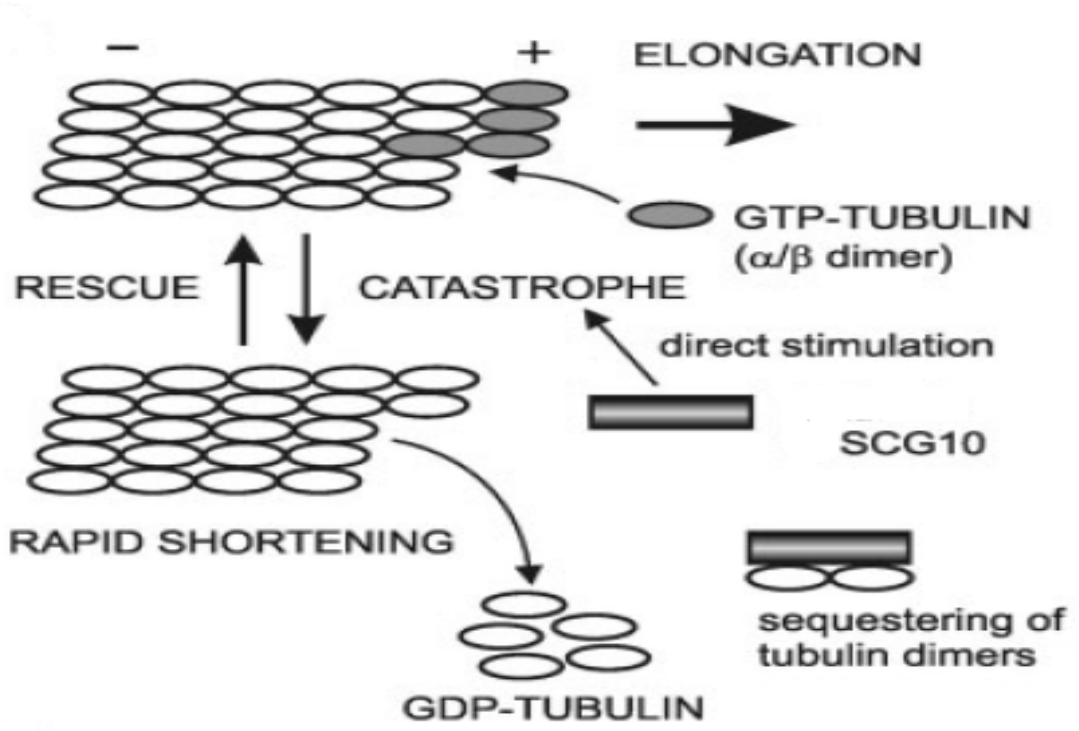

Figure 4.2. Shows the dynamic instability of microtubules in light of SCG10. Microtubules are polymer structures composed of α/β heterodimers. GTP-bound tubulin is added to the plus end of growing microtubules. Microtubules are also dynamic polymers which are capable of switching between phases of growth (rescue) and shrinkage (catastrophe). SCG10 increase the dynamic instability of microtubules by promoting catastrophe and by sequestering tubulin, thus dynamic instability is crucial in neurite extension and elongation (Taken from Grenningloh *et al.*,2003).

Recently it has been shown that gene silencing or immunodepletion of SCG10 suppresses neurite elongation and also increases the proportion of looped-shaped MITs, which induce growth cone pauses, so retarding growth cone movement (Mori *et al.,* 2006). Interestingly, drugs which suppress MIT dynamic instability (such as taxol and vinblastine, which block destabilising proteins) reduce neurite elongation and reduce growth cone motility (Letourneau and Ressler, 1984; Letourneau *et al.,* 1986; Rochlin *et al.,* 1996; Tanaka *et al.,* 1995; Zheng *et al.,* 1993; Yu and Baas, 1995). Additionally, elevated levels of SCG10 blocks neurite extension, due to its potent MIT depolymerizing effect (Reiderer *et al.,* 1997).

In a landmark study by Antonsson and colleagues, these investigators showed that phosphorylation of SCG10 inactivated its MIT depolymerizing activity as phosphorylated SCG10 is unable to sequester free tubulin and is therefore unable to promote MIT catastrophe (Antonsson *et al.,* 1997). These results indicate that SCG10 is crucial to neurite extension and growth cone guidance and that a fine

balance between SCG10 phosphorylation and expression is required for its proper function (Antonsson *et al.,* 1997).

4.4.2.4. SCG10-WDR47 interaction

Due to the localisation and potent destabilising effect of SCG10, it has been hypothesized that SCG10 may act antagonistically to MAPs by inducing destabilization of MITs to ensure a highly dynamic state of MITs within growth cones (Grenningloh *et al.,* 2003; Reiderer *et al.,* 1997). Thus the presence of both stabilizing and destabilising factors are required by migrating neurons to regulate MITs (Grenningloh *et al.,* 2003; Reiderer *et al.,* 1997).

The significance of the WDR47-SCG10 interaction could be to reduce the catastrophe promoting effect of SCG10, thereby reducing MIT dynamic instability. Dynamic instability is essential to neurite outgrowth, axonal elongation and growth cone turning and exploration (section 4.4.2.2.). Therefore, based on the previous Y2H screen of Reelin conducted by Kinnear and co-workers (Kinnear, 2007) and the novel interaction between WDR47 and SCG10 described in the present investigation, one could propose the following mechanism: Reelin signalling to downstream effectors such as MAP1B and tau would induce the partial stabilization of MITs. Upon Reelin internalization, it binds to WDR47 within neuronal vesicles where WDR47, in turn, binds to SCG10, possibly reducing the potent destabilising effects of SCG10. Thus, the interaction of WDR47 with SCG10 ultimately reduces MIT dynamics, this shift in balance in MIT dynamics results in an alteration in the migratory path of neurons.

The latter effect is supported by findings of Nixon and co-workers, who showed that when SCG10 is bound to the Golgi structure, it appears to be inactive (Nixon *et al.,* 2002). They found that SCG10 interacts with RGSZ1 (a regulator of G protein signalling) on the Golgi structure and that this interaction inhibited the MIT depolymerizing activity of SCG10 (Nixon *et al.,* 2002). Furthermore, Gong and colleagues recently used SCG10 in a Y2H analysis and identified a novel interaction between SCG10 and BRI_3 (a neuron-specific member of the integral membrane proteins) (Gong *et al.,* 2008). They hypothesized that BRI_3 may inhibit neurite extension by decreasing the dynamic instability of MITs induced by SCG10 (Gong *et al.,* 2008). Similarly, one could speculate that the WDR47-SCG10 interaction may serve to reduce the MIT dynamic instability and, ultimately, arresting neurite elongation. The WDR47-SCG10 interaction could render SCG10 inactive by incorporating it into a vesicular structure. Reelin could thus be an extracellular guidance cue that shifts the balance between stabilizing (via MAPs, such as tau and MAP1B) and destabilising (via WDR47-SCG10 interaction) factors within a growth cone, such that MITs are stabilized in the direction of growth.

Furthermore, WDR47 could induce the phosphorylation of SCG10 either directly or by inducing relevant kinases, as the non-phosphorylated form of SCG10 represents the most active form of SCG10 (Antonsson *et al.,* 1997). The Reelin signalling pathway activates cdk5 via the phosphorylation of Dab1, activated cdk5 is able to phosphorylate SCG10 thereby reducing its destabilising effects on MITs (Antonsson *et al.,* 1997). It therefore appears that in the Reelin pathway, one of the mechanisms that Reelin uses to exert its effects on neuronal migration is to reduce the MIT destabilising function of SCG10, either directly by binding to vesicle bound WDR47 or indirectly by inducing the phosphorylation, and hence, inactivation of SCG10. Additional studies need to be done to assess the phosphorylation state of SCG10 once bound to WDR47, and whether this interaction alters the degree of phosphorylation or what happens to SCG10 once WDR47 is no longer present in neuronal cells (knockdown of WDR47). It would also be interesting to measure the phosphorylation state of SCG10 before and after Reelin stimulation. Additionally, the MIT destabilising effect, as well as MIT dynamics and the amount of SCG10 as well as the phosphorylation state of SCG10 should be analysed in the *reeler* mouse cortex.

Li and colleagues identified an interaction between Rnd1 (subfamily of Rho GTPases) and the central domain of SCG10 using a Y2H screen (Li *et al.,* 2008). Rnd1 has been implicated in the regulation of the actin cytoskeleton, and in neurite extension via the inhibition of Rho-dependant pathways (Li *et al.,* 2008). The binding of Rnd1 to SCG10 is independent of the phosphorylation state of SCG10, and this interaction was shown to increase the MIT destabilising activity of SCG10 (Li *et al.,* 2008). Due to Rnd1s induced increase in SCG10 function, the MITs become more dynamically unstable which increases neurite outgrowth and axon formation (Li *et al.,* 2008). This study shows that once the destabilising effects of SCG10 increase, MIT dynamics instability increases which in turn increases neurite outgrowth. Thus, reinforcing the hypothesis we put forward in light of the reduction of MIT dynamics and arresting neurite elongation.

To reinforce the current hypothesis that WDR47 bound to internalized Reelin controls migration and lamination via the inhibition of cytoskeletal dynamics, Chai and colleagues recently showed that the Reelin signalling pathway increased the phosphorylation of n-cofilin (non-muscle cofilin) via the activation of LIM kinase 1 (LIMK1) (Chai *et al.,* 2009). Cofilin is an actin-binding protein and an essential regulator of actin dynamics (Bamburg, 1999). Cofilin acts as an actin depolymerizing protein that is responsible for promoting actin disassembly and provides actin monomers required for directional migration (Dawe *et al.,* 2003; Ghosh *et al.,* 2004; Jovceva *et al.,* 2007; Kiuchi *et al.,* 2007). Upon LIMK1 phosphorylation, cofilin no longer has the ability to bind to and disassemble actin filaments, which reduces actin dynamics and in turn inhibits neurite extension (Moriyama *et al.,* 1996; Zebda *et al.,* 2000, Chai *et al.,* 2009). Chai and colleagues showed that Reelin signalling

enhanced the activity of LIMK1, which increased the serine phosphorylation of cofilin and hence increased the stability of the actin cytoskeleton, resulting in the inhibition of neurite extension and migration (Chai *et al.,* 2009). Additionally, they showed that, in the reeler cortex, n-cofilin phosphorylation was significantly reduced (Chai *et al.,* 2009). From this study they concluded that Reelin's effect on the actin cytoskeleton (via the inhibition of actin dynamics) is responsible for Reelin's action as a positional and directional cue, suggesting that Reelin acts as a stop signal to migrating neurons via the reduction of cytoskeletal dynamics (Chai *et al.* ,2009). Thus, in light of the above study in which Reelin reduces actin dynamics to regulate neuronal migration, we hypothesise that Reelin additionally modulates MIT dynamics via the interaction between WDR47 and SCG10 ultimately inhibiting cytoskeletal dynamics as a whole to arrest neuronal migration.

It is not yet known whether or not internalised Reelin (hence WDR47) within neuronal vesicles (section 1.3.2.3.3) is targeted for proteosomal degradation. If the neuronal vesicles containing Reelin bound WDR47 are targeted for degradation, the binding of WDR47 to SCG10 could facilitate the removal of SCG10 from neuronal growth cone. This mechanism could be responsible for the down regulation of SCG10 mRNA in postnatal development, and may also serve to remove SCG10 in regions of plasticity in the adult brain once regeneration has been achieved.

Numerous theories have been posited for the function of Reelin during cortical development. Based on the results of the present investigation, one could envision the following scenario: The first wave of postmitotic neurons to leave the ventricular zone may migrate via somal translocation to their final cortical positions (section 1.3.2.1.1). Various extracellular guidance cues such as neuronal growth factor (NGF), which not only stimulates axonal or neurite outgrowth, but also activates the expression of SCG10 initiates migration and neurite extension (Riederer *et al.,* 1997; Grenningloh *et al.,* 2003). These neurons would initially encounter a high concentration of Reelin as the cortical distance is still relatively short. Upon binding of Reelin to its receptors on the surface of the migrating neuron and its consequential internalization, neurite elongation is inhibited by the inhibition of MIT dynamic instability via the downstream effects of Reelin, including its interaction with WDR47 and the binding of WDR47 to SCG10. Thus, once internalised Reelin binds to WDR47, it may activate WDR47 which in turn binds to SCG10 rendering SCG10 inactive (bound to the vesicular structure). Additionally, Reelin activated WDR47 bound to SCG10 could also recruit kinases to phosphorylate SCG10 (vesicle bound or free cytosolic SCG10), further inactivating SCG10 and reducing MIT dynamics. Later born neurons then migrate via glial-dependent locomotion (section 1.3.2.1.2) and encounter a concentration gradient of Reelin. It appears as if lower concentrations of Reelin are initially not enough to inhibit MIT dynamics although it is sufficient to detach neurons from their glial guides via the Reelin-integrin interaction (section 1.3.2.3.3). As the concentration of Reelin increases, neurons would

migrate via somal translocation, which is guided by cytoskeletal dynamics and motor proteins (section 1.3.2.1.1). Once migrating neurons have encountered a high enough concentration of Reelin (the closer they are to the marginal zone), MIT dynamics is inhibited (via the WDR47-SCG10 interaction) and neurons stop migrating and assume their final cortical positions.

This hypothesis could also explain the inside-out manner of lamination of the neocortex, as later born neurons only encounter a high enough concentration of Reelin once they have by passed their earlier born predecessors. Thus later born neurons traverse greater cortical distances and assume more superficial positions until they stop migration once MIT and actin dynamics have been inhibited. It also explains the outside-in manner of lamination observed in the *reeler* neocortex, as early born neurons do not stop migrating as there is no Reelin available to reduce cytoskeletal dynamics. Hence, later born neurons do not bypass their early born predecessors, instead they settle underneath earlier born neurons in an unorganised mass of neocortical neurons. Neurons also remain closely associated to their glial guides due to the absence of the Reelin-integrin interaction. However, it needs to be taken into account that other factors could also contribute to the *reeler* phenotype, as Reelin could interact with other extracellular factors which allow for the fine tuning of the normal neocortical architecture, one such factor is the microtubule associated protein LIS1. It is safe to say that a host of signalling pathways regulate neuronal migration and cortical lamination; these pathways ultimately control migration via their actions on the neuronal cytoskeleton. It is also not impossible that these pathways regulate each other, or interact in unison as is the case for the Reelin and the LIS1 signalling pathways.

4.5. LIMITATIONS OF THE PRESENT STUDY

4.5.1. Limitations of Yeast-two-hybrid analysis

The yeast two-hybrid system is a powerful, reliable and relatively inexpensive method to detect tissue specific protein-protein interactions, although like any assay it has its advantages and disadvantages.

This technique uses the yeast as a host system; this is both an advantage as well as a disadvantage. Yeast bears a greater similarity to higher eukaryotic systems in comparison to systems using a bacterial host (Sobhanifer, 2003). One of the major drawbacks of using *S. cerevisae* as a host is that a number of proteins' functions depend on their post-translational modifications (such as phosphorylation, disulphide bridge formation and glycosylation). Not all the enzymes responsible for these modifications for interaction with the particular bait occur in yeast and therefore, protein interactions that depend on post-translational modifications may not be detected (Van Criekinge and

Beyaert, 1999; Sobhanifer, 2003). Moreover, the yeast cells may not express the necessary chaperone proteins to fold the constructed fusion protein (Van Crieking and Beyaert, 1999).

Another limitation of the Y2H assay is the use of artificially constructed fusion proteins (Van Criekinge and Beyaert, 1999; Sobhanifer, 2003). The generation of chimeric bait and prey proteins may alter their native conformation, which, in turn, could alter both the activity and binding properties of the proteins (Van Criekinge and Beyaert, 1999; Sobhanifer, 2003).

An additional disadvantage of the Y2H system is the necessity for nuclear localisation of the proteins of interest. This is problematic since proteins which contain localisation signals to cellular compartments other than the nucleus will be exported to their proper cellular compartments thereby rendering them unavailable for analysis (Van Criekinge and Beyaert, 1999; Sobhanifer, 2003).

The Y2H assay also produces false positives, where the reporter genes are activated and detected even in the absence of protein interactions. These false positives may occur if the bait or prey constructs are able to auto activate transcription of the reporter genes (Van Criekinge and Beyaert, 1999; Sobhanifer, 2003).

Additionally, if the bait is mildly toxic to the yeast, some yeast diploids will be lost during the mating, so that interactions may be missed (a form of false negatives) (Van Criekinge and Beyaert, 1999; Sobhanifer, 2003). In the present study, the WDR47 construct was tested for auto-activation and toxicity. The results showed that this construct was not able to activate transcription autonomously nor was the construct toxic to the yeast host. In order to minimise the number of false positives in the present study, multiple reporter genes (both nutritional and colorimetric) and heterologous mating experiments were preformed to reduce non specific protein-protein interactions.

4.5.2. Limitations of *in vivo* co-localisation

The GT-17 hypothalamus cells used in the present study proved to be problematic as they were difficult to culture. Furthermore, the transfection efficiency of the cells was fairly low as they are difficult to transfect. Although this problem can be overcome by the use of endogenous WDR47, there is currently no commercially available WDR47 primary antibody, hence the present study made use of transfected WDR47.

Resolution is another obstacle when using fluorescent microscopy. Resolution depends on the wavelength of the light imaged and on the numerical aperture (NA) of the objective (Lalonde *et al.,* 2008). The resolution of a conventional light microscope (even with a high-NA objective) is limited

to approximately 200nm, suggesting that proteins could be contained or visualised within a co-localised space (volume) without biologically interacting (objects closer together than 200nm may appear as a single localised object) (Lalonde *et al.,* 2008). For the present study, z-stack images were taken 260nm apart, thus it remains possible that considerable distances may actually separate proteins that appear co-localised by fluorescence microscopy.

Despite the limitations of the *in vivo* co-localisation, it does, however, provide compelling evidence that WDR47 and SCG10 do co-localise although this interaction needs to be further verified using more sensitive *in vivo* techniques such as *in vivo* co-immunoprecipitation, which overcome the limitations of *in vivo* co-localisation.

4.6. FUTUTRE STUDIES

The present study has presented a novel interaction between WDR47 and SCG10 that directly links the Reelin signalling pathway to proteins which regulate microtubule dynamics and neuronal migration. However, further investigations of the current results are needed to fully grasp the significance of these findings in context of the pathophysiologies of neuronal migration disorders. The identification of the novel WDR47-interacting protein, not only furthers our understanding of the Reelin signalling pathway, but also sheds light on the function of WDR47. It should however be noted that further verification studies such as *in vivo* co-immunoprecipitation and bioluminescence resonance energy transfer (BRET), for example, need to be conducted in order to fully confirm the WDR47-SCG10 interaction. It also needs to be determined to which domains of SCG10 WDR47 binds, as this will aid in a better understanding of the WDR47-SCG10 interaction. Due to time constraints these could not be conducted as part of the present study, although they are currently underway in our laboratory.

Following this, it would be crucial to determine what effect, if any, the interaction of SCG10 with WDR47 has one tubulin dynamics. For this reason, siRNA knockdown studies, in which WDR47 is knocked down in GT1-7 cells, are currently underway in our laboratory. The effect of the WDR47-knockdown on tubulin would then be determined by fluorescent microscopy using tubulin specific antibodies. Additionally, by knocking down WDR47, one could also determine the effect WDR47 has on the phosphorylation status of SCG10. These experiments will give us more insight into the functional significance of the WDR47-SCG10 interaction.

4.7. CONCLUSION

This study identified four putative interactors of the N-terminal domain of WDR47 by Y2H analysis. *In vivo* 3D co-localisation verified that only the neuronal specific protein, SCG10, showed a true interaction with WDR47. The identification of SCG10 as a novel WDR47 interacting protein not only sheds light on the role and function of WDR47 but also aids in a better understanding of the Reelin pathway and cortical lamination. This interaction also has significant implications in the pathophysiologies of neurodevelopmental disorders. The data presented in the present study yielded exciting results that warrant future follow-up investigation. Ultimately, the goal of studies like this one, is to get a clearer understanding of the aetiologies of neurodevelopmental disorders, such as lissencephaly and more complex neurodevelopmental disorders such as OCD and schizophrenia. The identification of SCG10 as a WDR47-interacting protein, may provide investigators with alternative avenues of research into potential drug targets for OCD and schizophrenia pharmacotherapy.

APPENDIX I

1. DNA eXTRACTION SOLUTIONS

Cell Lysis Buffer

Sucrose	0.32M
Triton-X-100	1%
$MgCl_2$	5mM
Tris-HCl	10mM
H_2O	1l

3M NaAc

NaAc.$3H_2O$ (Merck)	40.18g
ddH_2O	50ml

Adjust pH to 5.2 with glacial acetic acid and adjust volume to 100ml with ddH_2O

DNA Extraction Buffer

NaCl	0.1M
Tris-HCl	0.01M
EDTA(pH8)	0.025M
SDS	0.5%
Protein K	0.1mg/ml

TBE Buffer (10X stock)

Tris-HCl	0.89M
Boric Acid	0.89M
Na_2EDTA(pH8)	20Mm

2. BACTERIAL PLASMID PURIFICATION SOLUTIONS

Cell Suspension Solution

50mM Tris-HCl, pH 7.5	2.5ml 1M Tris
10mM EDTA	1ml 0.5M EDTA
Sterile H_2O to a final volume of 50ml	

Cell Lysis Solution

0.2M NaOH	2.5ml 4M NaOH
1% SDS	5ml
Sterile H_2O to a final volume of 50ml	

Neutralisation Solution

1.32M KOAc, pH 4.8	13.2ml 5M KOAc
Sterile H_2O to a final volume of 50ml	

3. YEAST PLASMID PURIFICATION SOLUTIONS

Yeast Lysis Buffer

SDS	1%
Triton X-100	2%
NaCl	100mM
Tris, pH 8	10mM
EDTA, pH8	1mM

4. YEAST TRANSFORMATION REAGENTS

1M LiAc

LiAC	5.1g
Sterile H_2O to a final volume of 50ml	

100mM LiAc

1M LiAC	5ml
Sterile H_2O to a final volume of 50ml	

50% PEG 4000

PEG 4000	25g
Sterile H_2O to a final volume of 50ml	

5. ELECTROPHORESIS STOCK SOLUTIONS

10% Ammonium Persulphate

Ammonium persulphate (Merck)	1g
Sterile water	10ml
Mix well and stock at 4^0C	

20X SB Stock Solution

di-Sodium tetraborate decahydrate	38.14g
Sterile H_2O to a final volume of 1 litre	

1X SB Solution

20X SB solution	50ml

Sterile H_2O to a final volume of 1 litre

6. GELS

1% Agarose Gel

Agarose	1g
SB buffer (1X)	100ml

Microwave for 1 minute on maximum power (or until agarose has dissolved) and add 5µl ethidium bromide (10mg/ml) when temperature of ≈55^{0}C is reached.

2% Agarose Gel

Agarose	2g
SB buffer (1X)	100ml

Microwave for 1 minute on maximum power and add 5µl ethidium bromide (10mg/ml) when temperature of ≈55^{0}C is reached.

7. DYES

Ethidium Bromide Stock (10mg/ml)

Ethidium bromide (Sigma)	500mg
Sterile water	50ml

Stir well on magnetic stirrer for 4 hours and store in a dark container at 4^{0}C

Bromophenol Blue Loading Dye

Bromophenol blue	0.1% (w/v)

Sterile H_2O to a final volume of 100ml. Store at 4^{0}C

8. MOLECULAR SIZE MARKERS

Molecular Size Marker (Lambda λPst)

Bacteriophage Lambda genomic DNA	200µl
*Pst*I Restriction enzyme	3µl (30U)
Promega buffer H	30µl

Sterile H_2O to a final volume of 300µl

Incubate at 37^{0}C for 3 hours, heat inactivate enzyme at 65^{0}C for 10 minutes. Load 3µl on agarose gel containing EtBr.

9 . PCR BUFFER

10x NH_4 PCR Buffer (BIOLINE UK)

Ammonium sulphate	160mM
Tris-HCl (pH 8.8)	670mM
Tween-20	0.1%

10. SOLUTIONS USED FOR THE ESTABLISHMENT OF BACTERIAL COMPETENT CELLS

CAP-Buffer

$CaCl_2$	2.21g
Glycerol	37.5ml
PIPES	0.76g

Sterile water to a final volume of 250ml. Adjust pH to 7.0 and store at 4^0C.

11. BACTERIAL MEDIA

LB-Media

Bacto tryptone	5g
Yeast extract	2.5g
NaCl	5g

Sterile H_2O to a final volume of 500ml. Autoclave and add the appropriate antibiotic (Ampicillin 25mg/l, Kanamycin 5mg/l or Zeocin™ 10mg/l) to media when temperature of ≈55^0C is reached.

LB-Agar Plates

Bacto tryptone	5g
Yeast extract	2.5g
NaCl	5g
Bacto agar	8g

Sterile H_2O to a final volume of 500ml. Autoclave and add the appropriate antibiotic (Ampicillin 25mg/l, Kanamycin 5mg/l or Zeocin™ 10mg/l) to media when temperature of ~55^0C is reached, prior to pouring ~20, 90mm plates. These plates were then allowed to set for 2-5 hours and stored at room temperature for up to three weeks.

12. YEAST MEDIA

YPDA Media

Difco peptone	10g
Yeast extract	10g

Glucose	10g
L-adenine hemisulphate (0.2% stock solution)	7.5ml

Add sterile H_2O to a final volume of 500ml. Autoclave at 121^0C for 15 minutes.

YPDA Agar Plates

YPDA media	
Difco peptone	10g
Yeast extract	10g
Bacto agar	10g
Glucose	10g
L-adenine hemisulphate (0.2% stock solution)	7.5ml

Add sterile H_2O to a final volume of 500ml. and autoclave at 121^0C for 15 minutes. Allow to cool to a temperature of ~55^0C, before pouring ~20, 90mm plates. These plates were then allowed to set for 2-5 hours and stored at room temperature for up to three weeks.

SD^{-W} Media

Glucose	12g
Yeast nitrogen base without amino acids	4g
SD^{-W} amino acid supplement	0.4g

Add sterile H_2O to a final volume of 600ml. Adjust pH to 5.8 and autoclave at 121^0C for 15 minutes.

SD^{-W} Agar Plates

Glucose	12g
Bacto agar	12g
Yeast nitrogen base without amino acids	4g
SD^{-W} amino acid supplement	0.4g

Add sterile H_2O to a final volume of 600ml. Adjust pH to 5.8 and autoclave at 121^0C for 15 minutes. Allow to cool to a temperature of ~55^0C, before pouring ~20, 90mm plates. These plates were then allowed to set for 2-5 hours and stored at room temperature for up to three weeks.

SD^{-L} Media

Glucose	12g
Yeast nitrogen base without amino acids	4g
SD^{-L} amino acid supplement	0.4g

Add sterile H_2O to a final volume of 600ml. Adjust pH to 5.8 and autoclave at 121^{0}C for 15 minutes.

SD^{-L} Agar Plates

Glucose	12g
Bacto agar	12g
Yeast nitrogen base without amino acids	4g
SD^{-L} amino acid supplement	0.4g

Add sterile H_2O to a final volume of 600ml. Adjust pH to 5.8 and autoclave at 121^{0}C for 15 minutes. Allow to cool to a temperature of ~55^{0}C, before pouring ~20, 90mm plates. These plates were then allowed to set for 2-5 hours and stored at room temperature for up to three weeks.

SD^{-L-W} Media

Glucose	12g
Yeast nitrogen base without amino acids	4g
SD^{-L-W} amino acid supplement	0.4g

Add sterile H_2O to a final volume of 600ml. Adjust pH to 5.8 and autoclave at 121^{0}C for 15 minutes.

SD^{-L-W} Agar Plates

Glucose	12g
Bacto agar	12g
Yeast nitrogen base without amino acids	4g
SD^{-L-W} amino acid supplement	0.4g

Add sterile H_2O to a final volume of 600ml. Adjust pH to 5.8 and autoclave at 121^{0}C for 15 minutes. Allow to cool to a temperature of ~55^{0}C, before pouring ~20, 90mm plates. These plates were then allowed to set for 2-5 hours and stored at room temperature for up to three weeks.

TDO Media

Glucose	12g
Yeast nitrogen base without amino acids	4g
SD^{-L-W-H} amino acid supplement	0.4g

Add sterile H_2O to a final volume of 600ml. Adjust pH to 5.8 and autoclave at 121^{0}C for 15 minutes.

TDO Agar Plates

Glucose	12g
Bacto agar	12g
Yeast nitrogen base without amino acids	4g
SD^{-L-W-H} amino acid supplement	0.4g

Add sterile H_2O to a final volume of 600ml. Adjust pH to 5.8 and autoclave at 121^0C for 15 minutes. Allow to cool to a temperature of ~55^0C, before pouring ~20, 90mm plates. These plates were then allowed to set for 2-5 hours and stored at room temperature for up to three weeks.

QDO Media

Glucose	12g
Yeast nitrogen base without amino acids	4g
$SD^{-L-W-H-Ade}$ amino acid supplement	0.4g

Add sterile H_2O to a final volume of 600ml. Adjust pH to 5.8 and autoclave at 121^0C for 15 minutes.

QDO Agar Plates

Glucose	12g
Bacto agar	12g
Yeast nitrogen base without amino acids	4g
$SD^{-L-W-H-Ade}$ amino acid supplement	0.4g

Add sterile H_2O to a final volume of 600ml. Adjust pH to 5.8 and autoclave at 121^0C for 15 minutes. Allow to cool to a temperature of ~55^0C, before pouring ~20, 90mm plates. These plates were then allowed to set for 2-5 hours and stored at room temperature for up to three weeks.

X-α-Galactosidase Solution (5mg/ml)

X-α-Galactosidase	25mg
Dimethylformamide	1ml

Make a 25mg/ml stock. Dilute with dimethylformamide to 5mg/ml working solution.

13. EUKARYOTIC CELL CULTURE MEDIA

Complete Growth Media

DMEM (4.5g/L glucose, with L-glutamine)	178ml
Foetal calf serum	20ml
Penstrep	2ml

Pre-warm to 37^0C before use.

Serum-Free Media

DMEM (4.5g/L glucose, with L-glutamine) 100ml

Pre-warm to 37^0C before use.

APPENDIX II

CALCULATING YEAST MATING EFFICIENCIES (Calculations based on Clontech Manual)

Count number of colonies on all plates with 30-300 colonies after 4 days

$$\#\text{colony forming units (cfu)/ml} = \frac{\text{cfu} \times 1000\mu\text{l/ml}}{}$$

1. Number of cfu/ml on SD^{-L} plates = viability of prey partner
2. Number of cfu/ml on SD^{-W} plates = viability of bait partner
3. Number of cfu/ml on SD^{-L-W} plates = viability of diploids
4. Lowest Number of cfu/ml of SD^{-L} or SD^{-W} plates indicate limiting partner

$$\text{5. Mating efficiency} = \frac{\#\text{cfu/ml of diploids} \times 100}{\#\text{cfu/ml of limiting partner}}$$

Library titre

Count number of colonies on all plates with 30-300 colonies after 4 days

$$\#\text{cfu/ml} = \frac{\#\text{colonies plating volume(ml)} \times \text{dilution factor}}{}$$

colonies clones screened= # cfu/ml x final resuspension volume

Heamocytrometric cell count protocol

Haemocytometric cell count using a Neubauer haemocytometer (Superior, Berlin, Germany) was performed to determine the titre of bait culture used in the library mating experiment. Prior to aliquoting the sample onto the haemocytometer, a glass coverslip was placed over the counting surface. Approximately 50µl of a 1 in 10 dilution of bait culture was then pippeted into one of the V-shaped wells (Fig A). This allowed for the area under the coverslip to be filled with the sample through capillary action. The counting chamber was subsequently placed on a microscope (Nikon TMS, Nikon Instruments inc., New York U.S.A) stage and the counting area was brought into focus under low magnification. The organisation of the counting area is shown in Figure B and Figure C. The number of cells per millilitre was determined using the following formula:

number of cells/ml = number of cells x dilution factor x 10^4 (a constant used because the depth of the haemocytometer is 0.1mm)

A.

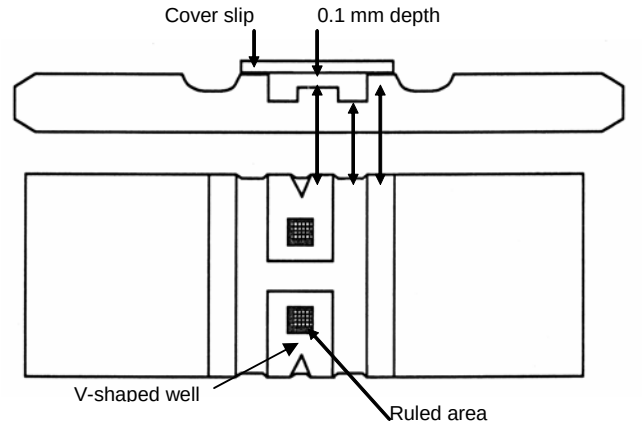

B.

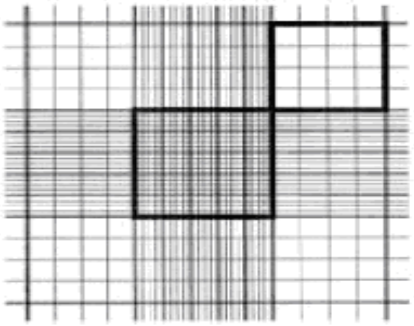

C.

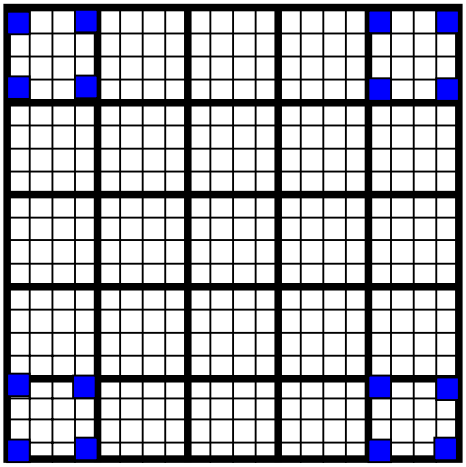

Neubauer heamocytometer, side and top view. The central platforms contain the ruled counting areas and are 0.1 mm under the cover slip, which is suspended on the raised ridges (taken from McNeel and Brown, 1992). b) **Magnified view of the ruled counting area** (taken from McNeel and Brown, 1992). c) **View of the central quadrant of the haemocyometer that was used to determine the number of cells per milliliter.** The number of cells per milliliter was determined as follows: The number of cells in each of the blue squares within the 4 outer larger squares (in the diagram) were counted and added together. This amount was multiplied by 4 to give an approximate number of cells each of the 4 large outer squares. The amount of cells in each of the 4 larger outer squares was then added together and divided by 4 to give an average number of cells for each of the 25 large squares of the central quadrant of the haemocytometer. This average number was then multiplied by 25 to yield a average number of cells within the large central quadrant. Number of cells per milliliter was then determined using the formula:

Cells/ml=number of cells x dilution factor x 10^4

APPENDIX III

LIST OF SUPPLIERS

Agarose	Whitehead Scientific
Ammonium acetate	B&M Scientific
Ammonium persulphate	Merck
Ampicillin	Roche
β-mercaptoethanol	Sigma
Bacteriophage Lambda gnomic DNA	Promega
Bacto Agar	Merck
Bacto tryptone	Fluka
*BamH*I	Promega
Bromophenol blue	Merck
Calcium chloride	Merck
Calf intestinal alkaline phosphatise	Promega
dATP	Boerhinger Mannheim
dCTP	Boerhinger Mannheim
dGTP	Boerhinger Mannheim
Dimethylformamide	Merck
di-Sodium tetraborate decahydrate	Merck
DMEM	Highveld biological
dNTP mix	TaKaRa
DTT	Roche
dTTP	Boerhinger Mannheim
*Eco*RI	Promega
EDTA	Boerhinger Mannheim
Ethanol	Boerhinger Mannheim
Ethidium bromide	Roche
Ex Taq™ polymerase	TaKaRa
Ex Taq™ polymerase Mg^{2+}-containing reaction buffer	TaKaRa
Foetal calf serum	Delta Bioproducts
GeneJuice®	Novagen
GFX® DNA purification kit	Amersham Pharmacia
Glass beads (450-600μm)	Sigma
Glucose	Kimix

Glycerol	Promega
Glycine	Kimix
HCl	Merck
Herring sperm DNA	Promega
*Hind*III	Promega
Isopropanol	Merck
K-acetate	Sigma
Kanamycin	Roche
LiAc	Sigma
$MgCl_2$	Bioline
$MgSO_4.7H_2O$	Merck
Molecular size marker (200bp)	Promega
Na_2CO_3	Merck
NaCl	BDH Chemicals
$Na_2HPO_4.7H_2O$	Merck
$Na_2H_2PO_4.H_2O$	Merck
NaOH	Sigma
*Nde*I	Promega
Oligonucleotide primers	Department of Molecular and Cell Biology, University of Cape Town (UCT), Cape Town, South Africa
pACT2	BD Biosciences
PBS	Sigma
PEG4000	Merck
Penicillin/streptomycin	Highveld Biological
Peptone	Difco
pGBKT7	BD Biosciences
Phenol/chloroform/isoamyl	Sigma
*Pst*I	Promega
QDO	BD Biosciences
*Sac*II	Promega
SD^{-Ade}	BD Biosciences
SD^{-L}	BD Biosciences
SD^{-L-W}	BD Biosciences
SD^{-Met}	BD Biosciences
SDS	Sigma
SD^{-Ura}	BD Biosciences

SD^{-w}	BD Biosciences
T4 DNA Ligase	Promega
Taq polymerase	Bioline
TDO	BD Biosciences
Tris	Merck
Tris-HCl	Merck
Triton X-100	Sigma
Trypsin	Highveld Biological
Tween 20	Merck
Whatman 3M paper	Whatman international
Wizard® Purefection plasmid purification kit	BD Bioscences
X-α-galactosidase	Southern Cross
Yeast extract	Difco
Yeast nitrogen base (without amino acids)	BD Biosciences

APPENDIX IV

BACTERIAL STRAIN PHENOTYPE

E.coli strain DH5α

Φ 80d *lacZ*Δ*M15* recA1, *end*A1, *Gry* A96 *thi*-1, *hsd*R17 *sup*E44, *rel*A1, *deoR* Δ(*lac*ZYA *argF*)u169

YEAST STRAIN PHENOTYPES

Yeast strain AH109

*MAT*a, *trp1-901*, *leu2-3, ura3-5, his3-200, gal4*Δ, *gal80*Δ, *LYS2::GAL1*$_{uas}$*-GAL1*$_{TATA}$*-HIS3, GAL2*$_{UAS}$*-GAL2*$_{TATA}$*-ADE2, URA3::MEL1*$_{UAS}$*-MEL1*$_{TATA}$*-lacZ* (James *et al.,* 1996)

Yeast strain Y187

*MAT*α*, ura3-52, his3-200, ade2-101, trp1-901, leu2-3, 112, gal4*Δ, *met*$^{-}$, *gal80*Δ, *URA3::GAL1*$_{UAS}$*-GAL1*$_{TATA}$*-lacZ* (Harper *et al.,* 1993)

APPENDIX V

Restriction maps of Yeast two-hybrid

A

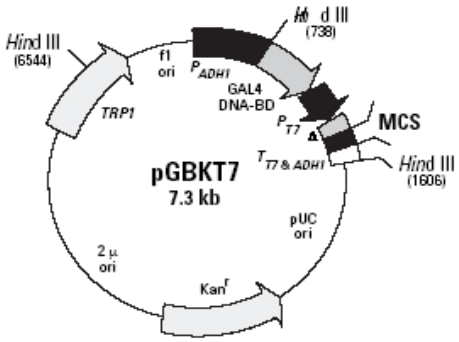

B

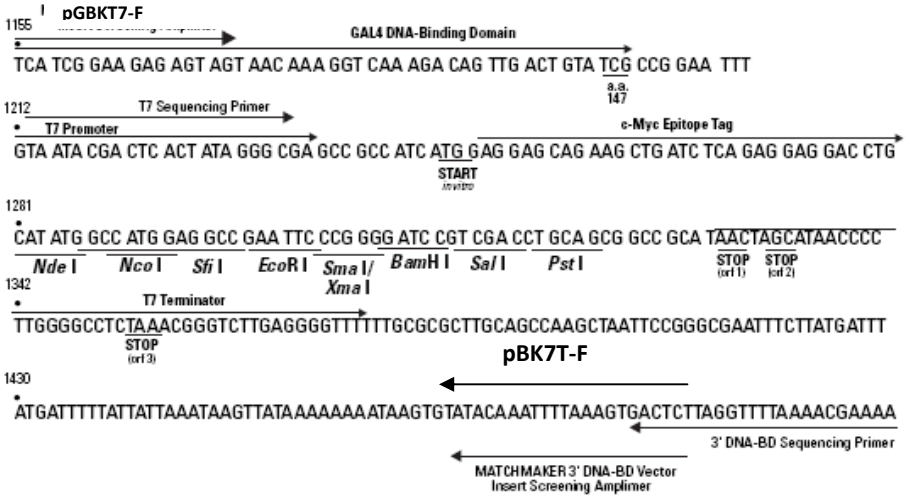

Figure 1. Restriction map and multiple cloning site of pGBKT7 Y2H bait vector.

A) The positions of the kanamycin resistance gene (*kan*), TRP1 and GAL4-BD coding sequences, f1 bacteriophage and pUC plasmid origins of replication, the truncated *S.cerivisiae* ADH1 promotor sequence (P_{ADH1}), the T7 RNA polymerase promoter, the T7 and c- Myc epitope tag are indicated on the map. B) Nucleotide sequence of the pGBKT7 MCS. The positions of all unique restriction enzyme recognition sequences, stop codons in the T7 terminator sequence, the GAL4-BD coding sequence, the T7 promoter sequence, c-Myc epitope tag and the positions of pGBKT7-F and pGBKT7-R screening primers and sequencing primers are indicated on the sequence (taken from Clontech MATCHMAKER vectors handbook).

A

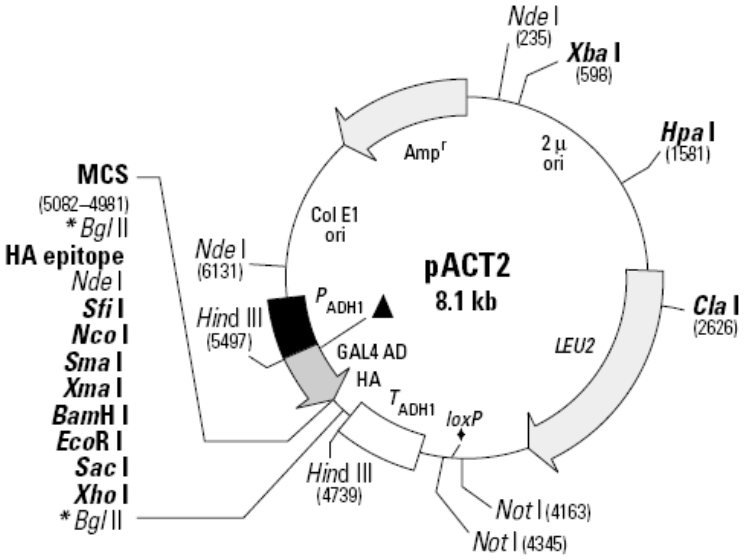

B

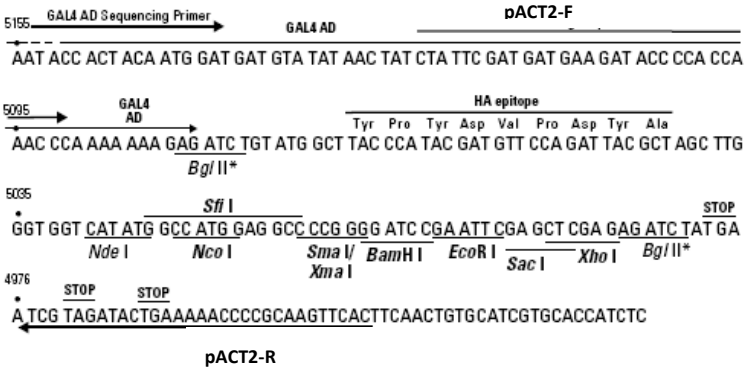

Figure 2. Restriction map and multiple cloning site of pACT2 Y2H prey vector. A) The positions of unique restriction sites are indicated in bold. The position of the ampicillin resistance gene (*Amp*^{r}), LEU2 and GAL4-AD coding sequences, and pBR322 plasmid origins, the *S.cerevisiae* ADH1 promoter, *S.cerevisiae* ADH1 termination sequence, Lox sites (Lox 1 and Lox 2), the heamagglutinin (HA) epitope tag and the MCS are indicated on the map. B) Nucleotide sequence of the pACT2 MCS. The positions of all unique restriction sites, stop codons, the position of the final codon (881) of GAL4-AD coding sequence, the positions of the pACT2-F and pACT2-R primers and the HA epitope tags are all indicated in the map (taken from Clontech MATCHMAKER vectors handbook).

Chromatogram of WDR47 sequence

TRACE

BioEdit version 7.0.9.0 (6/27/07)

Lane 11

Points 1783 to 13247

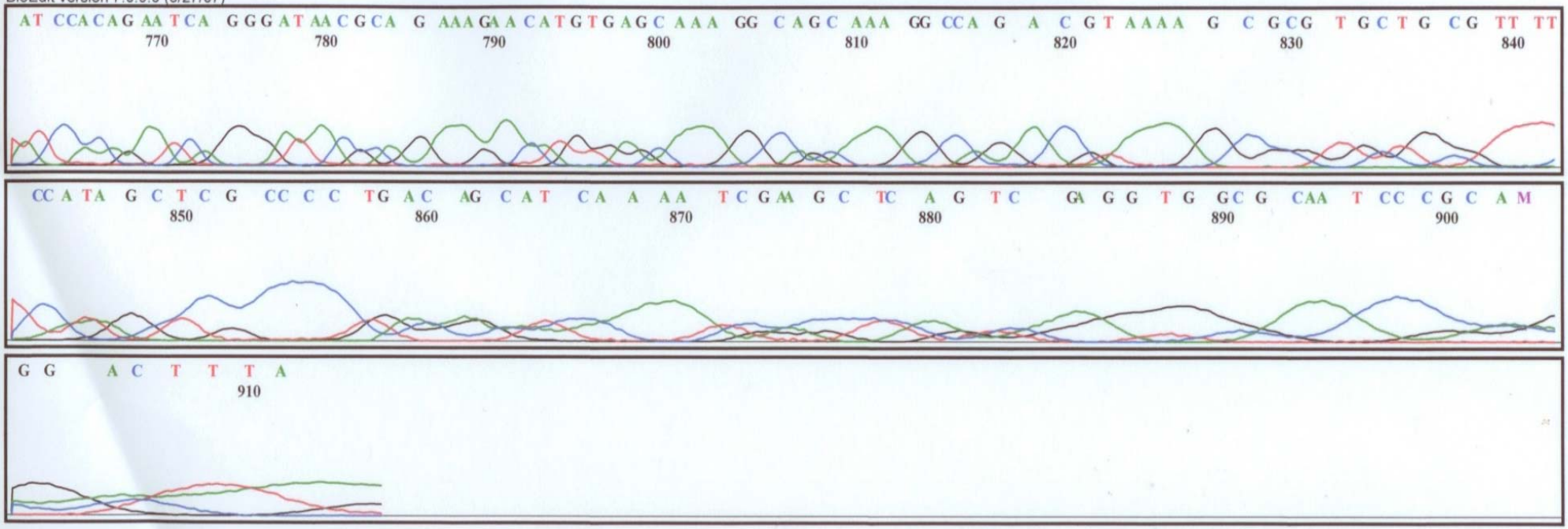

REFERENCES

http://www.clontech.com

http://www.ensembl.org

http://www.go.worldbank.org/

http://www.ncbi.nih.gov/publicat/ocdbrain.htm

http://www.ncbi.nlm.nih.gov/BLAST/

http://www.ncbi.nlm.nih.gov/PubMed

http://www.ncbi.nlm.nih.gov/Entrez

http://www.ncbi.nlm.nih.gov

http://www.who.int/healthinfo

Aboitiz, F., D. Morales, and J. Montiel. 2001. The Inverted Neurogenetic Gradient of the Mammalian Isocortex: Development and Evolution
Brain Res.Brain Res.Rev. 38, no. 1-2: 129-139.

Achte, K. A., E. Hillbom, and V. Aalberg. 1969. Psychoses Following War Brain Injuries
Acta Psychiatr.Scand. 45, no. 1: 1-18.

Alcantara, S., M. Ruiz, G. D'Arcangelo, F. Ezan, Lecea L. de, T. Curran, C. Sotelo, and E. Soriano. 1998. Regional and Cellular Patterns of Reelin MRNA Expression in the Forebrain of the Developing and Adult Mouse
J.Neurosci. 18, no. 19: 7779-7799.

Aligianis, I. A., C. A. Johnson, P. Gissen, D. Chen, D. Hampshire, K. Hoffmann, E. N. Maina, N. V. Morgan, L. Tee, J. Morton, J. R. Ainsworth, D. Horn, E. Rosser, T. R. Cole, I. Stolte-Dijkstra, K. Fieggen, J. Clayton-Smith, A. Megarbane, J. P. Shield, R. Newbury-Ecob, W. B. Dobyns, J. M. Graham, Jr., K. W. Kjaer, M. Warburg, J. Bond, R. C. Trembath, L. W. Harris, Y. Takai, S. Mundlos, D. Tannahill, C. G. Woods, and E. R. Maher. 2005. Mutations of the Catalytic Subunit of RAB3GAP Cause Warburg Micro Syndrome
Nat.Genet. 37, no. 3: 221-223.

Anderson, S. A., D. D. Eisenstat, L. Shi, and J. L. Rubenstein. 1997. Interneuron Migration From Basal Forebrain to Neocortex: Dependence on Dlx Genes
Science 278, no. 5337: 474-476.

Andressen, C., S. Arnhold, M. Puschmann, W. Bloch, J. Hescheler, R. Fassler, and K. Addicks. 1998. Beta1 Integrin Deficiency Impairs Migration and Differentiation of Mouse Embryonic Stem Cell Derived Neurons
Neurosci.Lett. 251, no. 3: 165-168.

Ang, E. S., Jr., T. F. Haydar, V. Gluncic, and P. Rakic. 2003. Four-Dimensional Migratory Coordinates of GABAergic Interneurons in the Developing Mouse Cortex
J.Neurosci. 23, no. 13: 5805-5815.

Antonsson, B., R. Lutjens, Paolo G. Di, D. Kassel, B. Allet, A. Bernard, S. Catsicas, and G. Grenningloh. 1997. Purification, Characterization, and in Vitro Phosphorylation of the Neuron-Specific Membrane-Associated Protein SCG10
Protein Expr.Purif. 9, no. 3: 363-371.

Arnaud, L., B. A. Ballif, E. Forster, and J. A. Cooper. 2003. Fyn Tyrosine Kinase Is a Critical Regulator of Disabled-1 During Brain Development
Curr.Biol. 13, no. 1: 9-17.

Arnaud, L., B. A. Ballif, and J. A. Cooper. 2003. Regulation of Protein Tyrosine Kinase Signaling by Substrate Degradation During Brain Development
Mol.Cell Biol. 23, no. 24: 9293-9302.

Assadi, A. H., G. Zhang, U. Beffert, R. S. McNeil, A. L. Renfro, S. Niu, C. C. Quattrocchi, B. A. Antalffy, M. Sheldon, D. D. Armstrong, A. Wynshaw-Boris, J. Herz, G. D'Arcangelo, and G. D. Clark. 2003. Interaction of Reelin Signaling and Lis1 in Brain Development
Nat.Genet. 35, no. 3: 270-276.

Augustine, G. J. 2001. How Does Calcium Trigger Neurotransmitter Release?
Curr.Opin.Neurobiol. 11, no. 3: 320-326.

Avila, J., J. Dominguez, and J. az-Nido. 1994. Regulation of Microtubule Dynamics by Microtubule-Associated Protein Expression and Phosphorylation During Neuronal Development
Int.J.Dev.Biol. 38, no. 1: 13-25.

Ayala, R., T. Shu, and L. H. Tsai. 2007. Trekking Across the Brain: the Journey of Neuronal Migration
Cell 128, no. 1: 29-43.

Baala, L., S. Briault, H. C. Etchevers, F. Laumonnier, A. Natiq, J. Amiel, N. Boddaert, C. Picard, A. Sbiti, A. Asermouh, T. ttie-Bitach, F. Encha-Razavi, A. Munnich, A. Sefiani, and S. Lyonnet. 2007. Homozygous Silencing of T-Box Transcription Factor EOMES Leads to Microcephaly With Polymicrogyria and Corpus Callosum Agenesis
Nat.Genet. 39, no. 4: 454-456.

Baas, P. W., L. A. White, and S. R. Heidemann. 1987. Microtubule Polarity Reversal Accompanies Regrowth of Amputated Neurites
Proc.Natl.Acad.Sci.U.S.A 84, no. 15: 5272-5276.

Baas, P. W., J. S. Deitch, M. M. Black, and G. A. Banker. 1988. Polarity Orientation of Microtubules in Hippocampal Neurons: Uniformity in the Axon and Nonuniformity in the Dendrite
Proc.Natl.Acad.Sci.U.S.A 85, no. 21: 8335-8339.

Bahn, S., M. Mimmack, M. Ryan, M. A. Caldwell, E. Jauniaux, M. Starkey, C. N. Svendsen, and P. Emson. 2002. Neuronal Target Genes of the Neuron-Restrictive Silencer Factor in Neurospheres Derived From Fetuses With Down's Syndrome: a Gene Expression Study
Lancet 359, no. 9303: 310-315.

Bailey, A., P. Luthert, A. Dean, B. Harding, I. Janota, M. Montgomery, M. Rutter, and P. Lantos. 1998. A Clinicopathological Study of Autism
Brain 121 (Pt 5): 889-905.

Ballif, B. A., L. Arnaud, and J. A. Cooper. 2003. Tyrosine Phosphorylation of Disabled-1 Is Essential for Reelin-Stimulated Activation of Akt and Src Family Kinases
Brain Res.Mol.Brain Res. 117, no. 2: 152-159.

Bamburg, J. R., D. Bray, and K. Chapman. 1986. Assembly of Microtubules at the Tip of Growing Axons
Nature 321, no. 6072: 788-790.

Bamburg, J. R. 1999. Proteins of the ADF/Cofilin Family: Essential Regulators of Actin Dynamics *Annu.Rev.Cell Dev.Biol.* 15: 185-230.

Barkovich, A. J., T. K. Koch, and C. L. Carrol. 1991. The Spectrum of Lissencephaly: Report of Ten Patients Analyzed by Magnetic Resonance Imaging *Ann.Neurol.* 30, no. 2: 139-146.

Barkovich, A. J., R. I. Kuzniecky, G. D. Jackson, R. Guerrini, and W. B. Dobyns. 2001. Classification System for Malformations of Cortical Development: Update 2001 *Neurology* 57, no. 12: 2168-2178.

Barkovich, A. J., R. I. Kuzniecky, G. D. Jackson, R. Guerrini, and W. B. Dobyns. 2005. A Developmental and Genetic Classification for Malformations of Cortical Development *Neurology* 65, no. 12: 1873-1887.

bdel Razek, A. A., A. Y. Kandell, L. G. Elsorogy, A. Elmongy, and A. A. Basett. 2009. Disorders of Cortical Formation: MR Imaging Features *AJNR Am.J.Neuroradiol.* 30, no. 1: 4-11.

Bearden, C. E., K. M. Hoffman, and T. D. Cannon. 2001. The Neuropsychology and Neuroanatomy of Bipolar Affective Disorder: a Critical Review *Bipolar.Disord.* 3, no. 3: 106-150.

Beffert, U., G. Morfini, H. H. Bock, H. Reyna, S. T. Brady, and J. Herz. 2002. Reelin-Mediated Signaling Locally Regulates Protein Kinase B/Akt and Glycogen Synthase Kinase 3beta *J.Biol.Chem.* 277, no. 51: 49958-49964.

Behar, D., J. L. Rapoport, C. J. Berg, M. B. Denckla, L. Mann, C. Cox, P. Fedio, T. Zahn, and M. G. Wolfman. 1984. Computerized Tomography and Neuropsychological Test Measures in Adolescents With Obsessive-Compulsive Disorder *Am.J.Psychiatry* 141, no. 3: 363-369.

Belmont, L. D. and T. J. Mitchison. 1996. Identification of a Protein That Interacts With Tubulin Dimers and Increases the Catastrophe Rate of Microtubules *Cell* 84, no. 4: 623-631.

Beltran-Valero de, Bernabe D., S. Currier, A. Steinbrecher, J. Celli, Beusekom E. van, Zwaag B. van der, H. Kayserili, L. Merlini, D. Chitayat, W. B. Dobyns, B. Cormand, A. E. Lehesjoki, J. Cruces, T. Voit, C. A. Walsh, Bokhoven H. van, and H. G. Brunner. 2002. Mutations in the O-Mannosyltransferase Gene POMT1 Give Rise to the Severe Neuronal Migration Disorder Walker-Warburg Syndrome *Am.J.Hum.Genet.* 71, no. 5: 1033-1043.

Beltran-Valero de, Bernabe D., T. Voit, C. Longman, A. Steinbrecher, V. Straub, Y. Yuva, R. Herrmann, J. Sperner, C. Korenke, C. Diesen, W. B. Dobyns, H. G. Brunner, Bokhoven H. van, M. Brockington, and F. Muntoni. 2004. Mutations in the FKRP Gene Can Cause Muscle-Eye-Brain Disease and Walker-Warburg Syndrome *J.Med.Genet.* 41, no. 5: e61.

Belvindrah, R., D. Graus-Porta, S. Goebbels, K. A. Nave, and U. Muller. 2007. Beta1 Integrins in Radial Glia but Not in Migrating Neurons Are Essential for the Formation of Cell Layers in the Cerebral Cortex *J.Neurosci.* 27, no. 50: 13854-13865.

Bennett, M. K., J. E. Garcia-Arraras, L. A. Elferink, K. Peterson, A. M. Fleming, C. D. Hazuka, and R. H. Scheller. 1993. The Syntaxin Family of Vesicular Transport Receptors *Cell* 74, no. 5: 863-873.

Bertrand, N., D. S. Castro, and F. Guillemot. 2002. Proneural Genes and the Specification of Neural Cell Types *Nat.Rev.Neurosci.* 3, no. 7: 517-530.

Bielas, S., H. Higginbotham, H. Koizumi, T. Tanaka, and J. G. Gleeson. 2004. Cortical Neuronal Migration Mutants Suggest Separate but Intersecting Pathways *Annu.Rev.Cell Dev.Biol.* 20: 593-618.

Bock, H. H., Y. Jossin, P. Liu, E. Forster, P. May, A. M. Goffinet, and J. Herz. 2003. Phosphatidylinositol 3-Kinase Interacts With the Adaptor Protein Dab1 in Response to Reelin Signaling and Is Required for Normal Cortical Lamination *J.Biol.Chem.* 278, no. 40: 38772-38779.

Bolton, D. 1996. Annotation: Developmental Issues in Obsessive-Compulsive Disorder *J.Child Psychol.Psychiatry* 37, no. 2: 131-137.

Bondallaz, P., A. Barbier, S. Soehrman, G. Grenningloh, and B. M. Riederer. 2006. The Control of Microtubule Stability in Vitro and in Transfected Cells by MAP1B and SCG10 *Cell Motil.Cytoskeleton* 63, no. 11: 681-695.

Borrell, V., B. K. Kaspar, F. H. Gage, and E. M. Callaway. 2006. In Vivo Evidence for Radial Migration of Neurons by Long-Distance Somal Translocation in the Developing Ferret Visual Cortex *Cereb.Cortex* 16, no. 11: 1571-1583.

Borson, N. D., W. L. Salo, and L. R. Drewes. 1992. A Lock-Docking Oligo(DT) Primer for 5' and 3' RACE PCR *PCR Methods Appl.* 2, no. 2: 144-148.

Boycott, K. M., S. Flavelle, A. Bureau, H. C. Glass, T. M. Fujiwara, E. Wirrell, K. Davey, A. E. Chudley, J. N. Scott, D. R. McLeod, and J. S. Parboosingh. 2005. Homozygous Deletion of the Very Low Density Lipoprotein Receptor Gene Causes Autosomal Recessive Cerebellar Hypoplasia With Cerebral Gyral Simplification *Am.J.Hum.Genet.* 77, no. 3: 477-483.

Bray, D. and M. B. Bunge. 1981. Serial Analysis of Microtubules in Cultured Rat Sensory Axons *J.Neurocytol.* 10, no. 4: 589-605.

Brooks, A. S., A. M. Bertoli-Avella, G. M. Burzynski, G. J. Breedveld, J. Osinga, L. G. Boven, J. A. Hurst, G. M. Mancini, M. H. Lequin, R. F. de Coo, I. Matera, Graaff E. de, C. Meijers, P. J. Willems, D. Tibboel, B. A. Oostra, and R. M. Hofstra. 2005. Homozygous Nonsense Mutations in KIAA1279 Are Associated With Malformations of the Central and Enteric Nervous Systems *Am.J.Hum.Genet.* 77, no. 1: 120-126.

Buck, K. B. and J. Q. Zheng. 2002. Growth Cone Turning Induced by Direct Local Modification of Microtubule Dynamics *J.Neurosci.* 22, no. 21: 9358-9367.

Bunge, M. B. 1973. Fine Structure of Nerve Fibers and Growth Cones of Isolated Sympathetic Neurons in Culture
J.Cell Biol. 56, no. 3: 713-735.

Buxton, P., X. M. Zhang, B. Walsh, A. Sriratana, I. Schenberg, E. Manickam, and T. Rowe. 2003. Identification and Characterization of Snapin As a Ubiquitously Expressed SNARE-Binding Protein That Interacts With SNAP23 in Non-Neuronal Cells
Biochem.J. 375, no. Pt 2: 433-440.

Calakos, N., M. K. Bennett, K. E. Peterson, and R. H. Scheller. 1994. Protein-Protein Interactions Contributing to the Specificity of Intracellular Vesicular Trafficking
Science 263, no. 5150: 1146-1149.

Cardoso, C., R. J. Leventer, J. J. Dowling, H. L. Ward, J. Chung, K. S. Petras, J. A. Roseberry, A. M. Weiss, S. Das, C. L. Martin, D. T. Pilz, W. B. Dobyns, and D. H. Ledbetter. 2002. Clinical and Molecular Basis of Classical Lissencephaly: Mutations in the LIS1 Gene (PAFAH1B1)
Hum.Mutat. 19, no. 1: 4-15.

Cardoso, C., R. J. Leventer, H. L. Ward, K. Toyo-Oka, J. Chung, A. Gross, C. L. Martin, J. Allanson, D. T. Pilz, A. H. Olney, O. M. Mutchinick, S. Hirotsune, A. Wynshaw-Boris, W. B. Dobyns, and D. H. Ledbetter. 2003. Refinement of a 400-Kb Critical Region Allows Genotypic Differentiation Between Isolated Lissencephaly, Miller-Dieker Syndrome, and Other Phenotypes Secondary to Deletions of 17p13.3
Am.J.Hum.Genet. 72, no. 4: 918-930.

Casarosa, S., C. Fode, and F. Guillemot. 1999. Mash1 Regulates Neurogenesis in the Ventral Telencephalon
Development 126, no. 3: 525-534.

Caspi, M., R. Atlas, A. Kantor, T. Sapir, and O. Reiner. 2000. Interaction between LIS1 and Doublecortin, Two Lissencephaly Gene Products
Hum.Mol.Genet. 9, no. 15: 2205-2213.

Castillo AR, Buchpiguel CA, de Araújo LA, Castillo JC, Asbahr FR, Maia AK, de Oliveira Latorre MR. 2005. Brain SPECT imaging in children and adolescents with obsessive-compulsive disorder. J. *Neural Transm.* 8: 1115-29

Caviness, V. S., Jr. and P. Rakic. 1978. Mechanisms of Cortical Development: a view from Mutations in Mice
Annu.Rev.Neurosci. 1: 297-326.

Caviness, V. S., Jr. 1982. Neocortical Histogenesis in Normal and Reeler Mice: a Developmental Study Based Upon [3H]Thymidine Autoradiography
Brain Res. 256, no. 3: 293-302.

Caviness, V. S. *et al*., 1988. The reeler malformation: Implications for neocortical histogenesis.

Chae, T., Y. T. Kwon, R. Bronson, P. Dikkes, E. Li, and L. H. Tsai. 1997. Mice Lacking P35, a Neuronal Specific Activator of Cdk5, Display Cortical Lamination Defects, Seizures, and Adult Lethality
Neuron 18, no. 1: 29-42.

Chai, X., E. Forster, S. Zhao, H. H. Bock, and M. Frotscher. 2009. Reelin Stabilizes the Actin Cytoskeleton of Neuronal Processes by Inducing N-Cofilin Phosphorylation at Serine3
J.Neurosci. 29, no. 1: 288-299.

Chapman, E. R. 2002. Synaptotagmin: a Ca(2+) Sensor That Triggers Exocytosis?
Nat.Rev.Mol.Cell Biol. 3, no. 7: 498-508.

Charbaut, E., P. A. Curmi, S. Ozon, S. Lachkar, V. Redeker, and A. Sobel. 2001. Stathmin Family Proteins Display Specific Molecular and Tubulin Binding Properties
J.Biol.Chem. 276, no. 19: 16146-16154.

Chen, Y. A. and R. H. Scheller. 2001. SNARE-Mediated Membrane Fusion
Nat.Rev.Mol.Cell Biol. 2, no. 2: 98-106.

Chenchik, A., Diatchenko, L., Chang, C. & Kuchibhatla, S. 1994.
Great Lengths™ cDNA Synthesis Kit for high yields of full-length cDNA. *Clontechniques* IX(1):9–12.

Chheda, M. G., U. Ashery, P. Thakur, J. Rettig, and Z. H. Sheng. 2001. Phosphorylation of Snapin by PKA Modulates Its Interaction With the SNARE Complex
Nat.Cell Biol. 3, no. 4: 331-338.

Chiang, G. G. and R. T. Abraham. 2005. Phosphorylation of Mammalian Target of Rapamycin (MTOR) at Ser-2448 Is Mediated by P70S6 Kinase
J.Biol.Chem. 280, no. 27: 25485-25490.

Chuckowree, J. A. and J. C. Vickers. 2003. Cytoskeletal and Morphological Alterations Underlying Axonal Sprouting After Localized Transection of Cortical Neuron Axons in Vitro
J.Neurosci. 23, no. 9: 3715-3725.

Conde, Lopez, V, de la Gandara Martin JJ, M. L. Blanco Lozano, Rodriguez P. Cerezo, Roig M. Martinez, and Francos A. de Dios. 1990. [Minor Neurological Signs in Obsessive-Compulsive Disorders]
Actas Luso.Esp.Neurol.Psiquiatr.Cienc.Afines 18, no. 3: 143-164.

Cooper, J. A. 2008. A Mechanism for Inside-Out Lamination in the Neocortex. *Trends Neurosci.* no. 3: 113-119.

Couillard-Despres, S., J. Winkler, G. Uyanik, and L. Aigner. 2001. Molecular Mechanisms of Neuronal Migration Disorders, Quo Vadis?
Curr.Mol.Med. 1, no. 6: 677-688.

Courchesne, E. 2004. Brain Development in Autism: Early Overgrowth Followed by Premature Arrest of Growth
Ment.Retard.Dev.Disabil.Res.Rev. 10, no. 2: 106-111.

Courchesne, E. and K. Pierce. 2005. Brain Overgrowth in Autism During a Critical Time in Development: Implications for Frontal Pyramidal Neuron and Interneuron Development and Connectivity
Int.J.Dev.Neurosci. 23, no. 2-3: 153-170.

Craig, A. M. and G. Banker. 1994. Neuronal Polarity
Annu.Rev.Neurosci. 17: 267-310.

Curmi, P. A., A. Maucuer, S. Asselin, M. Lecourtois, A. Chaffotte, J. M. Schmitter, and A. Sobel. 1994. Molecular Characterization of Human Stathmin Expressed in Escherichia Coli: Site-Directed Mutagenesis of Two Phosphorylatable Serines (Ser-25 and Ser-63)
Biochem.J. 300 (Pt 2): 331-338.

Curmi, P. A., S. S. Andersen, S. Lachkar, O. Gavet, E. Karsenti, M. Knossow, and A. Sobel. 1997. The Stathmin/Tubulin Interaction in Vitro
J.Biol.Chem. 272, no. 40: 25029-25036.

Curmi, P. A., O. Gavet, E. Charbaut, S. Ozon, S. Lachkar-Colmerauer, V. Manceau, S. Siavoshian, A. Maucuer, and A. Sobel. 1999. Stathmin and Its Phosphoprotein Family: General Properties, Biochemical and Functional Interaction With Tubulin
Cell Struct.Funct. 24, no. 5: 345-357.

Curran, T. and G. D'Arcangelo. 1998. Role of Reelin in the Control of Brain Development
Brain Res.Brain Res.Rev. 26, no. 2-3: 285-294.

Cusick, M. E., N. Klitgord, M. Vidal, and D. E. Hill. 2005. Interactome: Gateway into Systems Biology
Hum.Mol.Genet. 14 Spec No. 2: R171-R181.

D'Arcangelo, G., G. G. Miao, S. C. Chen, H. D. Soares, J. I. Morgan, and T. Curran. 1995. A Protein Related to Extracellular Matrix Proteins Deleted in the Mouse Mutant Reeler. *Nature* 374, no. 6524: 719-723.

D'Arcangelo, G., K. Nakajima, T. Miyata, M. Ogawa, K. Mikoshiba, and T. Curran. 1997. Reelin Is a Secreted Glycoprotein Recognized by the CR-50 Monoclonal Antibody
J.Neurosci. 17, no. 1: 23-31.

D'Arcangelo, G. and T. Curran. 1998. Reeler: New Tales on an Old Mutant Mouse
Bioessays 20, no. 3: 235-244.

D'Arcangelo, G., R. Homayouni, L. Keshvara, D. S. Rice, M. Sheldon, and T. Curran. 1999. Reelin Is a Ligand for Lipoprotein Receptors
Neuron 24, no. 2: 471-479.

D'Arcangelo, G. 2001. The Role of the Reelin Pathway in Cortical Development
Symp.Soc.Exp.Biol., no. 53: 59-73.

D'Arcangelo, G. 2005. The Reeler Mouse: Anatomy of a Mutant
Int.Rev.Neurobiol. 71: 383-417.

D'Arcangelo, G. 2005. Apoer2: a Reelin Receptor to Remember
Neuron 47, no. 4: 471-473.

D'Arcangelo, G. 2006. Reelin Mouse Mutants As Models of Cortical Development Disorders
Epilepsy Behav. 8, no. 1: 81-90.

Dabora, S. L., S. Jozwiak, D. N. Franz, P. S. Roberts, A. Nieto, J. Chung, Y. S. Choy, M. P. Reeve, E. Thiele, J. C. Egelhoff, J. Kasprzyk-Obara, D. Domanska-Pakiela, and D. J. Kwiatkowski. 2001. Mutational Analysis in a Cohort of 224 Tuberous Sclerosis Patients Indicates Increased Severity of TSC2, Compared With TSC1, Disease in Multiple Organs
Am.J.Hum.Genet. 68, no. 1: 64-80.

Dammermann, A., A. Desai, and K. Oegema. 2003. The Minus End in Sight
Curr.Biol. 13, no. 15: R614-R624.

Dawe, H. R., L. S. Minamide, J. R. Bamburg, and L. P. Cramer. 2003. ADF/Cofilin Controls Cell Polarity During Fibroblast Migration
Curr.Biol. 13, no. 3: 252-257.

De Carlos, J. A., L. Lopez-Mascaraque, and F. Valverde. 1996. Dynamics of Cell Migration From the Lateral Ganglionic Eminence in the Rat
J.Neurosci. 16, no. 19: 6146-6156.

de, Bergeyck, V, B. Naerhuyzen, A. M. Goffinet, and Rouvroit C. Lambert de. 1998. A Panel of Monoclonal Antibodies Against Reelin, the Extracellular Matrix Protein Defective in Reeler Mutant Mice
J.Neurosci.Methods 82, no. 1: 17-24.

DeFreitas, M. F., C. K. Yoshida, W. A. Frazier, D. L. Mendrick, R. M. Kypta, and L. F. Reichardt. 1995. Identification of Integrin Alpha 3 Beta 1 As a Neuronal Thrombospondin Receptor Mediating Neurite Outgrowth
Neuron 15, no. 2: 333-343.

Degreef, G., M. Ashtari, H. W. Wu, M. Borenstein, S. Geisler, and J. Lieberman. 1991. Follow Up MRI Study in First Episode Schizophrenia
Schizophr.Res. 5, no. 3: 204-206.

Deguchi, K., K. Inoue, W. E. Avila, D. Lopez-Terrada, B. A. Antalffy, C. C. Quattrocchi, M. Sheldon, K. Mikoshiba, G. D'Arcangelo, and D. L. Armstrong. 2003. Reelin and Disabled-1 Expression in Developing and Mature Human Cortical Neurons
J.Neuropathol.Exp.Neurol. 62, no. 6: 676-684.

DeLisi, L. E., P. Stritzke, H. Riordan, V. Holan, A. Boccio, M. Kushner, J. McClelland, Eyl O. Van, and A. Anand. 1992. The Timing of Brain Morphological Changes in Schizophrenia and Their Relationship to Clinical Outcome
Biol.Psychiatry 31, no. 3: 241-254.

Denaxa, M., C. H. Chan, M. Schachner, J. G. Parnavelas, and D. Karagogeos. 2001. The Adhesion Molecule TAG-1 Mediates the Migration of Cortical Interneurons From the Ganglionic Eminence Along the Corticofugal Fiber System
Development 128, no. 22: 4635-4644.

Dent, E. W., J. L. Callaway, G. Szebenyi, P. W. Baas, and K. Kalil. 1999. Reorganization and Movement of Microtubules in Axonal Growth Cones and Developing Interstitial Branches
J.Neurosci. 19, no. 20: 8894-8908.

Dent, E. W. and K. Kalil. 2001. Axon Branching Requires Interactions Between Dynamic Microtubules and Actin Filaments
J.Neurosci. 21, no. 24: 9757-9769.

Dent, E. W. and F. B. Gertler. 2003. Cytoskeletal Dynamics and Transport in Growth Cone Motility and Axon Guidance
Neuron 40, no. 2: 209-227.

des, Portes, V, J. M. Pinard, P. Billuart, M. C. Vinet, A. Koulakoff, A. Carrie, A. Gelot, E. Dupuis, J. Motte, Y. Berwald-Netter, M. Catala, A. Kahn, C. Beldjord, and J. Chelly. 1998. A Novel CNS Gene Required for Neuronal Migration and Involved in X-Linked Subcortical Laminar Heterotopia and Lissencephaly Syndrome
Cell 92, no. 1: 51-61.

Desai, A. and T. J. Mitchison. 1997. Microtubule Polymerization Dynamics
Annu.Rev.Cell Dev.Biol. 13: 83-117.

DeSilva, U., G. D'Arcangelo, V. V. Braden, J. Chen, G. G. Miao, T. Curran, and E. D. Green. 1997. The Human Reelin Gene: Isolation, Sequencing, and Mapping on Chromosome 7 *Genome Res.* 7, no. 2: 157-164.

Di, Paolo G., R. Lutjens, A. Osen-Sand, A. Sobel, S. Catsicas, and G. Grenningloh. 1997. Differential Distribution of Stathmin and SCG10 in Developing Neurons in Culture *J.Neurosci.Res.* 50, no. 6: 1000-1009.

Di, Paolo G., R. Lutjens, V. Pellier, S. A. Stimpson, M. H. Beuchat, S. Catsicas, and G. Grenningloh. 1997. Targeting of SCG10 to the Area of the Golgi Complex Is Mediated by Its NH2-Terminal Region *J.Biol.Chem.* 272, no. 8: 5175-5182.

Dickson, B. J. 2002. Molecular Mechanisms of Axon Guidance *Science* 298, no. 5600: 1959-1964.

Dobyns, W. B., O. Reiner, R. Carrozzo, and D. H. Ledbetter. 1993. Lissencephaly. A Human Brain Malformation Associated With Deletion of the LIS1 Gene Located at Chromosome 17p13 *JAMA* 270, no. 23: 2838-2842.

Dobyns, W. B., E. Andermann, F. Andermann, D. Czapansky-Beilman, F. Dubeau, O. Dulac, R. Guerrini, B. Hirsch, D. H. Ledbetter, N. S. Lee, J. Motte, J. M. Pinard, R. A. Radtke, M. E. Ross, D. Tampieri, C. A. Walsh, and C. L. Truwit. 1996. X-Linked Malformations of Neuronal Migration *Neurology* 47, no. 2: 331-339.

Douglas, R. J. and K. A. Martin. 2007. Mapping the Matrix: the Ways of Neocortex *Neuron* 56, no. 2: 226-238.

Doye, V., F. Soubrier, G. Bauw, M. C. Boutterin, L. Beretta, J. Koppel, J. Vandekerckhove, and A. Sobel. 1989. A Single CDNA Encodes Two Isoforms of Stathmin, a Developmentally Regulated Neuron-Enriched Phosphoprotein *J.Biol.Chem.* 264, no. 21: 12134-12137.

Drechsel, D. N., A. A. Hyman, M. H. Cobb, and M. W. Kirschner. 1992. Modulation of the Dynamic Instability of Tubulin Assembly by the Microtubule-Associated Protein Tau *Mol.Biol.Cell* 3, no. 10: 1141-1154.

Dulabon, L., E. C. Olson, M. G. Taglienti, S. Eisenhuth, B. McGrath, C. A. Walsh, J. A. Kreidberg, and E. S. Anton. 2000. Reelin Binds Alpha3beta1 Integrin and Inhibits Neuronal Migration *Neuron* 27, no. 1: 33-44.

Eash, D., D. Waggoner, J. Chung, D. Stevenson, and C. L. Martin. 2005. Calibration of 6q Subtelomere Deletions to Define Genotype/Phenotype Correlations *Clin.Genet.* 67, no. 5: 396-403.

Elias, L. A., D. D. Wang, and A. R. Kriegstein. 2007. Gap Junction Adhesion Is Necessary for Radial Migration in the Neocortex *Nature* 448, no. 7156: 901-907.

Emanuelsson, O., Heijne G. von, and G. Schneider. 2001. Analysis and Prediction of Mitochondrial Targeting Peptides *Methods Cell Biol.* 65: 175-187.

Emes, R. D. and C. P. Ponting. 2001. A New Sequence Motif Linking Lissencephaly, Treacher Collins and Oral-Facial-Digital Type 1 Syndromes, Microtubule Dynamics and Cell Migration
Hum.Mol.Genet. 10, no. 24: 2813-2820.

Etienne-Manneville, S. 2004. Actin and Microtubules in Cell Motility: Which One Is in Control?
Traffic. 5, no. 7: 470-477.

Farah, M. H., J. M. Olson, H. B. Sucic, R. I. Hume, S. J. Tapscott, and D. L. Turner. 2000. Generation of Neurons by Transient Expression of Neural BHLH Proteins in Mammalian Cells
Development 127, no. 4: 693-702.

Fasshauer, D., W. K. Eliason, A. T. Brunger, and R. Jahn. 1998. Identification of a Minimal Core of the Synaptic SNARE Complex Sufficient for Reversible Assembly and Disassembly
Biochemistry 37, no. 29: 10354-10362.

Fassler, R. and M. Meyer. 1995. Consequences of Lack of Beta 1 Integrin Gene Expression in Mice
Genes Dev. 9, no. 15: 1896-1908.

Fatemi, S. H., J. A. Earle, and T. McMenomy. 2000. Reduction in Reelin Immunoreactivity in Hippocampus of Subjects With Schizophrenia, Bipolar Disorder and Major Depression
Mol.Psychiatry 5, no. 6: 654-63, 571.

Fatemi, S. H., J. M. Stary, A. R. Halt, and G. R. Realmuto. 2001. Dysregulation of Reelin and Bcl-2 Proteins in Autistic Cerebellum
J.Autism Dev.Disord. 31, no. 6: 529-535.

Feng, L., N. S. Allen, S. Simo, and J. A. Cooper. 2007. Cullin 5 Regulates Dab1 Protein Levels and Neuron Positioning During Cortical Development
Genes Dev. 21, no. 21: 2717-2730.

Feng, L. and J. A. Cooper. 2009. Dual Functions of Dab1 During Brain Development
Mol.Cell Biol. 29, no. 2: 324-332.

Feng, Y. and C. A. Walsh. 2001. Protein-Protein Interactions, Cytoskeletal Regulation and Neuronal Migration
Nat.Rev.Neurosci. 2, no. 6: 408-416.

Ferland, R. J., J. N. Gaitanis, K. Apse, U. Tantravahi, C. A. Walsh, and V. L. Sheen. 2006. Periventricular Nodular Heterotopia and Williams Syndrome
Am.J.Med.Genet.A 140, no. 12: 1305-1311.

Fish, B. 1957. The Detection of Schizophrenia in Infancy; a Preliminary Report
J.Nerv.Ment.Dis. 125, no. 1: 1-24.

Fishman, R. B. and M. E. Hatten. 1993. Multiple Receptor Systems Promote CNS Neural Migration
J.Neurosci. 13, no. 8: 3485-3495.

Forscher, P. and S. J. Smith. 1988. Actions of Cytochalasins on the Organization of Actin Filaments and Microtubules in a Neuronal Growth Cone
J.Cell Biol. 107, no. 4: 1505-1516.

Forster, E., A. Tielsch, B. Saum, K. H. Weiss, C. Johanssen, D. Graus-Porta, U. Muller, and M. Frotscher. 2002. Reelin, Disabled 1, and Beta 1 Integrins Are Required for the Formation of

the Radial Glial Scaffold in the Hippocampus
Proc.Natl.Acad.Sci.U.S.A 99, no. 20: 13178-13183.

Francis, F., A. Koulakoff, D. Boucher, P. Chafey, B. Schaar, M. C. Vinet, G. Friocourt, N. McDonnell, O. Reiner, A. Kahn, S. K. McConnell, Y. Berwald-Netter, P. Denoulet, and J. Chelly. 1999. Doublecortin Is a Developmentally Regulated, Microtubule-Associated Protein Expressed in Migrating and Differentiating Neurons *Neuron* 23, no. 2: 247-256.

Frotscher, M., C. A. Haas, and E. Forster. 2003. Reelin Controls Granule Cell Migration in the Dentate Gyrus by Acting on the Radial Glial Scaffold
Cereb.Cortex 13, no. 6: 634-640.

Gavet, O., S. Ozon, V. Manceau, S. Lawler, P. Curmi, and A. Sobel. 1998. The Stathmin Phosphoprotein Family: Intracellular Localization and Effects on the Microtubule Network
J.Cell Sci. 111 (Pt 22): 3333-3346.

Georges-Labouesse, E., M. Mark, N. Messaddeq, and A. Gansmuller. 1998. Essential Role of Alpha 6 Integrins in Cortical and Retinal Lamination
Curr.Biol. 8, no. 17: 983-986.

Gerlitz, G., E. Darhin, G. Giorgio, B. Franco, and O. Reiner. 2005. Novel Functional Features of the Lis-H Domain: Role in Protein Dimerization, Half-Life and Cellular Localization
Cell Cycle 4, no. 11: 1632-1640.

Ghosh, M., X. Song, G. Mouneimne, M. Sidani, D. S. Lawrence, and J. S. Condeelis. 2004. Cofilin Promotes Actin Polymerization and Defines the Direction of Cell Motility
Science 304, no. 5671: 743-746.

Gilmore, E. C. and K. Herrup. 2000. Cortical Development: Receiving Reelin
Curr.Biol. 10, no. 4: R162-R166.

Glaser, T., L. Jepeal, J. G. Edwards, S. R. Young, J. Favor, and R. L. Maas. 1994. PAX6 Gene Dosage Effect in a Family With Congenital Cataracts, Aniridia, Anophthalmia and Central Nervous System Defects
Nat.Genet. 7, no. 4: 463-471.

Gleeson, J. G., K. M. Allen, J. W. Fox, E. D. Lamperti, S. Berkovic, I. Scheffer, E. C. Cooper, W. B. Dobyns, S. R. Minnerath, M. E. Ross, and C. A. Walsh. 1998. Doublecortin, a Brain-Specific Gene Mutated in Human X-Linked Lissencephaly and Double Cortex Syndrome, Encodes a Putative Signaling Protein
Cell 92, no. 1: 63-72.

Gleeson, J. G., P. T. Lin, L. A. Flanagan, and C. A. Walsh. 1999. Doublecortin Is a Microtubule-Associated Protein and Is Expressed Widely by Migrating Neurons
Neuron 23, no. 2: 257-271.

Gleeson, J. G. and C. A. Walsh. 2000. Neuronal Migration Disorders: From Genetic Diseases to Developmental Mechanisms
Trends Neurosci. 23, no. 8: 352-359.

Goffinet, A. M. 1979. An Early Development Defect in the Cerebral Cortex of the Reeler Mouse. A Morphological Study Leading to a Hypothesis Concerning the Action of the Mutant Gene
Anat.Embryol.(Berl) 157, no. 2: 205-216.

Gong, Y., J. Wu, H. Qiang, B. Liu, Z. Chi, T. Chen, B. Yin, X. Peng, and J. Yuan. 2008. BRI3 Associates With SCG10 and Attenuates NGF-Induced Neurite Outgrowth in PC12 Cells *BMB.Rep.* 41, no. 4: 287-293.

Gonzalez-Billault, C., J. A. Del Rio, J. M. Urena, E. M. Jimenez-Mateos, M. J. Barallobre, M. Pascual, L. Pujadas, S. Simo, A. L. Torre, R. Gavin, F. Wandosell, E. Soriano, and J. Avila. 2005. A Role of MAP1B in Reelin-Dependent Neuronal Migration *Cereb.Cortex* 15, no. 8: 1134-1145.

Goodwin, G. M., A. Martinez-Aran, D. C. Glahn, and E. Vieta. 2008. Cognitive Impairment in Bipolar Disorder: Neurodevelopment or Neurodegeneration? An ECNP Expert Meeting Report *Eur.Neuropsychopharmacol.* 18, no. 11: 787-793.

Gordon-Weeks, P. R. 1991. Control of Microtubule Assembly in Growth Cones *J.Cell Sci.Suppl* 15: 45-49.

Gordon-Weeks, P. R. and I. Fischer. 2000. MAP1B Expression and Microtubule Stability in Growing and Regenerating Axons *Microsc.Res.Tech.* 48, no. 2: 63-74.

Gordon-Weeks, P. R. 2004. Microtubules and Growth Cone Function *J.Neurobiol.* 58, no. 1: 70-83.

Gotthardt, M., M. Trommsdorff, M. F. Nevitt, J. Shelton, J. A. Richardson, W. Stockinger, J. Nimpf, and J. Herz. 2000. Interactions of the Low Density Lipoprotein Receptor Gene Family With Cytosolic Adaptor and Scaffold Proteins Suggest Diverse Biological Functions in Cellular Communication and Signal Transduction *J.Biol.Chem.* 275, no. 33: 25616-25624.

Grenningloh, G., S. Soehrman, P. Bondallaz, E. Ruchti, and H. Cadas. 2004. Role of the Microtubule Destabilising Proteins SCG10 and Stathmin in Neuronal Growth *J.Neurobiol.* 58, no. 1: 60-69.

Guerrini, R. and T. Filippi. 2005. Neuronal Migration Disorders, Genetics, and Epileptogenesis *J.Child Neurol.* 20, no. 4: 287-299.

Guerrini, R. and C. Marini. 2006. Genetic Malformations of Cortical Development *Exp.Brain Res.* 173, no. 2: 322-333.

Guerrini, R., W. B. Dobyns, and A. J. Barkovich. 2008. Abnormal Development of the Human Cerebral Cortex: Genetics, Functional Consequences and Treatment Options *Trends Neurosci.* 31, no. 3: 154-162.

Guidotti, A., J. Auta, J. M. Davis, V. Di-Giorgi-Gerevini, Y. Dwivedi, D. R. Grayson, F. Impagnatiello, G. Pandey, C. Pesold, R. Sharma, D. Uzunov, and E. Costa. 2000. Decrease in Reelin and Glutamic Acid Decarboxylase67 (GAD67) Expression in Schizophrenia and Bipolar Disorder: a Postmortem Brain Study *Arch.Gen.Psychiatry* 57, no. 11: 1061-1069.

Guidotti, A., C. Pesold, and E. Costa. 2000. New Neurochemical Markers for Psychosis: a Working Hypothesis of Their Operation *Neurochem.Res.* 25, no. 9-10: 1207-1218.

Guillemot, F., Z. Molnar, V. Tarabykin, and A. Stoykova. 2006. Molecular Mechanisms of Cortical Differentiation
Eur.J.Neurosci. 23, no. 4: 857-868.

Gupta, A., L. H. Tsai, and A. Wynshaw-Boris. 2002. Life Is a Journey: a Genetic Look at Neocortical Development
Nat.Rev.Genet. 3, no. 5: 342-355.

Hack, I., S. Hellwig, D. Junghans, B. Brunne, H. H. Bock, S. Zhao, and M. Frotscher. 2007. Divergent Roles of ApoER2 and Vldlr in the Migration of Cortical Neurons
Development 134, no. 21: 3883-3891.

Hardy, J., K. Duff, K. G. Hardy, J. Perez-Tur, and M. Hutton. 1998. Genetic Dissection of Alzheimer's Disease and Related Dementias: Amyloid and Its Relationship to Tau
Nat.Neurosci. 1, no. 5: 355-358.

Harrison, P. J. 1997. Schizophrenia: a Disorder of Neurodevelopment?
Curr.Opin.Neurobiol. 7, no. 2: 285-289.

Hatanaka, Y., S. Hisanaga, C. W. Heizmann, and F. Murakami. 2004. Distinct Migratory Behavior of Early- and Late-Born Neurons Derived From the Cortical Ventricular Zone
J.Comp Neurol. 479, no. 1: 1-14.

Hattori, M., H. Adachi, M. Tsujimoto, H. Arai, and K. Inoue. 1994. Miller-Dieker Lissencephaly Gene Encodes a Subunit of Brain Platelet-Activating Factor Acetylhydrolase [Corrected]
Nature 370, no. 6486: 216-218.

Hayashi, K., Y. Pan, H. Shu, T. Ohshima, J. W. Kansy, C. L. White, III, C. A. Tamminga, A. Sobel, P. A. Curmi, K. Mikoshiba, and J. A. Bibb. 2006. Phosphorylation of the Tubulin-Binding Protein, Stathmin, by Cdk5 and MAP Kinases in the Brain
J.Neurochem. 99, no. 1: 237-250.

Heidemann, S. R., J. M. Landers, and M. A. Hamborg. 1981. Polarity Orientation of Axonal Microtubules
J.Cell Biol. 91, no. 3 Pt 1: 661-665.

Henning, K. A., L. Li, N. Iyer, L. D. McDaniel, M. S. Reagan, R. Legerski, R. A. Schultz, M. Stefanini, A. R. Lehmann, L. V. Mayne, and E. C. Friedberg. 1995. The Cockayne Syndrome Group A Gene Encodes a WD Repeat Protein That Interacts With CSB Protein and a Subunit of RNA Polymerase II TFIIH
Cell 82, no. 4: 555-564.

Herbert, M. R. 2005. Large Brains in Autism: the Challenge of Pervasive Abnormality
Neuroscientist. 11, no. 5: 417-440.

Herculano-Houzel, S., C. E. Collins, P. Wong, and J. H. Kaas. 2007. Cellular Scaling Rules for Primate Brains
Proc.Natl.Acad.Sci.U.S.A 104, no. 9: 3562-3567.

Herz, J. and H. H. Bock. 2002. Lipoprotein Receptors in the Nervous System
Annu.Rev.Biochem. 71: 405-434.

Hiesberger, T., M. Trommsdorff, B. W. Howell, A. Goffinet, M. C. Mumby, J. A. Cooper, and J. Herz. 1999. Direct Binding of Reelin to VLDL Receptor and ApoE Receptor 2 Induces

Tyrosine Phosphorylation of Disabled-1 and Modulates Tau Phosphorylation
Neuron 24, no. 2: 481-489.

Hilfiker, S., P. Greengard, and G. J. Augustine. 1999. Coupling Calcium to SNARE-Mediated Synaptic Vesicle Fusion
Nat.Neurosci. 2, no. 2: 104-106.

Himi, T., T. Okazaki, H. Wang, T. H. McNeill, and N. Mori. 1994. Differential Localization of SCG10 and P19/Stathmin Messenger RNAs in Adult Rat Brain Indicates Distinct Roles for These Growth-Associated Proteins
Neuroscience 60, no. 4: 907-926.

Hirotsune, S., M. W. Fleck, M. J. Gambello, G. J. Bix, A. Chen, G. D. Clark, D. H. Ledbetter, C. J. McBain, and A. Wynshaw-Boris. 1998. Graded Reduction of Pafah1b1 (Lis1) Activity Results in Neuronal Migration Defects and Early Embryonic Lethality
Nat.Genet. 19, no. 4: 333-339.

Hollander, E., E. Schiffman, B. Cohen, M. A. Rivera-Stein, W. Rosen, J. M. Gorman, A. J. Fyer, L. Papp, and M. R. Liebowitz. 1990. Signs of Central Nervous System Dysfunction in Obsessive-Compulsive Disorder
Arch.Gen.Psychiatry 47, no. 1: 27-32.

Holz, M. K. and J. Blenis. 2005. Identification of S6 Kinase 1 As a Novel Mammalian Target of Rapamycin (MTOR)-Phosphorylating Kinase
J.Biol.Chem. 280, no. 28: 26089-26093.

Honda, T., H. Tabata, and K. Nakajima. 2003. Cellular and Molecular Mechanisms of Neuronal Migration in Neocortical Development
Semin.Cell Dev.Biol. 14, no. 3: 169-174.

Horwitz, S. B., H. J. Shen, L. He, P. Dittmar, R. Neef, J. Chen, and U. K. Schubart. 1997. The Microtubule-Destabilising Activity of Metablastin (P19) Is Controlled by Phosphorylation
J.Biol.Chem. 272, no. 13: 8129-8132.

Howell, B. W., R. Hawkes, P. Soriano, and J. A. Cooper. 1997. Neuronal Position in the Developing Brain Is Regulated by Mouse Disabled-1
Nature 389, no. 6652: 733-737.

Howell, B. W., F. B. Gertler, and J. A. Cooper. 1997. Mouse Disabled (MDab1): a Src Binding Protein Implicated in Neuronal Development
EMBO J. 16, no. 1: 121-132.

Howell, B. W., T. M. Herrick, and J. A. Cooper. 1999. Reelin-Induced Tyrosine [Corrected] Phosphorylation of Disabled 1 During Neuronal Positioning
Genes Dev. 13, no. 6: 643-648.

Howell, B. W., L. M. Lanier, R. Frank, F. B. Gertler, and J. A. Cooper. 1999. The Disabled 1 Phosphotyrosine-Binding Domain Binds to the Internalization Signals of Transmembrane Glycoproteins and to Phospholipids
Mol.Cell Biol. 19, no. 7: 5179-5188.

Howell, B. W., T. M. Herrick, J. D. Hildebrand, Y. Zhang, and J. A. Cooper. 2000. Dab1 Tyrosine Phosphorylation Sites Relay Positional Signals During Mouse Brain Development
Curr.Biol. 10, no. 15: 877-885.

Hua, S. and Z. Sun. 2001. Support Vector Machine Approach for Protein Subcellular Localization Prediction
Bioinformatics. 17, no. 8: 721-728.

Huang, Z. 2009. Molecular Regulation of Neuronal Migration During Neocortical Development
Mol.Cell Neurosci.

Hunter-Schaedle, K. E. 1997. Radial Glial Cell Development and Transformation Are Disturbed in Reeler Forebrain
J.Neurobiol. 33, no. 4: 459-472.

Hyde, T. M., J. C. Ziegler, and D. R. Weinberger. 1992. Psychiatric Disturbances in Metachromatic Leukodystrophy. Insights into the Neurobiology of Psychosis
Arch.Neurol. 49, no. 4: 401-406.

Ilangumaran, S., S. Ramanathan, and R. Rottapel. 2004. Regulation of the Immune System by SOCS Family Adaptor Proteins
Semin.Immunol. 16, no. 6: 351-365.

Ilardi, J. M., S. Mochida, and Z. H. Sheng. 1999. Snapin: a SNARE-Associated Protein Implicated in Synaptic Transmission
Nat.Neurosci. 2, no. 2: 119-124.

Illowsky, B. P., D. M. Juliano, L. B. Bigelow, and D. R. Weinberger. 1988. Stability of CT Scan Findings in Schizophrenia: Results of an 8 Year Follow-Up Study
J.Neurol.Neurosurg.Psychiatry 51, no. 2: 209-213.

Impagnatiello, F., A. R. Guidotti, C. Pesold, Y. Dwivedi, H. Caruncho, M. G. Pisu, D. P. Uzunov, N. R. Smalheiser, J. M. Davis, G. N. Pandey, G. D. Pappas, P. Tueting, R. P. Sharma, and E. Costa. 1998. A Decrease of Reelin Expression As a Putative Vulnerability Factor in Schizophrenia
Proc.Natl.Acad.Sci.U.S.A 95, no. 26: 15718-15723.

Jaskiw, G. E., D. M. Juliano, T. E. Goldberg, M. Hertzman, E. Urow-Hamell, and D. R. Weinberger. 1994. Cerebral Ventricular Enlargement in Schizophreniform Disorder Does Not Progress. A Seven Year Follow-Up Study
Schizophr.Res. 14, no. 1: 23-28.

Johnstone, E. C., T. J. Crow, C. D. Frith, J. Husband, and L. Kreel. 1976. Cerebral Ventricular Size and Cognitive Impairment in Chronic Schizophrenia
Lancet 2, no. 7992: 924-926.

Jossin, Y. and A. M. Goffinet. 2007. Reelin Signals Through Phosphatidylinositol 3-Kinase and Akt to Control Cortical Development and Through MTor to Regulate Dendritic Growth
Mol.Cell Biol. 27, no. 20: 7113-7124.

Jourdain, L., P. Curmi, A. Sobel, D. Pantaloni, and M. F. Carlier. 1997. Stathmin: a Tubulin-Sequestering Protein Which Forms a Ternary T2S Complex With Two Tubulin Molecules
Biochemistry 36, no. 36: 10817-10821.

Jovceva, E., M. R. Larsen, M. D. Waterfield, B. Baum, and J. F. Timms. 2007. Dynamic Cofilin Phosphorylation in the Control of Lamellipodial Actin Homeostasis
J.Cell Sci. 120, no. Pt 11: 1888-1897.

Kaas, J. H. 2000. Evolution of Somatosensory and Motor Cortex in Primates
Anat.Rec.A Discov.Mol.Cell Evol.Biol. 281, no. 1: 1148-1156.

Kaas, J. H. 2007. The Evolution of the Complex Sensory and Motor Systems of the Human Brain
Brain Res.Bull. 75, no. 2-4: 384-390.

Kabir, N., A. W. Schaefer, A. Nakhost, W. S. Sossin, and P. Forscher. 2001. Protein Kinase C Activation Promotes Microtubule Advance in Neuronal Growth Cones by Increasing Average Microtubule Growth Lifetimes
J.Cell Biol. 152, no. 5: 1033-1044.

Kalil, K. and E. W. Dent. 2005. Touch and Go: Guidance Cues Signal to the Growth Cone Cytoskeleton
Curr.Opin.Neurobiol. 15, no. 5: 521-526.

Kanatani, S., H. Tabata, and K. Nakajima. 2005. Neuronal Migration in Cortical Development
J.Child Neurol. 20, no. 4: 274-279.

Kato, M., S. Das, K. Petras, K. Kitamura, K. Morohashi, D. N. Abuelo, M. Barr, D. Bonneau, A. F. Brady, N. J. Carpenter, K. L. Cipero, F. Frisone, T. Fukuda, R. Guerrini, E. Iida, M. Itoh, A. F. Lewanda, Y. Nanba, A. Oka, V. K. Proud, P. Saugier-Veber, S. L. Schelley, A. Selicorni, R. Shaner, M. Silengo, F. Stewart, N. Sugiyama, J. Toyama, A. Toutain, A. L. Vargas, M. Yanazawa, E. H. Zackai, and W. B. Dobyns. 2004. Mutations of ARX Are Associated With Striking Pleiotropy and Consistent Genotype-Phenotype Correlation
Hum.Mutat. 23, no. 2: 147-159.

Kawauchi, T., K. Chihama, Y. Nabeshima, and M. Hoshino. 2003. The in Vivo Roles of STEF/Tiam1, Rac1 and JNK in Cortical Neuronal Migration
EMBO J. 22, no. 16: 4190-4201.

Kawauchi, T., K. Chihama, Y. V. Nishimura, Y. Nabeshima, and M. Hoshino. 2005. MAP1B Phosphorylation Is Differentially Regulated by Cdk5/P35, Cdk5/P25, and JNK
Biochem.Biophys.Res.Commun. 331, no. 1: 50-55.

Keays, D. A. 2007. Neuronal Migration: Unraveling the Molecular Pathway With Humans, Mice, and a Fungus
Mamm.Genome 18, no. 6-7: 425-430.

Keays, D. A., G. Tian, K. Poirier, G. J. Huang, C. Siebold, J. Cleak, P. L. Oliver, M. Fray, R. J. Harvey, Z. Molnar, M. C. Pinon, N. Dear, W. Valdar, S. D. Brown, K. E. Davies, J. N. Rawlins, N. J. Cowan, P. Nolan, J. Chelly, and J. Flint. 2007. Mutations in Alpha-Tubulin Cause Abnormal Neuronal Migration in Mice and Lissencephaly in Humans
Cell 128, no. 1: 45-57.

Kemper, T. L. and M. Bauman. 1998. Neuropathology of Infantile Autism
J.Neuropathol.Exp.Neurol. 57, no. 7: 645-652.

Kim, D. H., H. Iijima, K. Goto, J. Sakai, H. Ishii, H. J. Kim, H. Suzuki, H. Kondo, S. Saeki, and T. Yamamoto. 1996. Human Apolipoprotein E Receptor 2. A Novel Lipoprotein Receptor of the Low Density Lipoprotein Receptor Family Predominantly Expressed in Brain
J.Biol.Chem. 271, no. 14: 8373-8380.

Kinnear, C. 2007. Molecular genetic strategies to identify obsessive-compulsive disorder (OCD) and schizophrenia candidate genes in SA sub-population groups.

Kiuchi, T., K. Ohashi, S. Kurita, and K. Mizuno. 2007. Cofilin Promotes Stimulus-Induced Lamellipodium Formation by Generating an Abundant Supply of Actin Monomers *J.Cell Biol.* 177, no. 3: 465-476.

Klar, A., M. Baldassare, and T. M. Jessell. 1992. F-Spondin: a Gene Expressed at High Levels in the Floor Plate Encodes a Secreted Protein That Promotes Neural Cell Adhesion and Neurite Extension *Cell* 69, no. 1: 95-110.

Kondo-Iida, E., K. Kobayashi, M. Watanabe, J. Sasaki, T. Kumagai, H. Koide, K. Saito, M. Osawa, Y. Nakamura, and T. Toda. 1999. Novel Mutations and Genotype-Phenotype Relationships in 107 Families With Fukuyama-Type Congenital Muscular Dystrophy (FCMD) *Hum.Mol.Genet.* 8, no. 12: 2303-2309.

Kriegstein, A. and J. G. Parnavelas. 2006. Progress in Corticogenesis *Cereb.Cortex* 16 Suppl 1: i1-i2.

Kriegstein, A. R. and M. Gotz. 2003. Radial Glia Diversity: a Matter of Cell Fate *Glia* 43, no. 1: 37-43.

Kriegstein, A. R. and S. C. Noctor. 2004. Patterns of Neuronal Migration in the Embryonic Cortex *Trends Neurosci.* 27, no. 7: 392-399.

Kriegstein, A. R. and S. C. Noctor. 2004. Patterns of Neuronal Migration in the Embryonic Cortex *Trends Neurosci.* 27, no. 7: 392-399.

Kubo K, and Nakajima K. 2002. Secreted reelin molecules form heterodimers. *Neurosci Res.* 43, no. 4: 381-8

Lambert de, Rouvroit C. and A. M. Goffinet. 1998. The Reeler Mouse As a Model of Brain Development *Adv.Anat.Embryol.Cell Biol.* 150: 1-106.

Lamparello, P., M. Baybis, J. Pollard, E. M. Hol, D. D. Eisenstat, E. Aronica, and P. B. Crino. 2007. Developmental Lineage of Cell Types in Cortical Dysplasia With Balloon Cells *Brain* 130, no. Pt 9: 2267-2276.

Lee, J. E. 1997. Basic Helix-Loop-Helix Genes in Neural Development *Curr.Opin.Neurobiol.* 7, no. 1: 13-20.

Lenane, M. C., S. E. Swedo, H. Leonard, D. L. Pauls, W. Sceery, and J. L. Rapoport. 1990. Psychiatric Disorders in First Degree Relatives of Children and Adolescents With Obsessive Compulsive Disorder *J.Am.Acad.Child Adolesc.Psychiatry* 29, no. 3: 407-412.

Letourneau, P. C. and A. H. Ressler. 1984. Inhibition of Neurite Initiation and Growth by Taxol *J.Cell Biol.* 98, no. 4: 1355-1362.

Letourneau, P. C., T. A. Shattuck, and A. H. Ressler. 1986. Branching of Sensory and Sympathetic Neurites in Vitro Is Inhibited by Treatment With Taxol *J.Neurosci.* 6, no. 7: 1912-1917.

Lew, J. and J. H. Wang. 1995. Neuronal Cdc2-Like Kinase *Trends Biochem.Sci.* 20, no. 1: 33-37.

Li, D. and R. Roberts. 2001. WD-Repeat Proteins: Structure Characteristics, Biological Function, and Their Involvement in Human Diseases
Cell Mol.Life Sci. 58, no. 14: 2085-2097.

Li, Y. H., S. Ghavampur, P. Bondallaz, L. Will, G. Grenningloh, and A. W. Puschel. 2009. Rnd1 Regulates Axon Extension by Enhancing the Microtubule Destabilising Activity of SCG10
J.Biol.Chem. 284, no. 1: 363-371.

Lim, S. S., P. J. Sammak, and G. G. Borisy. 1989. Progressive and Spatially Differentiated Stability of Microtubules in Developing Neuronal Cells
J.Cell Biol. 109, no. 1: 253-263.

Lin, C. H. and P. Forscher. 1993. Cytoskeletal Remodeling During Growth Cone-Target Interactions
J.Cell Biol. 121, no. 6: 1369-1383.

Lo, Nigro C., C. S. Chong, A. C. Smith, W. B. Dobyns, R. Carrozzo, and D. H. Ledbetter. 1997. Point Mutations and an Intragenic Deletion in LIS1, the Lissencephaly Causative Gene in Isolated Lissencephaly Sequence and Miller-Dieker Syndrome
Hum.Mol.Genet. 6, no. 2: 157-164.

Longman, C., M. Brockington, S. Torelli, C. Jimenez-Mallebrera, C. Kennedy, N. Khalil, L. Feng, R. K. Saran, T. Voit, L. Merlini, C. A. Sewry, S. C. Brown, and F. Muntoni. 2003. Mutations in the Human LARGE Gene Cause MDC1D, a Novel Form of Congenital Muscular Dystrophy With Severe Mental Retardation and Abnormal Glycosylation of Alpha-Dystroglycan
Hum.Mol.Genet. 12, no. 21: 2853-2861.

Lutjens, R., M. Igarashi, V. Pellier, H. Blasey, Paolo G. Di, E. Ruchti, C. Pfulg, J. K. Staple, S. Catsicas, and G. Grenningloh. 2000. Localization and Targeting of SCG10 to the Trans-Golgi Apparatus and Growth Cone Vesicles
Eur.J.Neurosci. 12, no. 7: 2224-2234.

Ma, Q., C. Kintner, and D. J. Anderson. 1996. Identification of Neurogenin, a Vertebrate Neuronal Determination Gene
Cell 87, no. 1: 43-52.

Magdaleno, S. M. and T. Curran. 2001. Brain Development: Integrins and the Reelin Pathway
Curr.Biol. 11, no. 24: R1032-R1035.

Manna, T., G. Grenningloh, H. P. Miller, and L. Wilson. 2007. Stathmin Family Protein SCG10 Differentially Regulates the Plus and Minus End Dynamics of Microtubules at Steady State in Vitro: Implications for Its Role in Neurite Outgrowth
Biochemistry 46, no. 11: 3543-3552.

Marenco, S. and D. R. Weinberger. 2000. The Neurodevelopmental Hypothesis of Schizophrenia: Following a Trail of Evidence From Cradle to Grave
Dev.Psychopathol. 12, no. 3: 501-527.

Marin-Padilla, M. 1998. Cajal-Retzius Cells and the Development of the Neocortex
Trends Neurosci. 21, no. 2: 64-71.

Matsumoto, N., R. J. Leventer, J. A. Kuc, S. K. Mewborn, L. L. Dudlicek, M. B. Ramocki, D. T. Pilz, P. L. Mills, S. Das, M. E. Ross, D. H. Ledbetter, and W. B. Dobyns. 2001. Mutation Analysis of the DCX Gene and Genotype/Phenotype Correlation in Subcortical Band Heterotopia
Eur.J.Hum.Genet. 9, no. 1: 5-12.

Maucuer, A., V. Doye, and A. Sobel. 1990. A Single Amino Acid Difference Distinguishes the Human and the Rat Sequences of Stathmin, a Ubiquitous Intracellular Phosphoprotein Associated With Cell Regulations
FEBS Lett. 264, no. 2: 275-278.

Maucuer, A., J. Moreau, M. Mechali, and A. Sobel. 1993. Stathmin Gene Family: Phylogenetic Conservation and Developmental Regulation in Xenopus
J.Biol.Chem. 268, no. 22: 16420-16429.

Mayer, H., S. Duit, C. Hauser, W. J. Schneider, and J. Nimpf. 2006. Reconstitution of the Reelin Signaling Pathway in Fibroblasts Demonstrates That Dab1 Phosphorylation Is Independent of Receptor Localization in Lipid Rafts
Mol.Cell Biol. 26, no. 1: 19-27.

Mikoshiba, K., Y. Nishimura, and Y. Tsukada. 1983. Absence of Bundle Structure in the Neocortex of the Reeler Mouse at the Embryonic Stage. Studies by Scanning Electron Microscopic Fractography
Dev.Neurosci. 6, no. 1: 18-25.

Mimori-Kiyosue, Y. and S. Tsukita. 2003. "Search-and-Capture" of Microtubules Through Plus-End-Binding Proteins (+TIPs)
J.Biochem. 134, no. 3: 321-326.

Mione, M. C., J. F. Cavanagh, B. Harris, and J. G. Parnavelas. 1997. Cell Fate Specification and Symmetrical/Asymmetrical Divisions in the Developing Cerebral Cortex
J.Neurosci. 17, no. 6: 2018-2029.

Mitchison, T. and M. Kirschner. 1984. Dynamic Instability of Microtubule Growth
Nature 312, no. 5991: 237-242.

Miyata, T. and M. Ogawa. 2007. Twisting of Neocortical Progenitor Cells Underlies a Spring-Like Mechanism for Daughter-Cell Migration
Curr.Biol. 17, no. 2: 146-151.

Mizuguchi, R., M. Sugimori, H. Takebayashi, H. Kosako, M. Nagao, S. Yoshida, Y. Nabeshima, K. Shimamura, and M. Nakafuku. 2001. Combinatorial Roles of Olig2 and Neurogenin2 in the Coordinated Induction of Pan-Neuronal and Subtype-Specific Properties of Motoneurons
Neuron 31, no. 5: 757-771.

Moqadam, F. & Siebert, P. 1994. Rapid Amplification of the 3' end of cDNAs with the 3'-AmpliFINDER™ RACE Kit.
Clontechniques IX(3):6–9.

Mori, N. and H. Morii. 2002. SCG10-Related Neuronal Growth-Associated Proteins in Neural Development, Plasticity, Degeneration, and Aging
J.Neurosci.Res. 70, no. 3: 264-273.

Morii, H., Y. Shiraishi-Yamaguchi, and N. Mori. 2006. SCG10, a Microtubule Destabilising Factor, Stimulates the Neurite Outgrowth by Modulating Microtubule Dynamics in Rat Hippocampal Primary Cultured Neurons
J.Neurobiol. 66, no. 10: 1101-1114.

Moriyama, K., K. Iida, and I. Yahara. 1996. Phosphorylation of Ser-3 of Cofilin Regulates Its Essential Function on Actin
Genes Cells 1, no. 1: 73-86.

Nadarajah, B., J. E. Brunstrom, J. Grutzendler, R. O. Wong, and A. L. Pearlman. 2001. Two Modes of Radial Migration in Early Development of the Cerebral Cortex
Nat.Neurosci. 4, no. 2: 143-150.

Nadarajah, B. and J. G. Parnavelas. 2002. Modes of Neuronal Migration in the Developing Cerebral Cortex
Nat.Rev.Neurosci. 3, no. 6: 423-432.

Nadarajah, B., P. Alifragis, R. O. Wong, and J. G. Parnavelas. 2003. Neuronal Migration in the Developing Cerebral Cortex: Observations Based on Real-Time Imaging
Cereb.Cortex 13, no. 6: 607-611.

Nadarajah, B. 2003. Radial Glia and Somal Translocation of Radial Neurons in the Developing Cerebral Cortex
Glia 43, no. 1: 33-36.

Nair, R. and B. Rost. 2002. Inferring Sub-Cellular Localization Through Automated Lexical Analysis
Bioinformatics. 18 Suppl 1: S78-S86.

Nakajima, K., K. Mikoshiba, T. Miyata, C. Kudo, and M. Ogawa. 1997. Disruption of Hippocampal Development in Vivo by CR-50 MAb Against Reelin
Proc.Natl.Acad.Sci.U.S.A 94, no. 15: 8196-8201.

Neer, E. J., C. J. Schmidt, and T. Smith. 1993. LIS Is More
Nat.Genet. 5, no. 1: 3-4.

Neer, E. J., C. J. Schmidt, R. Nambudripad, and T. F. Smith. 1994. The Ancient Regulatory-Protein Family of WD-Repeat Proteins
Nature 371, no. 6495: 297-300.

Nery, S., G. Fishell, and J. G. Corbin. 2002. The Caudal Ganglionic Eminence Is a Source of Distinct Cortical and Subcortical Cell Populations
Nat.Neurosci. 5, no. 12: 1279-1287.

Nikolic, M., M. M. Chou, W. Lu, B. J. Mayer, and L. H. Tsai. 1998. The P35/Cdk5 Kinase Is a Neuron-Specific Rac Effector That Inhibits Pak1 Activity
Nature 395, no. 6698: 194-198.

Nixon, A. B., G. Grenningloh, and P. J. Casey. 2002. The Interaction of RGSZ1 With SCG10 Attenuates the Ability of SCG10 to Promote Microtubule Disassembly
J.Biol.Chem. 277, no. 20: 18127-18133.

Noctor, S. C., A. C. Flint, T. A. Weissman, R. S. Dammerman, and A. R. Kriegstein. 2001. Neurons Derived From Radial Glial Cells Establish Radial Units in Neocortex
Nature 409, no. 6821: 714-720.

Nogales, E. and H. W. Wang. 2006. Structural Intermediates in Microtubule Assembly and Disassembly: How and Why?
Curr.Opin.Cell Biol. 18, no. 2: 179-184.

Ogawa, M., T. Miyata, K. Nakajima, K. Yagyu, M. Seike, K. Ikenaka, H. Yamamoto, and K. Mikoshiba. 1995. The Reeler Gene-Associated Antigen on Cajal-Retzius Neurons Is a Crucial Molecule for Laminar Organization of Cortical Neurons
Neuron 14, no. 5: 899-912.

Ognibene, E., W. Adriani, S. Macri, and G. Laviola. 2007. Neurobehavioural Disorders in the Infant Reeler Mouse Model: Interaction of Genetic Vulnerability and Consequences of Maternal Separation
Behav.Brain Res. 177, no. 1: 142-149.

Ognibene, E., W. Adriani, O. Granstrem, S. Pieretti, and G. Laviola. 2007. Impulsivity-Anxiety-Related Behavior and Profiles of Morphine-Induced Analgesia in Heterozygous Reeler Mice
Brain Res. 1131, no. 1: 173-180.

Ohshima, T., J. M. Ward, C. G. Huh, G. Longenecker, Veeranna, H. C. Pant, R. O. Brady, L. J. Martin, and A. B. Kulkarni. 1996. Targeted Disruption of the Cyclin-Dependent Kinase 5 Gene Results in Abnormal Corticogenesis, Neuronal Pathology and Perinatal Death
Proc.Natl.Acad.Sci.U.S.A 93, no. 20: 11173-11178.

Ohshima, T., M. Hirasawa, H. Tabata, T. Mutoh, T. Adachi, H. Suzuki, K. Saruta, T. Iwasato, S. Itohara, M. Hashimoto, K. Nakajima, M. Ogawa, A. B. Kulkarni, and K. Mikoshiba. 2007. Cdk5 Is Required for Multipolar-to-Bipolar Transition During Radial Neuronal Migration and Proper Dendrite Development of Pyramidal Neurons in the Cerebral Cortex
Development 134, no. 12: 2273-2282.

Okazaki, T., H. Wang, E. Masliah, M. Cao, S. A. Johnson, M. Sundsmo, T. Saitoh, and N. Mori. 1995. SCG10, a Neuron-Specific Growth-Associated Protein in Alzheimer's Disease
Neurobiol.Aging 16, no. 6: 883-894.

Oyler, G. A., G. A. Higgins, R. A. Hart, E. Battenberg, M. Billingsley, F. E. Bloom, and M. C. Wilson. 1989. The Identification of a Novel Synaptosomal-Associated Protein, SNAP-25, Differentially Expressed by Neuronal Subpopulations
J.Cell Biol. 109, no. 6 Pt 1: 3039-3052.

Ozon, S., A. Maucuer, and A. Sobel. 1997. The Stathmin Family -- Molecular and Biological Characterization of Novel Mammalian Proteins Expressed in the Nervous System
Eur.J.Biochem. 248, no. 3: 794-806.

Ozon, S., T. Byk, and A. Sobel. 1998. SCLIP: a Novel SCG10-Like Protein of the Stathmin Family Expressed in the Nervous System
J.Neurochem. 70, no. 6: 2386-2396.

Ozon, S., Mestikawy S. El, and A. Sobel. 1999. Differential, Regional, and Cellular Expression of the Stathmin Family Transcripts in the Adult Rat Brain
J.Neurosci.Res. 56, no. 5: 553-564.

Pantaloni, D., Clainche C. Le, and M. F. Carlier. 2001. Mechanism of Actin-Based Motility
Science 292, no. 5521: 1502-1506.

Pardo, C. A. and C. G. Eberhart. 2007. The Neurobiology of Autism
Brain Pathol. 17, no. 4: 434-447.

Parrini, E., A. Ramazzotti, W. B. Dobyns, D. Mei, F. Moro, P. Veggiotti, C. Marini, E. H. Brilstra, Bernardina B. Dalla, L. Goodwin, A. Bodell, M. C. Jones, M. Nangeroni, S. Palmeri, E. Said, J. W. Sander, P. Striano, Y. Takahashi, Maldergem L. Van, G. Leonardi, M. Wright, C. A.

Walsh, and R. Guerrini. 2006. Periventricular Heterotopia: Phenotypic Heterogeneity and Correlation With Filamin A Mutations
Brain 129, no. Pt 7: 1892-1906.

Pauls, D. L., J. P. Alsobrook, W. Goodman, S. Rasmussen, and J. F. Leckman. 1995. A Family Study of Obsessive-Compulsive Disorder. *Am.J.Psychiatry* 152, no. 1: 76-84.

Pearlman, A. L. and A. M. Sheppard. 1996. Extracellular Matrix in Early Cortical Development *Prog.Brain Res.* 108: 117-134.

Pearlman, A. L., P. L. Faust, M. E. Hatten, and J. E. Brunstrom. 1998. New Directions for Neuronal Migration
Curr.Opin.Neurobiol. 8, no. 1: 45-54.

Persico, A. M., L. D'Agruma, N. Maiorano, A. Totaro, R. Militerni, C. Bravaccio, T. H. Wassink, C. Schneider, R. Melmed, S. Trillo, F. Montecchi, M. Palermo, T. Pascucci, S. Puglisi-Allegra, K. L. Reichelt, M. Conciatori, R. Marino, C. C. Quattrocchi, A. Baldi, L. Zelante, P. Gasparini, and F. Keller. 2001. Reelin Gene Alleles and Haplotypes As a Factor Predisposing to Autistic Disorder
Mol.Psychiatry 6, no. 2: 150-159.

Pesold, C., F. Impagnatiello, M. G. Pisu, D. P. Uzunov, E. Costa, A. Guidotti, and H. J. Caruncho. 1998. Reelin Is Preferentially Expressed in Neurons Synthesizing Gamma-Aminobutyric Acid in Cortex and Hippocampus of Adult Rats
Proc.Natl.Acad.Sci.U.S.A 95, no. 6: 3221-3226.

Petroski, M. D. and R. J. Deshaies. 2005. Function and Regulation of Cullin-RING Ubiquitin Ligases *Nat.Rev.Mol.Cell Biol.* 6, no. 1: 9-20.

Piao, X., B. S. Chang, A. Bodell, K. Woods, B. Benzeev, M. Topcu, R. Guerrini, H. Goldberg-Stern, L. Sztriha, W. B. Dobyns, A. J. Barkovich, and C. A. Walsh. 2005. Genotype-Phenotype Analysis of Human Frontoparietal Polymicrogyria Syndromes
Ann.Neurol. 58, no. 5: 680-687.

Pinto Lord, M. C. and V. S. Caviness, Jr. 1979. Determinants of Cell Shape and Orientation: a Comparative Golgi Analysis of Cell-Axon Interrelationships in the Developing Neocortex of Normal and Reeler Mice
J.Comp Neurol. 187, no. 1: 49-69.

Poirier, K., D. A. Keays, F. Francis, Y. Saillour, N. Bahi, S. Manouvrier, C. Fallet-Bianco, L. Pasquier, A. Toutain, F. P. Tuy, T. Bienvenu, S. Joriot, S. Odent, D. Ville, I. Desguerre, A. Goldenberg, M. L. Moutard, J. P. Fryns, Esch H. van, R. J. Harvey, C. Siebold, J. Flint, C. Beldjord, and J. Chelly. 2007. Large Spectrum of Lissencephaly and Pachygyria Phenotypes Resulting From De Novo Missense Mutations in Tubulin Alpha 1A (TUBA1A)
Hum.Mutat. 28, no. 11: 1055-1064.

Pollard, T. D. and G. G. Borisy. 2003. Cellular Motility Driven by Assembly and Disassembly of Actin Filaments
Cell 112, no. 4: 453-465.

Polleux, F., K. L. Whitford, P. A. Dijkhuizen, T. Vitalis, and A. Ghosh. 2002. Control of Cortical Interneuron Migration by Neurotrophins and PI3-Kinase Signaling
Development 129, no. 13: 3147-3160.

Quraishi, S. and S. Frangou. 2002. Neuropsychology of Bipolar Disorder: a Review
J.Affect.Disord. 72, no. 3: 209-226.

Rakic, P. 1995. Radial Versus Tangential Migration of Neuronal Clones in the Developing Cerebral Cortex
Proc.Natl.Acad.Sci.U.S.A 92, no. 25: 11323-11327.

Rakic, S. and N. Zecevic. 2003. Emerging Complexity of Layer I in Human Cerebral Cortex
Cereb.Cortex 13, no. 10: 1072-1083.

Rakic, P. The radial edifice of cortical architecture: from neuronal silhouettes to genetic engineering.
Brain Res. Rev. 55, 204-219

Ravelli, R. B., B. Gigant, P. A. Curmi, I. Jourdain, S. Lachkar, A. Sobel, and M. Knossow. 2004. Insight into Tubulin Regulation From a Complex With Colchicine and a Stathmin-Like Domain
Nature 428, no. 6979: 198-202.

Reiner, O., R. Carrozzo, Y. Shen, M. Wehnert, F. Faustinella, W. B. Dobyns, C. T. Caskey, and D. H. Ledbetter. 1993. Isolation of a Miller-Dieker Lissencephaly Gene Containing G Protein Beta-Subunit-Like Repeats
Nature 364, no. 6439: 717-721.

Reiner, O., U. Albrecht, M. Gordon, K. A. Chianese, C. Wong, O. Gal-Gerber, T. Sapir, L. D. Siracusa, A. M. Buchberg, C. T. Caskey, and . 1995. Lissencephaly Gene (LIS1) Expression in the CNS Suggests a Role in Neuronal Migration
J.Neurosci. 15, no. 5 Pt 2: 3730-3738.

Reiner, O. 2000. LIS1. Let's Interact Sometimes... (Part 1)
Neuron 28, no. 3: 633-636.

Ribeiro, Mdo C., Sousa S. Gama de, M. M. Freitas, I. Carrilho, and I. Fernandes. 2007. Bilateral Perisylvian Polymicrogyria and Chromosome 1 Anomaly
Pediatr.Neurol. 36, no. 6: 418-420.

Rice, D. S., M. Sheldon, G. D'Arcangelo, K. Nakajima, D. Goldowitz, and T. Curran. 1998. Disabled-1 Acts Downstream of Reelin in a Signaling Pathway That Controls Laminar Organization in the Mammalian Brain
Development 125, no. 18: 3719-3729.

Rice, D. S. and T. Curran. 1999. Mutant Mice With Scrambled Brains: Understanding the Signaling Pathways That Control Cell Positioning in the CNS
Genes Dev. 13, no. 21: 2758-2773.

Rice, D. S. and T. Curran. 2001. Role of the Reelin Signaling Pathway in Central Nervous System Development. *Annu.Rev.Neurosci.* 24: 1005-1039.

Rice, D. S., S. Nusinowitz, A. M. Azimi, A. Martinez, E. Soriano, and T. Curran. 2001. The Reelin Pathway Modulates the Structure and Function of Retinal Synaptic Circuitry
Neuron 31, no. 6: 929-941.

Rickmann, M. and J. R. Wolff. 1981. Differentiation of 'Preplate' Neurons in the Pallium of the Rat.
Bibl.Anat., no. 19: 142-146.

Riederer, B. M., V. Pellier, B. Antonsson, Paolo G. Di, S. A. Stimpson, R. Lutjens, S. Catsicas, and G. Grenningloh. 1997. Regulation of Microtubule Dynamics by the Neuronal Growth-Associated Protein SCG10
Proc.Natl.Acad.Sci.U.S.A 94, no. 2: 741-745.

Roberts, G. W. 1991. Schizophrenia: a Neuropathological Perspective
Br.J.Psychiatry 158: 8-17.

Roberts, R. C., L. Xu, J. K. Roche, and B. Kirkpatrick. 2005. Ultrastructural Localization of Reelin in the Cortex in Post-Mortem Human Brain
J.Comp Neurol. 482, no. 3: 294-308.

Robin, N. H., C. J. Taylor, D. M. Donald-McGinn, E. H. Zackai, P. Bingham, K. J. Collins, D. Earl, D. Gill, T. Granata, R. Guerrini, N. Katz, V. Kimonis, J. P. Lin, D. R. Lynch, S. N. Mohammed, R. F. Massey, M. McDonald, R. C. Rogers, M. Splitt, C. A. Stevens, M. D. Tischkowitz, N. Stoodley, R. J. Leventer, D. T. Pilz, and W. B. Dobyns. 2006. Polymicrogyria and Deletion 22q11.2 Syndrome: Window to the Etiology of a Common Cortical Malformation
Am.J.Med.Genet.A 140, no. 22: 2416-2425.

Rochlin, M. W., K. M. Wickline, and P. C. Bridgman. 1996. Microtubule Stability Decreases Axon Elongation but Not Axoplasm Production
J.Neurosci. 16, no. 10: 3236-3246.

Roll, P., G. Rudolf, S. Pereira, B. Royer, I. E. Scheffer, A. Massacrier, M. P. Valenti, N. Roeckel-Trevisiol, S. Jamali, C. Beclin, C. Seegmuller, M. N. Metz-Lutz, A. Lemainque, M. Delepine, C. Caloustian, Martin A. de Saint, N. Bruneau, D. Depetris, M. G. Mattei, E. Flori, A. Robaglia-Schlupp, N. Levy, B. A. Neubauer, R. Ravid, C. Marescaux, S. F. Berkovic, E. Hirsch, M. Lathrop, P. Cau, and P. Szepetowski. 2006. SRPX2 Mutations in Disorders of Language Cortex and Cognition
Hum.Mol.Genet. 15, no. 7: 1195-1207.

Rosenberg DR, Keshavan MS, O'Hearn KM, Dick EL, Bagwell WW, Seymour AB, Montrose DM, Pierri JN, Birmaher B. 1997. Frontostriatal measurement in treatment-naive children with obsessive-compulsive disorder. *Arch Gen Psychiatry*. 54, no. 9: 824-30

Rosenberg DR, Keshavan MS. A.E. Bennett Research Award. Toward a neurodevelopmental model of of obsessive--compulsive disorder. 1997. *Biol psychiatry*. 43, no. 9: 623-40

Royaux, I., Rouvroit C. Lambert de, G. D'Arcangelo, D. Demirov, and A. M. Goffinet. 1997. Genomic Organization of the Mouse Reelin Gene
Genomics 46, no. 2: 240-250.

Ruder, C., T. Reimer, I. gado-Martinez, R. Hermosilla, A. Engelsberg, R. Nehring, B. Dorken, and A. Rehm. 2005. EBAG9 Adds a New Layer of Control on Large Dense-Core Vesicle Exocytosis Via Interaction With Snapin
Mol.Biol.Cell 16, no. 3: 1245-1257.

Sabry, J. H., T. P. O'Connor, L. Evans, A. Toroian-Raymond, M. Kirschner, and D. Bentley. 1991. Microtubule Behavior During Guidance of Pioneer Neuron Growth Cones in Situ
J.Cell Biol. 115, no. 2: 381-395.

Sanada, K., A. Gupta, and L. H. Tsai. 2004. Disabled-1-Regulated Adhesion of Migrating Neurons to Radial Glial Fiber Contributes to Neuronal Positioning During Early Corticogenesis
Neuron 42, no. 2: 197-211.

Sapir, T., D. Horesh, M. Caspi, R. Atlas, H. A. Burgess, S. G. Wolf, F. Francis, J. Chelly, M. Elbaum, S. Pietrokovski, and O. Reiner. 2000. Doublecortin Mutations Cluster in Evolutionarily Conserved Functional Domains
Hum.Mol.Genet. 9, no. 5: 703-712.

Schaefer, A. W., N. Kabir, and P. Forscher. 2002. Filopodia and Actin Arcs Guide the Assembly and Transport of Two Populations of Microtubules With Unique Dynamic Parameters in Neuronal Growth Cones
J.Cell Biol. 158, no. 1: 139-152.

Schiffmann, S. N., B. Bernier, and A. M. Goffinet. 1997. Reelin MRNA Expression During Mouse Brain Development
Eur.J.Neurosci. 9, no. 5: 1055-1071.

Schmid, R. S., S. Shelton, A. Stanco, Y. Yokota, J. A. Kreidberg, and E. S. Anton. 2004. Alpha3beta1 Integrin Modulates Neuronal Migration and Placement During Early Stages of Cerebral Cortical Development
Development 131, no. 24: 6023-6031.

Schmid, R. S., R. Jo, S. Shelton, J. A. Kreidberg, and E. S. Anton. 2005. Reelin, Integrin and DAB1 Interactions During Embryonic Cerebral Cortical Development
Cereb.Cortex 15, no. 10: 1632-1636.

Schubart, U. K., M. D. Banerjee, and J. Eng. 1989. Homology Between the CDNAs Encoding Phosphoprotein P19 and SCG10 Reveals a Novel Mammalian Gene Family Preferentially Expressed in Developing Brain
DNA 8, no. 6: 389-398.

Schulze, E. and M. Kirschner. 1986. Microtubule Dynamics in Interphase Cells
J.Cell Biol. 102, no. 3: 1020-1031.

Senzaki, K., M. Ogawa, and T. Yagi. 1999. Proteins of the CNR Family Are Multiple Receptors for Reelin
Cell 99, no. 6: 635-647.

Sheen, V. L., J. W. Wheless, A. Bodell, E. Braverman, P. D. Cotter, K. A. Rauen, O. Glenn, K. Weisiger, S. Packman, C. A. Walsh, and E. H. Sherr. 2003. Periventricular Heterotopia Associated With Chromosome 5p Anomalies
Neurology 60, no. 6: 1033-1036.

Sheen, V. L., V. S. Ganesh, M. Topcu, G. Sebire, A. Bodell, R. S. Hill, P. E. Grant, Y. Y. Shugart, J. Imitola, S. J. Khoury, R. Guerrini, and C. A. Walsh. 2004. Mutations in ARFGEF2 Implicate Vesicle Trafficking in Neural Progenitor Proliferation and Migration in the Human Cerebral Cortex
Nat.Genet. 36, no. 1: 69-76.

Sheldon, M., D. S. Rice, G. D'Arcangelo, H. Yoneshima, K. Nakajima, K. Mikoshiba, B. W. Howell, J. A. Cooper, D. Goldowitz, and T. Curran. 1997. Scrambler and Yotari Disrupt the Disabled Gene and Produce a Reeler-Like Phenotype in Mice
Nature 389, no. 6652: 730-733.

Sheppard, A. M. and A. L. Pearlman. 1997. Abnormal Reorganization of Preplate Neurons and Their Associated Extracellular Matrix: an Early Manifestation of Altered Neocortical Development in the Reeler Mutant Mouse
J.Comp Neurol. 378, no. 2: 173-179.

Shu, T., R. Ayala, M. D. Nguyen, Z. Xie, J. G. Gleeson, and L. H. Tsai. 2004. Ndel1 Operates in a Common Pathway With LIS1 and Cytoplasmic Dynein to Regulate Cortical Neuronal Positioning
Neuron 44, no. 2: 263-277.

Sidman, R. L., S. H. Appel, and J. F. Fullier. 1965. Neurological Mutants of the Mouse
Science 150, no. 3695: 513-516.

Smith, S. J. 1988. Neuronal Cytomechanics: the Actin-Based Motility of Growth Cones
Science 242, no. 4879: 708-715.

Smith, T. F., C. Gaitatzes, K. Saxena, and E. J. Neer. 1999. The WD Repeat: a Common Architecture for Diverse Functions
Trends Biochem.Sci. 24, no. 5: 181-185.

Sobhanifer, S. 2003. Yeast two hybrid assay: A fishing tale.
BioTeach Journal.1, 81-85

Sollner, T., S. W. Whiteheart, M. Brunner, H. Erdjument-Bromage, S. Geromanos, P. Tempst, and J. E. Rothman. 1993. SNAP Receptors Implicated in Vesicle Targeting and Fusion
Nature 362, no. 6418: 318-324.

Sprecher, E., A. Ishida-Yamamoto, M. Mizrahi-Koren, D. Rapaport, D. Goldsher, M. Indelman, O. Topaz, I. Chefetz, H. Keren, T. J. O'brien, D. Bercovich, S. Shalev, D. Geiger, R. Bergman, M. Horowitz, and H. Mandel. 2005. A Mutation in SNAP29, Coding for a SNARE Protein Involved in Intracellular Trafficking, Causes a Novel Neurocutaneous Syndrome Characterized by Cerebral Dysgenesis, Neuropathy, Ichthyosis, and Palmoplantar Keratoderma
Am.J.Hum.Genet. 77, no. 2: 242-251.

Stein, R., N. Mori, K. Matthews, L. C. Lo, and D. J. Anderson. 1988. The NGF-Inducible SCG10 MRNA Encodes a Novel Membrane-Bound Protein Present in Growth Cones and Abundant in Developing Neurons
Neuron 1, no. 6: 463-476.

Stolt, P. C., H. Jeon, H. K. Song, J. Herz, M. J. Eck, and S. C. Blacklow. 2003. Origins of Peptide Selectivity and Phosphoinositide Binding Revealed by Structures of Disabled-1 PTB Domain Complexes
Structure. 11, no. 5: 569-579.

Stoothoff, W. H. and G. V. Johnson. 2005. Tau Phosphorylation: Physiological and Pathological Consequences
Biochim.Biophys.Acta 1739, no. 2-3: 280-297.

Strasser, V., D. Fasching, C. Hauser, H. Mayer, H. H. Bock, T. Hiesberger, J. Herz, E. J. Weeber, J. D. Sweatt, A. Pramatarova, B. Howell, W. J. Schneider, and J. Nimpf. 2004. Receptor Clustering Is Involved in Reelin Signaling
Mol.Cell Biol. 24, no. 3: 1378-1386.

Sugiura, Y. and N. Mori. 1995. SCG10 Expresses Growth-Associated Manner in Developing Rat Brain, but Shows a Different Pattern to P19/Stathmin or GAP-43
Brain Res.Dev.Brain Res. 90, no. 1-2: 73-91.

Super, H., E. Soriano, and H. B. Uylings. 1998. The Functions of the Preplate in Development and Evolution of the Neocortex and Hippocampus
Brain Res.Brain Res.Rev. 27, no. 1: 40-64.

Sussel, L., O. Marin, S. Kimura, and J. L. Rubenstein. 1999. Loss of Nkx2.1 Homeobox Gene Function Results in a Ventral to Dorsal Molecular Respecification Within the Basal Telencephalon: Evidence for a Transformation of the Pallidum into the Striatum
Development 126, no. 15: 3359-3370.

Tabata, H. and K. Nakajima. 2003. Multipolar Migration: the Third Mode of Radial Neuronal Migration in the Developing Cerebral Cortex
J.Neurosci. 23, no. 31: 9996-10001.

Takahashi, S., Y. Kawarabayasi, T. Nakai, J. Sakai, and T. Yamamoto. 1992. Rabbit Very Low Density Lipoprotein Receptor: a Low Density Lipoprotein Receptor-Like Protein With Distinct Ligand Specificity
Proc.Natl.Acad.Sci.U.S.A 89, no. 19: 9252-9256.

Tamamaki, N., K. E. Fujimori, and R. Takauji. 1997. Origin and Route of Tangentially Migrating Neurons in the Developing Neocortical Intermediate Zone
J.Neurosci. 17, no. 21: 8313-8323.

Tanaka, D., Y. Nakaya, Y. Yanagawa, K. Obata, and F. Murakami. 2003. Multimodal Tangential Migration of Neocortical GABAergic Neurons Independent of GPI-Anchored Proteins
Development 130, no. 23: 5803-5813.

Tanaka, E., T. Ho, and M. W. Kirschner. 1995. The Role of Microtubule Dynamics in Growth Cone Motility and Axonal Growth
J.Cell Biol. 128, no. 1-2: 139-155.

Tanaka, E. and M. W. Kirschner. 1995. The Role of Microtubules in Growth Cone Turning at Substrate Boundaries
J.Cell Biol. 128, no. 1-2: 127-137.

Tanaka, E. M. and M. W. Kirschner. 1991. Microtubule Behavior in the Growth Cones of Living Neurons During Axon Elongation
J.Cell Biol. 115, no. 2: 345-363.

Tanaka, J., M. Kira, and K. Sobue. 1993. Gelsolin Is Localized in Neuronal Growth Cones
Brain Res.Dev.Brain Res. 76, no. 2: 268-271.

Tanaka, T., F. F. Serneo, H. C. Tseng, A. B. Kulkarni, L. H. Tsai, and J. G. Gleeson. 2004. Cdk5 Phosphorylation of Doublecortin Ser297 Regulates Its Effect on Neuronal Migration
Neuron 41, no. 2: 215-227.

Tararuk, T., N. Ostman, W. Li, B. Bjorkblom, A. Padzik, J. Zdrojewska, V. Hongisto, T. Herdegen, W. Konopka, M. J. Courtney, and E. T. Coffey. 2006. JNK1 Phosphorylation of SCG10 Determines Microtubule Dynamics and Axodendritic Length
J.Cell Biol. 173, no. 2: 265-277.

Tassi L, Colombo N, Garbelli R, Francione S, Lo Russo G, Mai R, Cardinale F, Cossu M, Ferrario A, Galli C, Bramerio M, Citterio A, Spreafico R. 2002. Focal cortical dysplasia: neuropathological subtypes, EEG, neuroimaging and surgical outcome. *Brain*. 125, pt. 8: 1719-32

Taylor, D. C., M. A. Falconer, C. J. Bruton, and J. A. Corsellis. 1971. Focal Dysplasia of the Cerebral Cortex in Epilepsy
J.Neurol.Neurosurg.Psychiatry 34, no. 4: 369-387.

Taylor, K. R., A. K. Holzer, J. F. Bazan, C. A. Walsh, and J. G. Gleeson. 2000. Patient Mutations in Doublecortin Define a Repeated Tubulin-Binding Domain
J.Biol.Chem. 275, no. 44: 34442-34450.

Tessier-Lavigne, M. and C. S. Goodman. 1996. The Molecular Biology of Axon Guidance
Science 274, no. 5290: 1123-1133.

Tian, J. H., Z. X. Wu, M. Unzicker, L. Lu, Q. Cai, C. Li, C. Schirra, U. Matti, D. Stevens, C. Deng, J. Rettig, and Z. H. Sheng. 2005. The Role of Snapin in Neurosecretion: Snapin Knock-Out Mice Exhibit Impaired Calcium-Dependent Exocytosis of Large Dense-Core Vesicles in Chromaffin Cells
J.Neurosci. 25, no. 45: 10546-10555.

Togano, T., M. Kurachi, M. Watanabe, G. Grenningloh, and M. Igarashi. 2005. Role of Ser50 Phosphorylation in SCG10 Regulation of Microtubule Depolymerization
J.Neurosci.Res. 80, no. 4: 475-480.

Tordjman, S., D. Drapier, O. Bonnot, R. Graignic, S. Fortes, D. Cohen, B. Millet, C. Laurent, and P. L. Roubertoux. 2007. Animal Models Relevant to Schizophrenia and Autism: Validity and Limitations
Behav.Genet. 37, no. 1: 61-78.

Toro, C. T. and J. F. Deakin. 2007. Adult Neurogenesis and Schizophrenia: a Window on Abnormal Early Brain Development?
Schizophr.Res. 90, no. 1-3: 1-14.

Trimble, W. S., D. M. Cowan, and R. H. Scheller. 1988. VAMP-1: a Synaptic Vesicle-Associated Integral Membrane Protein
Proc.Natl.Acad.Sci.U.S.A 85, no. 12: 4538-4542.

Trinczek, B., J. Biernat, K. Baumann, E. M. Mandelkow, and E. Mandelkow. 1995. Domains of Tau Protein, Differential Phosphorylation, and Dynamic Instability of Microtubules
Mol.Biol.Cell 6, no. 12: 1887-1902.

Troelstra, C., Gool A. van, Wit J. de, W. Vermeulen, D. Bootsma, and J. H. Hoeijmakers. 1992. ERCC6, a Member of a Subfamily of Putative Helicases, Is Involved in Cockayne's Syndrome and Preferential Repair of Active Genes
Cell 71, no. 6: 939-953.

Trommsdorff, M., J. P. Borg, B. Margolis, and J. Herz. 1998. Interaction of Cytosolic Adaptor Proteins With Neuronal Apolipoprotein E Receptors and the Amyloid Precursor Protein
J.Biol.Chem. 273, no. 50: 33556-33560.

Trommsdorff, M., M. Gotthardt, T. Hiesberger, J. Shelton, W. Stockinger, J. Nimpf, R. E. Hammer, J. A. Richardson, and J. Herz. 1999. Reeler/Disabled-Like Disruption of Neuronal Migration in Knockout Mice Lacking the VLDL Receptor and ApoE Receptor2
Cell 97, no. 6: 689-701.

Tsuang, M. T., R. F. Woolson, and J. A. Fleming. 1979. Long-Term Outcome of Major Psychoses. I. Schizophrenia and Affective Disorders Compared With Psychiatrically Symptom-Free

Surgical Conditions
A*rch.Gen.Psychiatry* 36, no. 12: 1295-1301.

Tueting, P., E. Costa, Y. Dwivedi, A. Guidotti, F. Impagnatiello, R. Manev, and C. Pesold. 1999. The Phenotypic Characteristics of Heterozygous Reeler Mouse
Neuroreport 10, no. 6: 1329-1334.

Uher, B. F. and J. A. Golden. 2000. Neuronal Migration Defects of the Cerebral Cortex: a Destination Debacle
Clin.Genet. 58, no. 1: 16-24.

Utsunomiya-Tate, N., K. Kubo, S. Tate, M. Kainosho, E. Katayama, K. Nakajima, and K. Mikoshiba. 2000. Reelin Molecules Assemble Together to Form a Large Protein Complex, Which Is Inhibited by the Function-Blocking CR-50 Antibody
Proc.Natl.Acad.Sci.U.S.A 97, no. 17: 9729-9734.

Van, Criekinge W. and R. Beyaert. 1999. Yeast Two-Hybrid: State of the Art
Biol.Proced.Online. 2: 1-38.

van, Reeuwijk J., M. Janssen, Elzen C. van den, Bernabe D. Beltran-Valero de, P. Sabatelli, L. Merlini, M. Boon, H. Scheffer, M. Brockington, F. Muntoni, M. A. Huynen, A. Verrips, C. A. Walsh, P. G. Barth, H. G. Brunner, and Bokhoven H. van. 2005. POMT2 Mutations Cause Alpha-Dystroglycan Hypoglycosylation and Walker-Warburg Syndrome
J.Med.Genet. 42, no. 12: 907-912.

van, Reeuwijk J., S. Maugenre, Elzen C. van den, A. Verrips, E. Bertini, F. Muntoni, L. Merlini, H. Scheffer, H. G. Brunner, P. Guicheney, and Bokhoven H. van. 2006. The Expanding Phenotype of POMT1 Mutations: From Walker-Warburg Syndrome to Congenital Muscular Dystrophy, Microcephaly, and Mental Retardation
Hum.Mutat. 27, no. 5: 453-459.

Vander and Ploegh. 1992. The WD40 repeats.

varez-Buylla, A., M. Theelen, and F. Nottebohm. 1990. Proliferation "Hot Spots" in Adult Avian Ventricular Zone Reveal Radial Cell Division
Neuron 5, no. 1: 101-109.

Venkatasubramanian G, Rao NP, Behere RV. 2009. Neuroanatomical, neurochemical, and neurodevelopmental basis of obsessive-Compulsive symptoms in schizophrenia. *Indn Journal of psychiatry.* 31, no. 1: 3-10

Vites, O., J. S. Rhee, M. Schwarz, C. Rosenmund, and R. Jahn. 2004. Reinvestigation of the Role of Snapin in Neurotransmitter Release
J.Biol.Chem. 279, no. 25: 26251-26256.

Walsh, C. and C. L. Cepko. 1993. Clonal Dispersion in Proliferative Layers of Developing Cerebral Cortex
Nature 362, no. 6421: 632-635.

Walter-Yohrling, J., X. Cao, M. Callahan, W. Weber, S. Morgenbesser, S. L. Madden, C. Wang, and B. A. Teicher. 2003. Identification of Genes Expressed in Malignant Cells That Promote Invasion
Cancer Res. 63, no. 24: 8939-8947.

Ware, M. L., S. F. Tavazoie, C. B. Reid, and C. A. Walsh. 1999. Coexistence of Widespread Clones and Large Radial Clones in Early Embryonic Ferret Cortex
Cereb.Cortex 9, no. 6: 636-645.

Watt, N. F. 1972. Longitudinal Changes in the Social Behavior of Children Hospitalized for Schizophrenia As Adults
J.Nerv.Ment.Dis. 155, no. 1: 42-54.

Weinberger, D. R., E. F. Torrey, A. N. Neophytides, and R. J. Wyatt. 1979. Lateral Cerebral Ventricular Enlargement in Chronic Schizophrenia
Arch.Gen.Psychiatry 36, no. 7: 735-739.

Weinberger, D. R., L. E. DeLisi, G. P. Perman, S. Targum, and R. J. Wyatt. 1982. Computed Tomography in Schizophreniform Disorder and Other Acute Psychiatric Disorders
Arch.Gen.Psychiatry 39, no. 7: 778-783.

Weinberger, D. R. 1987. Implications of Normal Brain Development for the Pathogenesis of Schizophrenia
Arch.Gen.Psychiatry 44, no. 7: 660-669.

Weinberger, D. R. 1987. The pathogenesis of schizophrenia: a neurodevelopmental hypothesis.

Wichterle, H., J. M. Garcia-Verdugo, D. G. Herrera, and A. varez-Buylla. 1999. Young Neurons From Medial Ganglionic Eminence Disperse in Adult and Embryonic Brain
Nat.Neurosci. 2, no. 5: 461-466.

Wichterle, H., D. H. Turnbull, S. Nery, G. Fishell, and A. varez-Buylla. 2001. In Utero Fate Mapping Reveals Distinct Migratory Pathways and Fates of Neurons Born in the Mammalian Basal Forebrain
Development 128, no. 19: 3759-3771.

Witte, H., D. Neukirchen, and F. Bradke. 2008. Microtubule Stabilization Specifies Initial Neuronal Polarization
J.Cell Biol. 180, no. 3: 619-632.

Witte, H. and F. Bradke. 2008. The Role of the Cytoskeleton During Neuronal Polarization
Curr.Opin.Neurobiol. 18, no. 5: 479-487.

Yamada, K. M., B. S. Spooner, and N. K. Wessells. 1971. Ultrastructure and Function of Growth Cones and Axons of Cultured Nerve Cells
J.Cell Biol. 49, no. 3: 614-635.

Yao, G., X. N. Chen, L. Flores-Sarnat, G. M. Barlow, G. Palka, J. B. Moeschler, B. McGillivray, R. P. Morse, and J. R. Korenberg. 2006. Deletion of Chromosome 21 Disturbs Human Brain Morphogenesis
Genet.Med. 8, no. 1: 1-7.

Yokota, Y., H. T. Gashghaei, C. Han, H. Watson, K. J. Campbell, and E. S. Anton. 2007. Radial Glial Dependent and Independent Dynamics of Interneuronal Migration in the Developing Cerebral Cortex
PLoS.One. 2, no. 8: e794.

Yu, W. and P. W. Baas. 1995. The Growth of the Axon Is Not Dependent Upon Net Microtubule Assembly at Its Distal Tip
J.Neurosci. 15, no. 10: 6827-6833.

Yun, M., L. Keshvara, C. G. Park, Y. M. Zhang, J. B. Dickerson, J. Zheng, C. O. Rock, T. Curran, and H. W. Park. 2003. Crystal Structures of the Dab Homology Domains of Mouse Disabled 1 and 2
J.Biol.Chem. 278, no. 38: 36572-36581.

Zaki, M., M. Shehab, A. A. El-Aleem, G. bdel-Salam, H. B. Koeller, Y. Ilkin, M. E. Ross, W. B. Dobyns, and J. G. Gleeson. 2007. Identification of a Novel Recessive RELN Mutation Using a Homozygous Balanced Reciprocal Translocation
Am.J.Med.Genet.A 143A, no. 9: 939-944.

Zebda, N., O. Bernard, M. Bailly, S. Welti, D. S. Lawrence, and J. S. Condeelis. 2000. Phosphorylation of ADF/Cofilin Abolishes EGF-Induced Actin Nucleation at the Leading Edge and Subsequent Lamellipod Extension
J.Cell Biol. 151, no. 5: 1119-1128.

Zhang, Z. and D. S. Galileo. 1998. Retroviral Transfer of Antisense Integrin Alpha6 or Alpha8 Sequences Results in Laminar Redistribution or Clonal Cell Death in Developing Brain
J.Neurosci. 18, no. 17: 6928-6938.

Zheng, J., R. E. Buxbaum, and S. R. Heidemann. 1993. Investigation of Microtubule Assembly and Organization Accompanying Tension-Induced Neurite Initiation
J.Cell Sci. 104 (Pt 4): 1239-1250.

Zhou, F. Q., C. M. Waterman-Storer, and C. S. Cohan. 2002. Focal Loss of Actin Bundles Causes Microtubule Redistribution and Growth Cone Turning
J.Cell Biol. 157, no. 5: 839-849.

Zollino, M., C. Colosimo, O. Zuffardi, E. Rossi, A. Tosolini, C. A. Walsh, and G. Neri. 2003. Cryptic T(1;12)(Q44;P13.3) Translocation in a Previously Described Syndrome With Polymicrogyria, Segregating As an Apparently X-Linked Trait
Am.J.Med.Genet.A 117A, no. 1: 65-71.